PONTIFICIA UNIVERSIDAD CATOLICA DE CHILE

ESCUELA DE INGENIERIA

DEVELOPING A DECISION TOOL TO SELECT LOCATIONS AND CHARACTERISTICS OF PARABOLIC TROUGH CONCENTRATOR PLANTS IN CHILE, BASED ON THE LEVELIZED COST OF ENERGY

MATIAS A HÄNEL

Thesis submitted to the Office of Research and Graduate Studies in partial fulfillment of the requirements for the Degree of Master of Science in

Advisor:

RODRIGO ESCOBAR

Santiago de Chile, January 2010

© 2010, Matías Hänel

PONTIFICIA UNIVERSIDAD CATOLICA DE CHILE

ESCUELA DE INGENIERIA

DEVELOPING A DECISION TOOL TO SELECT LOCATIONS AND CHARACTERISTICS OF PARABOLIC TROUGH CONCENTRATOR PLANTS IN CHILE, BASED ON THE LEVELIZED COST OF ENERGY

MATIAS A HÄNEL

Members of the Committee:

RODRIGO ESCOBAR

JULIO VERGARA

ANDRES OLIVARES

VLADIMIR MARIANOV

Thesis submitted to the Office of Research and Graduate Studies in partial fulfillment of the requirements for the Degree of Master of Science in Engineering

Santiago de Chile, January 2010

A mis papás e Ignacia que me han apoyado.

ACKNOWLEDGMENTS

I would like to acknowledge the support of my advisor, Dr. Rodrigo Escobar of the Pontificia Universidad Católica de Chile, who guided me throughout this work.

I also would like to show my gratitude to the people who gave me their advice during the development of this thesis and to my officemates Alberto, Cristián, Alan, Sebastien and Teresita and especially my friend Ignacio.

TABLE OF CONTENTS

List of Figures vi
List of Tables ix
List of Acronyms x
Resumen xi
Abstract xii
1. Introduction 1
1.1 Energy in Chile 1
1.2 Electricity in Chile 3
1.3 Renewable energies in Chile 6
1.4 Climate change 8
1.5 Solar energy 12
1.6 Chapter Summary 30
2. Thesis Objectives 31
2.1 Current Knowledge in the Field 31
2.2 Objectives 32
2.3 Hypothesis 33
2.4 Methodology 33
3. Thermodynamic Model 34
3.1 Introduction 34
3.2 Common information 37
3.3 Models 50
3.4 Chapter Summary 56
4. Simulation Results 58
4.1 Introduction 58
4.2 Results for direct energy production in Antofagasta 59
4.3 Results for indirect storage with fossil back-up in Antofagasta 63
4.4 Results for indirect storage without fossil back-up in Antofagasta 67
4.5 Results for direct storage with fossil back-up in Antofagasta 68
4.6 Results for direct storage without fossil back-up in Antofagasta 72

4.7 Models in Antofagasta comparison 73
4.8 Monthly energy comparison for the three cities and five models 80
4.9 Validation of the thermodynamic model 86
4.10 Chapter Summary 88
5. Economic Model 90
5.1 Introduction 90
5.2 Economic concepts 91
5.3 Inputs and Assumptions 93
5.4 Chapter summary 102
6. Economic Results 103
6.1 Introduction 103
6.2 Results for plants without back-up 103
6.3 Results for plants with back-up 106
6.4 Chapter summary 108
7. Tool Developed 112
7.1 Introduction 112
7.2 Results 113
7.3 Weather variability 120
7.4 Discount rate sensitization 123
7.5 Chapter Summary 125
8. Conclusions 126
References 128

LIST OF FIGURES

Figure 1-1: Production and consumption of crude oil in Chile (CNE, 2008) 1
Figure 1-4: Unavailability of natural gas from Argentina (CNE, 2008) 2
Figure 1-5: Imported natural gas for the regions II through VIII in the last years (CNE, 2008) 3
Figure 1-7: Electric systems in Chile (CNE, 2008) 4
Figure 1-8: Installed capacity distribution of SING and SIC (CNE, 2008) 4
Figure 1-9: Electricity generated in SING and SIC (CNE, 2008) 5
Figure 1-10: Marginal costSING and SIC in US/MWh (CNE, 2008) 5
Figure 1-11: Projected CO2 emissions by system (CNE, 2008) 6
Figure 1-12: Consequences of climate change (IPCC, 2007) 8
Figure 1-13: GHG concentration (IPCC, 2007) 9
Figure 1-14: GHG emissions by activity (IEA, 2006) 9
Figure 1-15: Temperature change (IPCC, 2007) (ATSE, 2009) 10
Figure 1-16: CO_2 emissions from various generating technologies (ATSE, 2009) 11
Figure 1-18: Earth received radiation (Boyle, 2004) 13
Figure 1-19: Renewable energy resources (Völker, Heinsath, Morin, & Varas, 2009) ... 14
Figure 1-20: DNI resource distribution (Völker, Heinsath, Morin, & Varas, 2009) 14
Figure 1-21: DNI Global Horizontal Solar Radiation (SWERA) 15
Figure 1-23: Photovoltaic cell 17
Figure 1-24: PS10 Central receiver 19
Figure 1-25: Manzanares chimney prototype 20
Figure 1-26: Dish Stirling system (Plataforma Solar de Almeria) 21
Figure 1-27: Receiver with secondary reflector and Fresnel mirror (Ausra) 22
Figure 1-28: Parabolic power plant (Solarmillennium) 24
Figure 1-29: Parabolic trough (Völker, Heinsath, Morin, & Varas, 2009) 24
Figure 1-31: Schott PTR 70 Receiver (Schott AG) 26
Figure 1-32: Collector structure (Pilkington Solar International, 1996) 26
Figure 1-33: Tracking system and Articulated joint 27
Figure 1-34: Mirror cleaning 27
Figure 1-35: Thermal storage (Völker, Heinsath, Morin, & Varas, 2009) 28
Figure 1-36: Land use for a 100MW plant (Völker, Heinsath, Morin, & Varas, 2009) .. 29
Figure 3-1: Direct power production (Kearney, et al., 2003) 34
Figure 3-2: Indirect storage with back-up (Kearney, et al., 2003) 35
Figure 3-3 : Indirect storage without back-up (Kearney, et al., 2003) 36
Figure 3-4: Direct storage with back-up (Kearney, et al., 2003) 36
Figure 3-5: Direct storage with back-up (Kearney, et al., 2003) 37
Figure 3-6: Radiation data for Calama for one day 38
Figure 3-7: Radiation data for Calama in January 39
Figure 3-8: Average monthly radiation data for Calama for a year 39
Figure 3-9: Water diagram from EES software 40
Figure 3-10: Therminol VP1 heat capacity vs. Temperature 41

Figure 3-11: Heat losses vs. temperature difference (Therminol) 44
Figure 3-12: Rankine cycle T-s for water 46
Figure 3-13: Cooling curve of cold storage tank during standby over a period of 6 weeks (Herrmann, Kelly, & Price, 2004).....47
Figure 3-14: Information flow for direct power production 50
Figure 3-15: Information flow for indirect TES with back-up 51
Figure 3-16: Information flow for indirect TES without back-up 53
Figure 3-17: Information flow for direct TES with back-up.....54
Figure 3-18: Information flow for direct TES without back-up 55
Figure 4-1: HTF flow in direct production 59
Figure 4-2: Steam flow in direct production.....60
Figure 4-3: Electric energy for direct production 60
Figure 4-4: Absorbed energy in solar field for direct production 61
Figure 4-5: Lost energy in solar field for direct production.....61
Figure 4-6: Monthly delivered electric energy.....62
Figure 4-7: Gain and losses in solar field per month for direct production 62
Figure 4-8: Hourly average electric energy in direct production model per month.....63
Figure 4-9: VP1 flow in solar field for indirect TES 63
Figure 4-10: Hitec XL flow in the VP1-Hitec heat exchanger 64
Figure 4-11: Hot tank level for indirect storage.....64
Figure 4-12: Cold tank level for indirect storage.....65
Figure 4-13: Solar fraction for indirect TES.....65
Figure 4-14: Monthly thermal energy to power block by source for indirect storage 66
Figure 4-15: Delivered electric energy in indirect TES model.....67
Figure 4-16: Electric energy by month for indirect TES without back-up 68
Figure 4-17: Average electric energy by month for indirect TES without back-up 68
Figure 4-18: Hitec flow in solar field for direct storage 69
Figure 4-20: Cold tank level for direct TES.....70
Figure 4-21: Solar fraction for direct TES 71
Figure 4-22: Thermal energy to power block by month per source for direct TES.....71
Figure 4-23: Electric energy delivered monthly for direct TES 72
Figure 4-24 Electric energy by month for direct TES without back-up 72
Figure 4-25: Hourly average electric power for direct TES without back-up 73
Figure 4-26: Solar electricity during the summer in Antofagasta.....74
Figure 4-28: Solar electric energy per model in winter in Antofagasta.....75
Figure 4-29: Solar electricity for direct production on a mostly cloudy day in Antofagasta 75
Figure 4-30: Solar electricity for indirect TES on a mostly cloudy day in Antofagasta..76
Figure 4-31: Solar electricity for direct TES on a mostly cloudy day in Antofagasta.....76
Figure 4-33: Solar electricity for indirect TES on a partly cloudy day in Antofagasta ...77
Figure 4-34: Solar electricity for direct TES on a partly cloudy day in Antofagasta 77

Figure 4-35: Solar electricity for direct production on a mostly sunny day in Antofagasta 78
Figure 4-37: Solar electricity for direct TES on a mostly sunny day in Antofagasta 79
Figure 4-39: Tank levels per model during autumn in Antofagasta 80
Figure 4-41: Average energy per site and model 81
Figure 4-42: Yearly electric generation for all models and sites 82
Figure 4-43: Solar fraction and tank levels for Direct TES Calama in summer 83
Figure 4-44: Solar fraction and tank levels for direct TES Calama in autumn.....83
Figure 4-45: Solar fraction and tank levels for direct TES Calama in winter.....84
Figure 4-46: Energy production in direct production model in Antofagasta 84
Figure 4-47: Energy in direct production model for Calama 85
Figure 4-48: Thermal energy to power block per source in Calama for Direct TES with BU 85
Figure 4-50: Gross electric production vs. radiation for the different plants and models88
Figure 5-1: Cost model diagram 91
Figure 6-1: LEC for different locations and models 109
Figure 6-3: Annual energy by model 111
Figure 6-4: LEC by model and site 111
Figure 7-1: LEC and energy for Calama or locations with 3200kWh/m2 year 114
Figure 7-2:LEC and energy for Copiapo or locations with 2500kWh/m2 year.....114
Figure 7-3: LEC and energy for Antofagasta or locations with 1800kWh/m2 year 115
Figure 7-4: LEC and energy for Santiago or locations with 1500kWh/m2 year 116
Figure 7-5: LEC for different sites for direct TES technology 117
Figure 7-6: LEC for different sites for direct TES with back-up technology 117
Figure 7-7: LEC for different sites for indirect TES technology 118
Figure 7-8: LEC for different sites for indirect TES with back-up technology 118
Figure 7-9: LEC for different sites for Direct Production technology.....119
Figure 7-10: Best LEC by model 119
Figure 7-11: LEC and energy for +-10% radiation in Copiapo for direct TES no BU..120
Figure 7-12: LEC difference for +-10% radiation in Copiapo for direct TES no BU ...121
Figure 7-13: LEC and energy for +-10% radiation in Copiapo for direct TES with BU 121
Figure 7-14: LEC and energy for +-10% radiation in Copiapo for indirect TES no BU 122
Figure 7-15: LEC and energy for +-10% radiation in Copiapo for indirect TES with BU 122
Figure 7-16: LEC and energy for +-10% radiation in Copiapo for direct production ...123
Figure 7-17: LEC difference for +-10% radiation in Copiapo for direct production 123
Figure 7-18: LEC vs. Discount Rate 124
Figure 7-19: LEC vs Discount Rate 124
Figure 7-20: Best LEC for Calama by type of technology 125

LIST OF TABLES

Table 1-1: CO_2 Emissions reductions from CSP plants (The Western Governors' Association's Clean and Diversified Energy, 2006) 12
Table 1-2: Photovoltaic LCOE (Energy, 2006) 17
Table 1-3: Technologies concentrating ration, stage, efficiency and cost (Völker, Heinsath, Morin, & Varas, 2009) 28
Table 3-1: Weather data table 38
Table 3-2: Differences between models 57
Table 4-1: Summary of results 73
Table 4-2: Electric production and radiation 88
Table 5-1: Storage cost (Kearney D. , et al., 2003) 95
Table 5-2: Sale cost (CDEC-SIC) 99
Table 5-3: Economic output example 101
Table 5-4: Cost drivers summary example 102
Table 6-1: Solar Field Amplifiers and Areas 104
Table 6-2: Economic results for Antofagasta, no back-up 104
Table 6-3: Economic results for Calama, no back-up 105
Table 6-4: Economic results for Santiago, no back-up 105
Table 6-5: Economic results for Antofagasta 106
Table 6-6: Economic results for Calama 106
Table 6-7: Economic results for Santiago 107
Table 6-8: Cost drivers for no back-up models 107
Table 6-9: Cost drivers for back-up models 108

LIST OF ACRONYMS

BU: Back-up

CNE: *Comisión Nacional de Energía*-National Energy Commission

CSP: Concentrating Solar Power

CT: Cold Tank

DMC: *Dirección Meteorológica de Chile*- Chilean Bureau of Meteorology

GHG: Green House Gases

HCE: Heat Collecting Element

HT: Hot Tank

HTF: Heat Transfer Fluid

HX: Heat Exchanger

IPCC: Intergovernmental Panel on Climate Change

IRR: Internal Return Rate

LEC: Levelized Electric Cost

NPV: Net Present Value

PV: Present Value

SEGS: Solar Electric Generating Systems

SF: Solar Field

SIC: *Sistema Interconectado Central*- Main Interconnected System

SING: *Sistema Interconectado Norte Grande*- Interconnected System for the *Norte Grande* Region of Chile

TES: Thermal Energy Storage

US$: United States Dollar

RESUMEN

Dada la demanda actual de energía, su proyección futura de crecimiento y que Chile es un país importador de combustibles fósiles, es interesante evaluar la posibilidad de instalar plantas de potencia que usen energías primarias renovables y de disponibilidad local. Una de las tecnologías para producción de energía prometedoras es la energía solar de potencia, especialmente la de concentradores cilindro-parabólicos, que tiene mayor experiencia comercial que otras tecnologías. Esto se puede ver en las plantas SEGS en Estados Unidos y otras en el mundo. Se suma además que Chile es reconocido como un país con uno de los mejores niveles de radiación en el mundo.

El alcance de la tesis es evaluar termodinámicamente diferentes modelos de plantas solares, con ciertas características en común, para poder realizar comparaciones. También realizar una comparación económica para entender como las distintas configuraciones se relacionan con los costos de las plantas. De los modelos térmicos y económicos estudiados, se creó una herramienta de selección. Esta herramienta es útil para seleccionar el tipo de planta y el área optima de la misma, basado en la irradiación especifica anual del lugar donde está planeada la planta. La herramienta está basada en el costo nivelado de la energía, precio que revela el valor presente del proyecto. Las principales conclusiones basadas en el LEC son que existe un modelo óptimo, para distintos niveles de radiación. Este modelo óptimo tiene a su vez un área de apertura de colectores, que es inversamente proporcional a la radiación del lugar. La disponibilidad de sistema de respaldo fósil puede bajar el LEC en lugares con niveles de radiación menores, pero puede subir el costo de la electricidad para lugares con mayor radiación.

La variabilidad en la radiación también fue estudiada y se concluye que la dispersión del LEC es menor si se sobredimensiona el área de colectores, por lo que para el caso de tener incertidumbre se recomienda aumentar el área de colectores.

ABSTRACT

Due to the current and growing energy demand in an importing fossil fuel country such as Chile, it's interesting to evaluate the possibility of installing power plants that use renewable and locally available primary energy as resource for producing electricity. One of the promising technologies is solar power, especially parabolic trough concentrators. Currently, there are more commercial facilities producing electricity using that technology than any other concentrating technology. This can be seen in the use of SEGS in the United States and other countries around the world. Chile is recognized having one of the best radiation levels in the world, which makes this option particularly interesting for our nation.

The purpose of the thesis is to evaluate the various modes of thermal plants. An economical evaluation of those plants was performed in order to elucidate how the different technologies are connected to their costs. A selection tool was developed based on the economic and thermal model studied in order to assess the best technology and solar field size. This tool can be used to choose parabolic trough concentrating plant technologies and solar field areas based on the specific annual irradiance of the site selected for the plant. The tool is based on the levelized electric cost, which is the sale price of electricity for net present value of the project equal to zero. The study showed that the optimal model depends on the radiation level. The optimal solar field size of this model was found to be inversely proportional to local irradiation.

One of the ways in which the models vary is the use of a fossil back-up system, which can lower the LEC in low solar energy sites. However, higher radiation can increase the LEC.

The variability in the radiation also was studied, and it was found that the LEC spread diminishes if the solar field is oversized. As a result, if there is a lack of certainty, a larger than optimal field area is recommended.

1. INTRODUCTION

1.1 Energy in Chile

Primary Energy in Chile

Chile is not a fossil energy producer; the country uses imported fuels to satisfy its internal consumption. See Figure 1-1, which is based on data from the *Comision Nacional de Energia* (National Energy Commission, CNE).

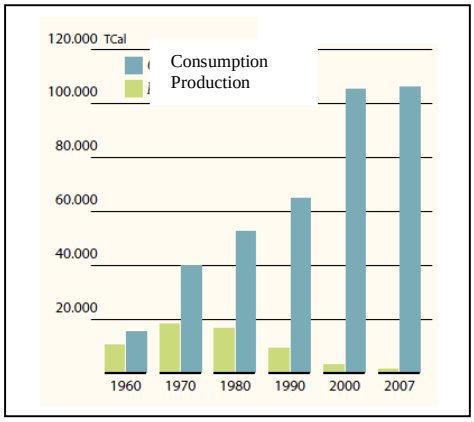

Figure 1-1: Production and consumption of crude oil in Chile (CNE, 2008)

Figure 1-2 clearly shows that the country's coal production is insufficient to satisfy internal demand. As a result, almost all of the coal is imported.

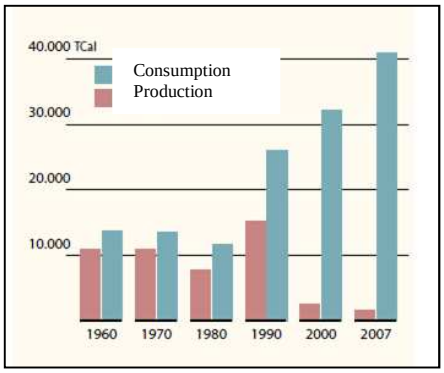

Figure 1-2: Production and consumption of coal in Chile (CNE, 2008)

Figure 1-3 shows that internal production is not sufficient to meet gas consumption.

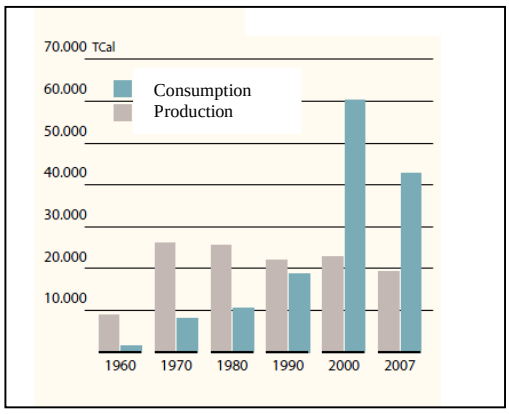

Figure 1-3: Production and consumption of natural gas in Chile (CNE, 2008)

There was a significant increase in gas consumption in 2000 due to the gas connection to Argentina which made it possible to generate electricity less expensively using gas turbines. However, the gas flow from that country has since been restricted, as seen in the figure below.

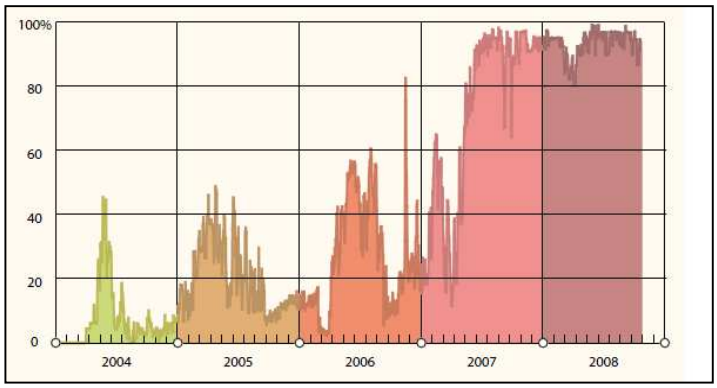

Figure 1-4: Unavailability of natural gas from Argentina (CNE, 2008)

GNL Quinteros, a regasification port for liquefied natural gas, was opened in 2009 in order to provide gas to central Chile. The plant was designed to provide 10 million cubic meters of natural gas per day. That quantity would be sufficient to meet gas needs for a

year like 2002, when there were no shortages, but probably would not satisfy current needs.

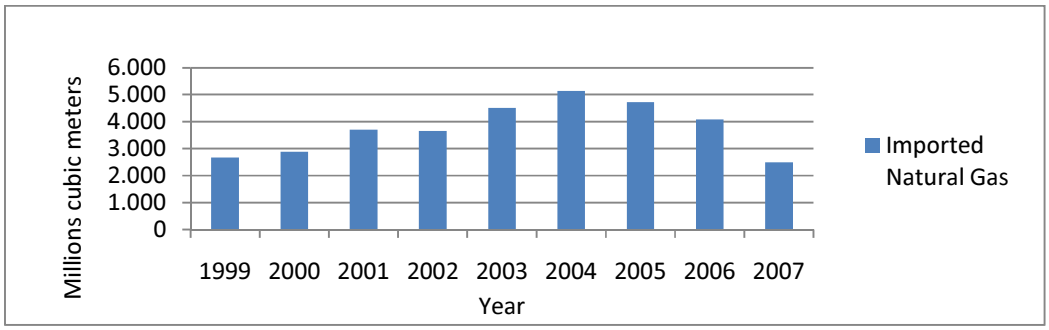

Figure 1-5: Imported natural gas for the regions II through VIII in the last years (CNE, 2008)

Figure 1-6 shows that Chile is highly dependent on fossil fuels, with an important contribution of electricity and biomass in final energy use.

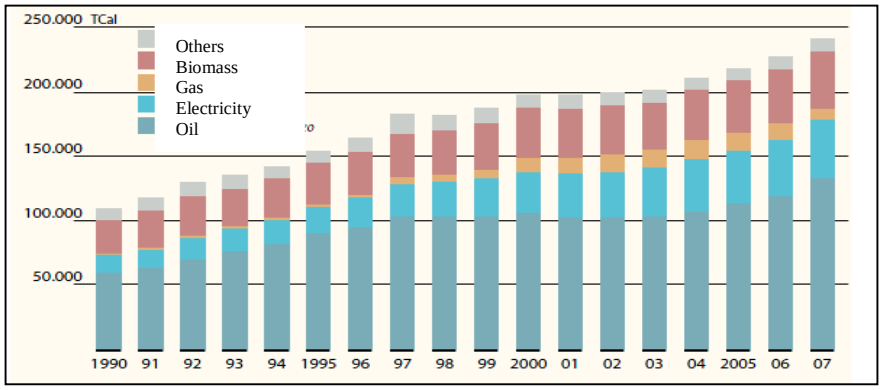

Figure 1-6: Final primary energy consumption in Chile (CNE, 2008)

1.2 Electricity in Chile

The electric market in Chile is based on four transmission systems. The northern system produces, transports and delivers energy to Regions I, II and XV. This system, which is called SING or *Sistema Interconectado Norte Grande*, mainly provides power for mining activities and, to a lesser extent, to the cities in that area, which is less populated

than other parts of Chile. The installed capacity of SING in 2008 was 3,600 MW, 99.64 % of which came from thermal systems.

The central systems is the SIC, or *Sistema Interconectado Central*, which had an installed capacity of 9,650 MW in 2008. This network covers Regions III through X, Region XIV and the Metropolitan Region, which is home to Santiago, a city of some six million people. Hydroelectricity provides 56% of the system's capacity, and the remaining 44% is mainly produced by thermal power plants.

The southern systems are the *Sistema de Aysén* and *Sistema de Magallanes*, which produce electricity for Regions XI and XII, respectively. That two systems account for almost 130 MW of installed capacity.

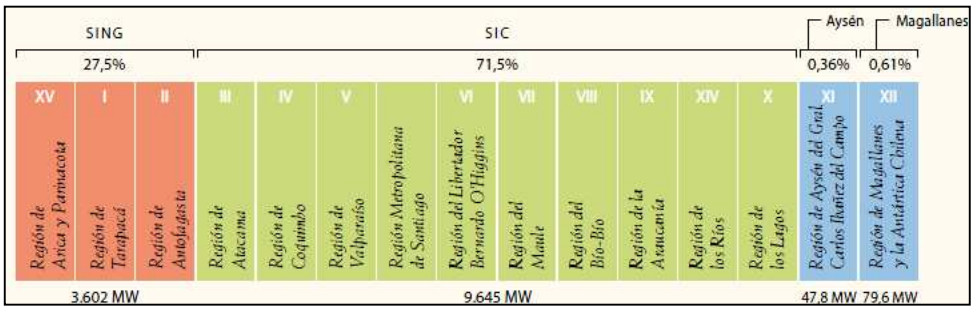

Figure 1-7: Electric systems in Chile (CNE, 2008)

SING and SIC are the most important power systems in Chile. The primary energy used in the two systems is shown in Figure1-8. Hydroelectricity is the leading source, followed closely by natural gas. The use of coal is increasing.

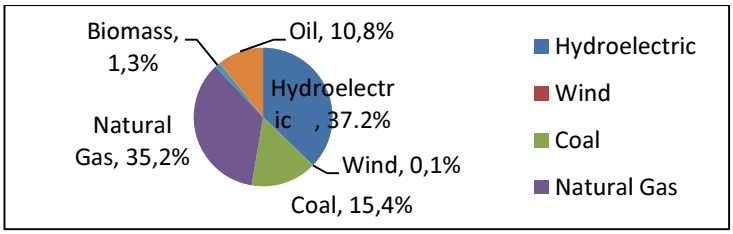

Figure 1-8: Installed capacity distribution of SING and SIC (CNE, 2008)

Figure 1-9 presents yearly electric energy use by primary energy source produced in both main systems through October 2008. Hydro plays a leading role in the production, and oil and coal are very important, as well. Wind power has been marginal, as only a few wind farms contribute power to the systems.

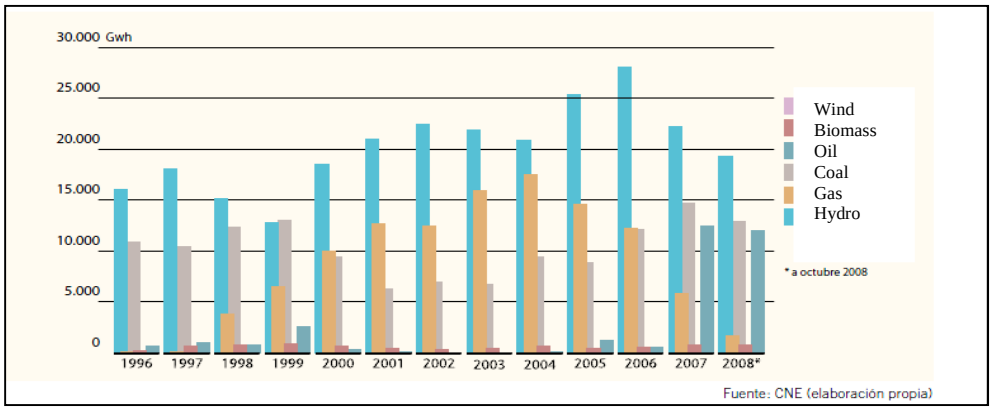

Figure 1-9: Electricity generated in SING and SIC (CNE, 2008)

The marginal cost is the price that has to be paid to produce the final unit of energy. Figure 1-10 shows observed high marginal costs of electricity that are correlated to the prices of fossil fuels over the past year. The average monthly marginal cost is shown for the Crucero substation for SING and Quillota for SIC.

Figure 1-10: Marginal costs in SING and SIC in UDS/MWh (CNE, 2008)

1.3 Renewable energies in Chile

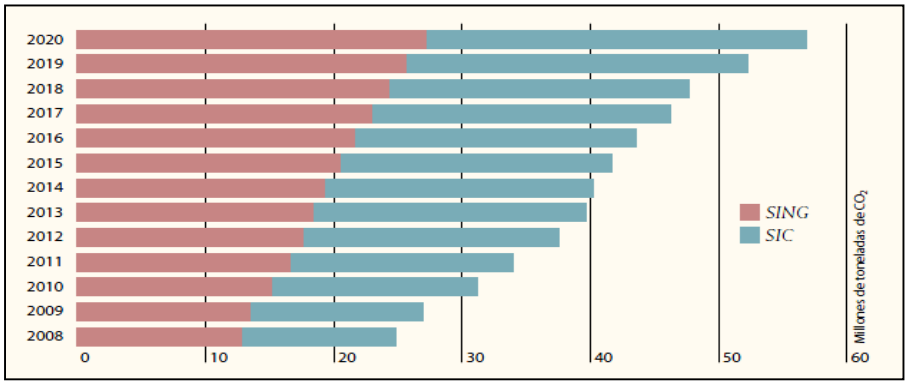

Figure 1-11: Projected CO2 emissions by system (CNE, 2008)

Projections suggest that the energy market and thus carbon dioxide emissions will increase. This is due to the limited amount of hydro resources available, the low cost of using thermal power plants and barriers to entry of renewables such as limited data on wind power, limited data on radiation produced by photovoltaic electricity and scant available information on thermal use of solar power or geothermal studies. . In addition to this lack of information, the development of this renewable energy was not regulated under Chilean law until 2004, when renewables were mentioned explicitly in the country's legislation as Non-Conventional Renewable Energies (E*nergias Renovables No Convencionales* ERNC). The term "non-conventional" was added to differentiate large to small scale hydro projects at 20GW of installed capacity.

According to Law No. 20,257, ERNC are:

- Forms of energy that use biomass as primary energy either directly or as a derivate bio fuel.
- Those that use hydraulic power as a primary source and have a maximum output of 20GW.
- Those using geothermal energy as primary energy.

- Forms of energy that use solar power as primary energy.
- Those that use the energy of wind as primary energy.
- Those that use the energy of the seas as primary energy.
- Other determined by CNE.

Benefits for ERNC

- All of the electric energy generators, including ERNC, can sell their energy to major consumers such as mines or distributors.
- ERNC plants with less than 9MW of installed capacity have the right to connect to transmission lines.
- ERNC power plants can transmit their power free of charge if they have less than 9MW of installed capacity, or pay some of the transmission costs if the installed capacity is less than 20MW.

The country's energy law also was changed in order to increase the participation of ERNC in the generating matrix. The goal is for at least 5% of the power generated to come through ERNC in 2010 and for this number to increase to 10% by 2024. This law would force electricity companies with more than 200MW of installed capacity to produce 5% of their energy using renewable systems in 2010 and to increase the use of renewables in their production pool plants by 0.5% each year. Those that fail to meet these goals will be penalized 0.4 UTM/MWh, or approximately 30US/MWh. This modification is increasing the cost of energy because the generating companies are transferring the cost to the consumers, and there is no investment in renewable energy (Galetovic, 2007). According to Libertad y Desarrollo, 2008 , a conservative estimate for 2025 suggests that 17TWh could be generated with renewables in Chile in a profitable manner. The question that one must ask in regard to this is at what point renewable will become financially self-sufficient in the short term..

1.4 Climate change

Introduction

The fourth assessment report (AR4) from the Intergovernmental Panel on Climate Change (IPCC) has confirmed that the global warming process is continuing. This is reflected in global temperature increases, melting of snow and ice reservoirs, rises in average sea levels, and other developments (IPCC, 2007). As described in Figure 1-12, the global surface temperature has increased by approximately 1°C over the past 150 years and 0.7ºC in the past 50 years. Eleven of the past 12 years were the warmest since 1850. The data on sea levels shows that they are increasing, and satellite information has confirmed a decrease in snow and ice coverage.

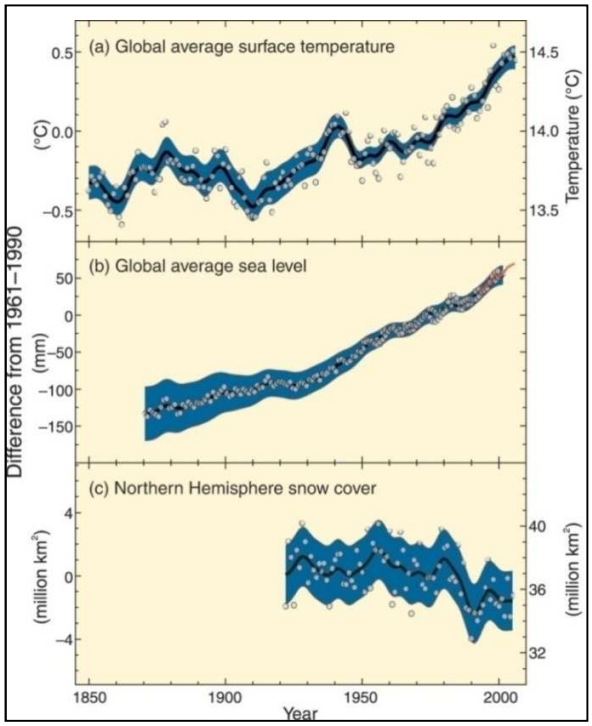

Figure 1-12: Consequences of climate change (IPCC, 2007)

It is clear that global warming is progressing and that it is directly correlated to greenhouse gas emissions (GHG). The atmospheric concentration of GHG such as CO_2,

methane and nitrous oxide produced as a result of anthropogenic activities increased by 70% between 1970 and 2004, with current values far exceeding pre-industrial levels. This is mainly due to the sustained use of fossil fuels and human activities are the principal cause of these emissions. Global warming's effects can include changes to and the destruction of ecosystems, increasing numbers of climate-related natural disasters, and potential water and food shortages.

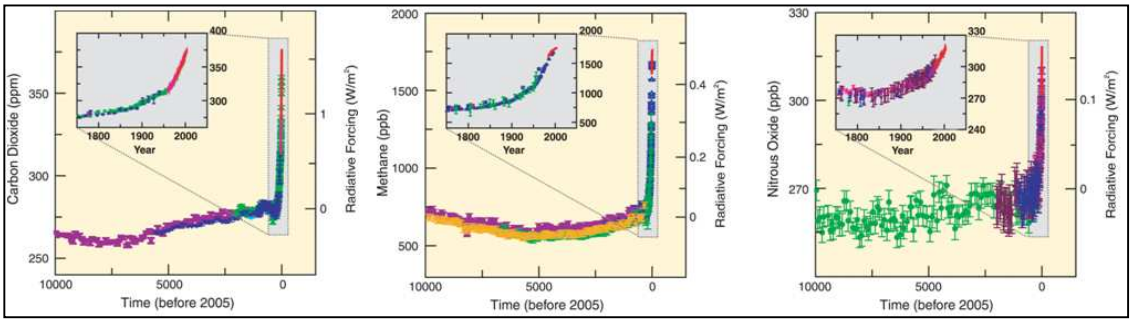

Figure 1-13: GHG concentration (IPCC, 2007)

One way to stop climate change is to adopt sustainable energy technologies. Energy production is the main contributor to CO_2 emissions and this should be the main focus of any efforts to ameliorate global warming.

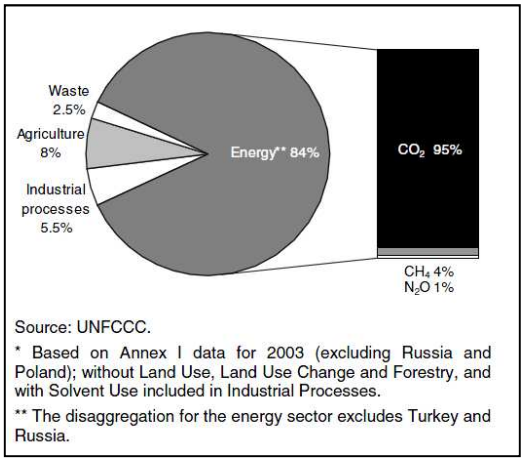

Figure 1-14: GHG emissions by activity (IEA, 2006)

Effects of climate change

One of the main problems of global warming is the rise of the sea levels that would force millions of inhabitants of coastal cities to move inland. Changes in temperatures also could affect life. Figure 1-15 shows the estimated temperature change in each continent.

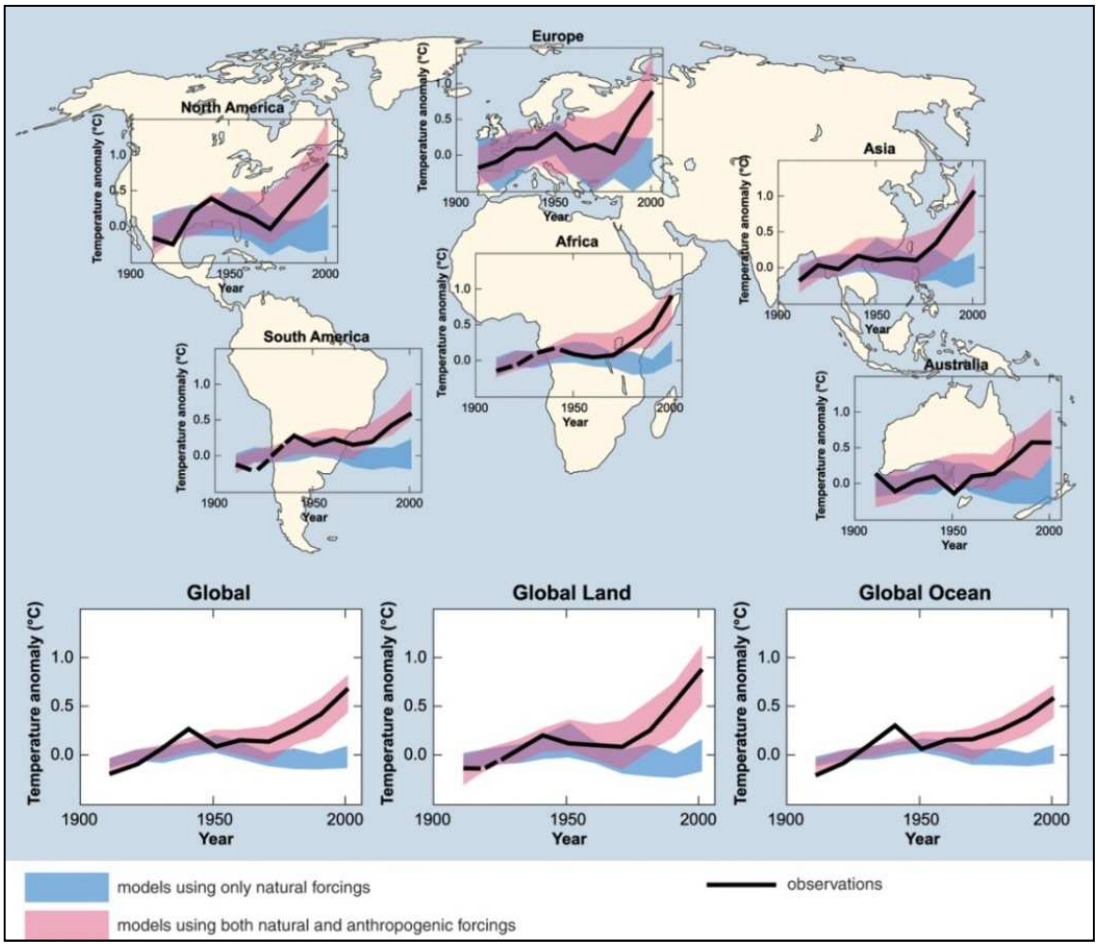

Figure 1-15: Temperature change (IPCC, 2007) (ATSE, 2009)

This global change is thought to be primarily caused by anthropogenic emissions. It is urgent that changes be made to halt this trend.

Power technologies and their emissions

Emissions from various power technologies are plotted in Figure 1-16. The left side compares different types of technologies and the right side compares technologies that emit lower amounts of carbon dioxide on a different scale. The black bar stands for emissions during operation and the grey bar refers to the construction, dismantling and other stages.

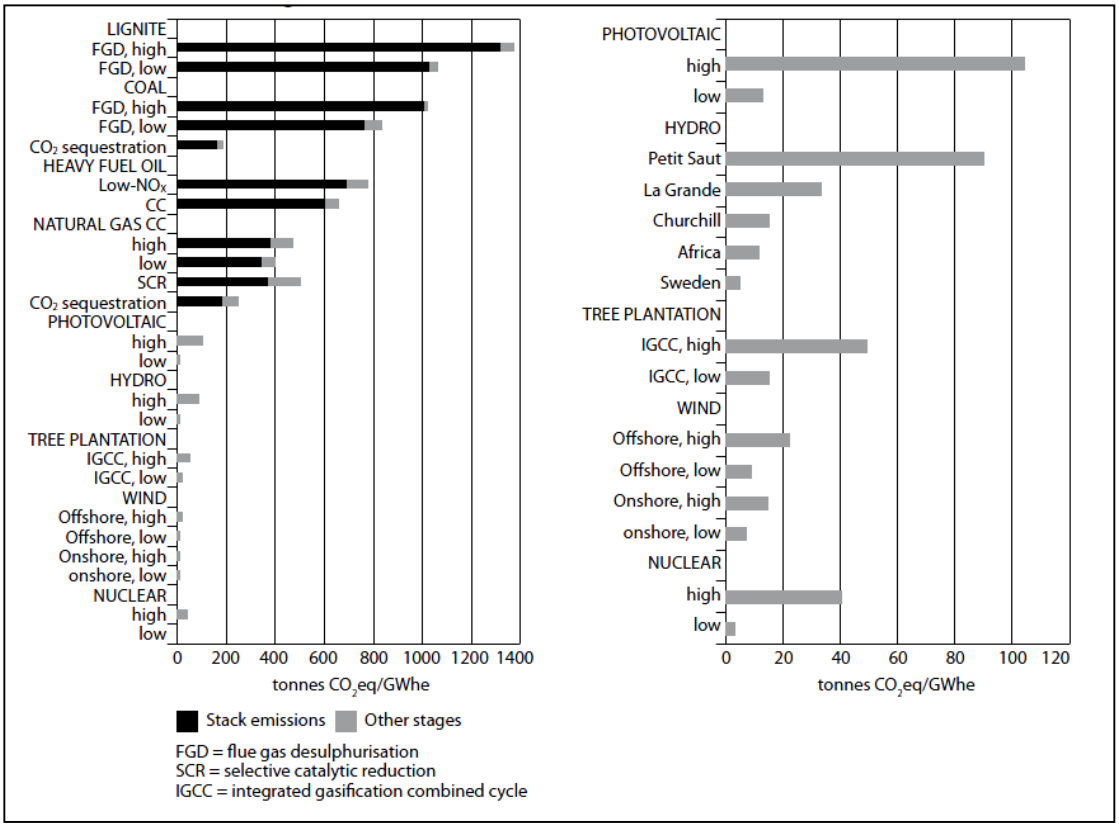

Figure 1-16: CO_2 emissions from various generating technologies (ATSE, 2009)

Figure 1-16 does not include concentrating solar plants. Data on that type of plant is presented in the table below.

Table 1-1: CO_2 Emissions reductions from CSP plants (The Western Governors' Association's Clean and Diversified Energy, 2006)

Emissions Reduction by CSP Plants				
Pollutant	Proxy Fossil Plant Emissions Rate (lb/MBtu)	CSP Plant Capacity		
		100 MW (tons/year)	2,100 MW (tons/year)	4,000 MW (tons/year)
NO_x	0.0060	**7.4**	**156**	**297**
CO	0.0036	**4.5**	**95**	**181**
VOC	0.0021	**2.6**	**54**	**103**
CO_2	154	**191,000**	**4,000,000**	**7,600,000**

As can be seen in the Table 1-1 and Figure 1-16, moving from a fossil plant to a solar one generates a significant reduction in ERNC emissions.

One of the conclusions reached at the International Solar Energy Society World Congress 2009 in Johannesburg, South Africa (ISES World Congress 2009, 2009)was that:

The global target of 100% renewable energies is both attainable and necessary by the middle of the current century. This is motivated on grounds of ecological, economic and social sustainability.

Experts in this field agree that renewable energies can supply the world's energy needs with economic factors in mind.

1.5 Solar energy

What is solar energy?

The earth has an elliptical orbit around the sun, which generates its energy by nuclear fusion of hydrogen nuclei into helium. The average distance between Earth and the sun is $1{,}495 \cdot 10^{11}$ m. An almost constant solar radiation per square meter can be observed in the outer part of the atmosphere and it is known as solar constant with a value of $1{,}367 W/m^2$.

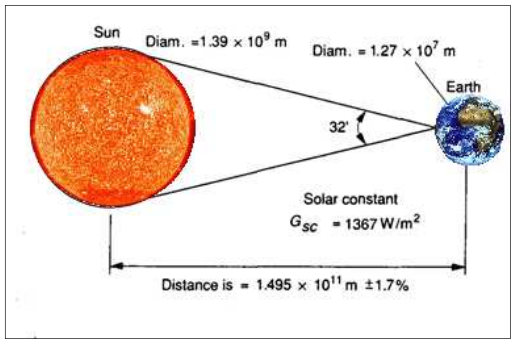

Figure 1-17: Solar distance and radiation (Duffie & Beckman, 1980)

Due to the characteristics of the sun, the radiated light has an energy distribution along the wavelength of the light. Most of the energy radiated is in the visible and the near infrared spectrum, as it can be seen in Figure 1-18. Only a small part of the energy from sunlight passes that through the atmosphere reaches the Earth due to scattering, energy absorption and reflection in the atmosphere. The amount depends on how much air mass the light has to travel through. This effect can be seen in Figure 1-18.

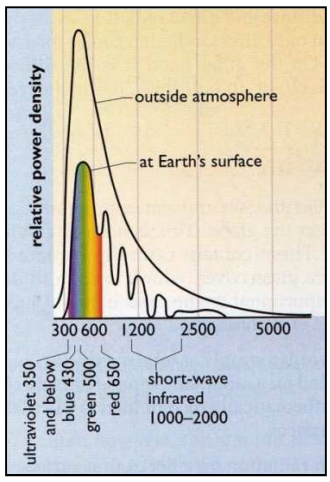

Figure 1-18: Earth received radiation (Boyle, 2004)

But is solar energy or even renewable energy resources as a whole enough to provide energy to the human race? Figure 1-19 presents data that suggests that the solar resource could meet the planet's demand for energy.

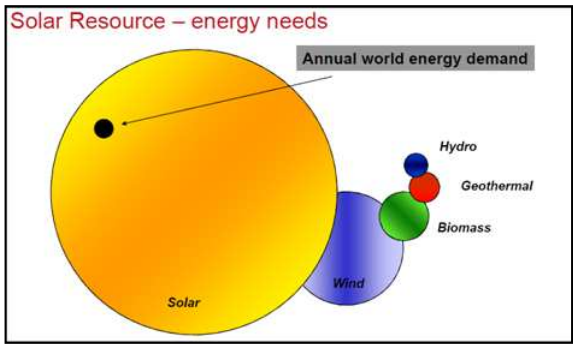

Figure 1-19: Renewable energy resources (Völker, Heinsath, Morin, & Varas, 2009)

Figure 1-20 shows the direct normal irradiation that is, the power that reaches a surface. In this case it refers to the number of light rays that reach a normal surface over the course of one hour. Light can be decomposed from global into direct and diffuse light. Direct rays are those that only move from the sun to the Earth. Diffuse rays have no direction. Northern Chile has a high potential for solar energy due to the fact that its radiation levels are higher than most other locations in the world.

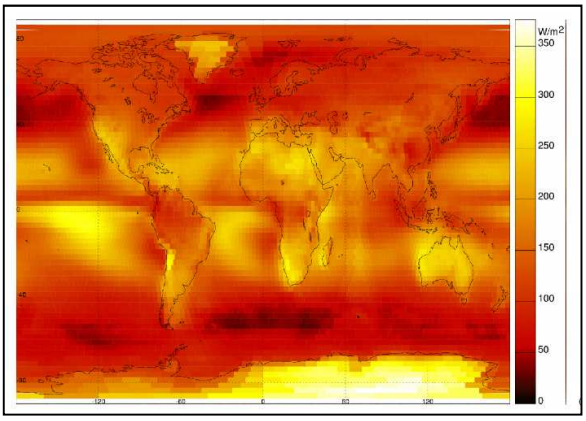

Figure 1-20: DNI resource distribution (Völker, Heinsath, Morin, & Varas, 2009)

Figure 1-21 shows the radiation on a horizontal surface for South America. It clearly indicates that the northern part of Chile presents the best conditions in the region.

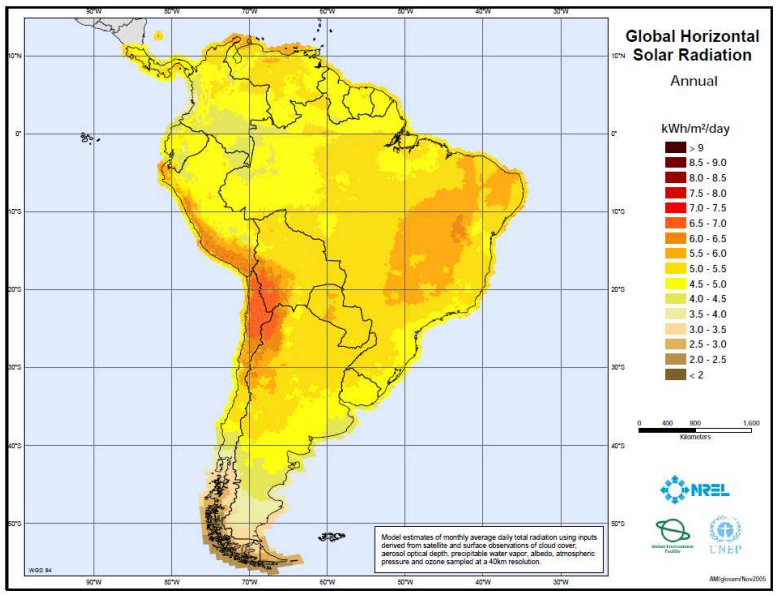

Figure 1-21: DNI Global Horizontal Solar Radiation (SWERA)

Figure 1-22 shows the average energy per square meter that is received daily. On the left side is a map developed by Ortega et al, 2008 with solar data from the Solarimetric Registry registered by Professor Sarmiento. On the right side, the same data is plotted using an estimation done with satellites based on a Brazilian model. It can be seen that the northern part of Chile has a good resource. The central part of Chile is a good location too for solar projects, comparing it with Spain or USA where several solar project are commercially working. But how can we harvest solar energy?

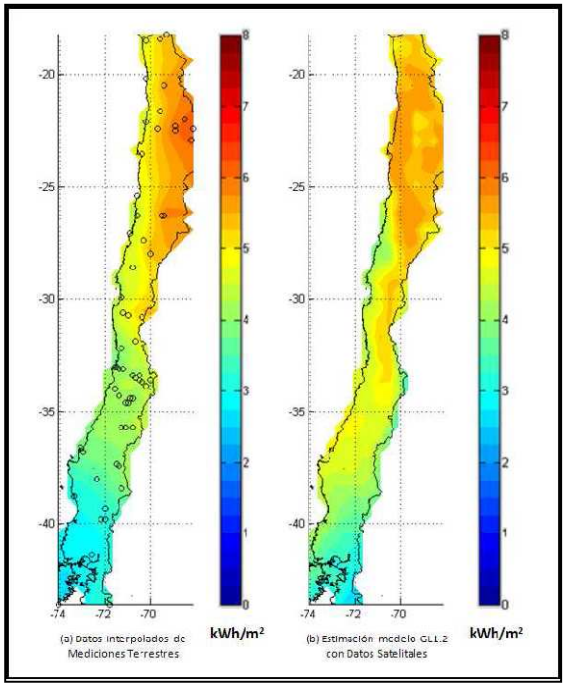

Figure 1-22: Solar resource in Chile, left map from Prof. Sarmiento registry and right side by Ortega et al (Ortega, Escobar, & Colle, 2008)

Solar Energy Technologies

Solar power plants in regions with high solar radiation levels are a promising option for electric energy supply that is compatible with the environment, produces no CO_2 emissions during operation and dependencies not dependent on the availability of fossil fuels.

There are several options for transforming solar radiation into electricity. There are various costs associated with these options, and each presents advantages and disadvantages.

Photovoltaic

Photovoltaic cells are devices that convert light into electric current using the photoelectric effect. Photovoltaic production has been doubling every 2 years, increasing by an average of 48 percent each year since 2002, which makes it the world's fastest-growing energy technology. At the end of 2008, global photovoltaic installations totaled 15,200 MW (PRLOG, 2009).

Figure 1-23: Photovoltaic cell

The table below shows the costs for 2006, 2011 and 2020:

Table 1-2: Photovoltaic LCOE (Energy, 2006)

	Current US Market Price Range	Target for PV LCOE in 2011 (cent/kWh)	Target for PV LCOE in 2020 (cent/kWh)
Residential	25-32	13-18	8-10
Commercial	18-22	9-10	6-8
Utility	15-22	10-15	5-7

Advantages of photovoltaic energy production:

- The electricity produced by solar cells is clean and silent (Nieuwlaar & Alsema, 1997).
- This technology is visually unobtrusive.
- It takes advantage of unused space on rooftops.
- A photovoltaic system can be sized to meet energy requirements.

Disadvantages of photovoltaic energy production:

- Some toxic chemicals, such as cadmium and arsenic, are used in the photovoltaic production process.
- This is a variable energy source, with intermittent energy production dependent on the sun.
- It is expensive to store the energy that is produced.

Solar power tower

The solar tower system or central receiver consists of a field of heliostat mirrors with a two axis tracking system that concentrates the light into a single receiver mounted at the top of a tower.

In the central receiver, steam can be produced directly or an oil or salt can be heated and transfer its heat to water in a heat exchanger for a rankine cycle. The latter options are more suitable for thermal storage than direct steam generation.

Figure 1-24: PS10 Central receiver

Another option is to compress air to heat it in the receiver and expand it in a Brayton cycle.

The U.S. National Renewable Energy Laboratory (NREL) has estimated that electricity could be produced from power towers for 5.5 cents per kWh by 2020 (Sargent & Lundy LLC Consulting Group, 2003).

Advantages:

- This approach is suitable for generating electricity in deserts and sun-rich wastelands.
- The energy produced is quite clean (Völker, Heinsath, Morin, & Varas, 2009).
- The energy can be stored in thermal storage systems and dispatched later.
- There is no need for flat expanses of land (Völker, Heinsath, Morin, & Varas, 2009).

Disadvantages:

- This type of system is not modular.
- It requires a large area (Völker, Heinsath, Morin, & Varas, 2009).
- There is almost no commercial experience with this type of energy production.

Solar chimney

Solar chimney systems consist of three parts:

- The *collector* is used to produce hot air using the green-house effect. The soil is heated so that it can act as thermal storage during night.
- *Wind turbines* are placed vertically in the chimney or horizontally in the collector.
- The most important part of the plant is the chimney, whichacts as a thermal engine. It can be said that:
    - The higher the chimney, the more energy produced. (Bernardes, Voß, & Weinrebe, 2003)
    - The efficiency of the chimney does not depend on how high the temperature rises but on the outside temperature.

Figure 1-25: Manzanares chimney prototype

Advantages:

- This technology is suitable for generating electricity in deserts and sun-rich wastelands.
- It provides variable power 24 hours a day using solar energy alone (Bernardes, Voß, & Weinrebe, 2003).

- No fuel is needed.
- It is reliable and a less prone to problems than other power plants.

Disadvantages:

- The structure itself is massive and requires a lot of engineering expertise and materials to construct.
- There is no commercial experience with this technology.

Dish Stirling

Dish Stirling is composed of a circular parabolic mirror with a point focus and a Stirling engine with a receiver in the focus point of the circular parabolic mirror. The concentrator has a concentration ratio of 300 to 4,000. The mirror size is related to the local radiation and the engine output. The dish-engine ensemble is mounted on a two axis tracking system. The systems may have fired back-up to replace the solar resource.

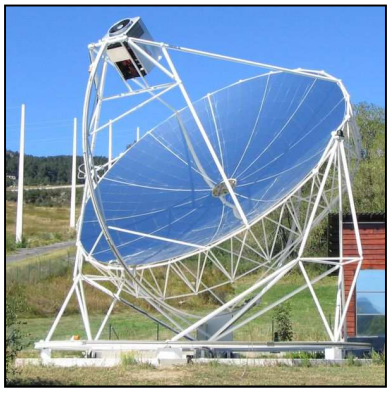

Figure 1-26: Dish Stirling system (Plataforma Solar de Almeria)

This system is generally 10 to 50 kW per unit, which means that it is very modular and can be used for distributed generation in a small number of concentrators or a large solar power plant.

The advantages of this technology include:

- High versatility due to modularity
- High efficiency of the stirling engine (>=30%) (Sandia National Laboratories, 2004)
- It can be hybridized with fuel back-up.

The disadvantages include:

- There are currently no commercial plants using it.
- It is difficult to store energy.

Linear Fresnel

Linear Fresnel Reflectors focus solar energy using a series of essentially flat mirrors on a stationary linear receiver (Ford, 2008). These mirrors are mounted on a single axis tracking system to concentrate light on the receiver.

Figure 1-27: Receiver with secondary reflector and Fresnel mirror (Ausra)

The receiver can have a secondary reflector to decrease losses and augment solar concentration.

Advantages of this technology:

- Researchers claim that it is less expensive than a parabolic trough power plant (Völker, Heinsath, Morin, & Varas, 2009 and Ford, 2008).
- It can include storage (Völker, Heinsath, Morin, & Varas, 2009).
- It is suitable for direct steam generation (Völker, Heinsath, Morin, & Varas, 2009).
- The receiver is stationary (Völker, Heinsath, Morin, & Varas, 2009).

Disadvantages of this technology:

- It is only being used in three commercial plants (5MW at Kimberlina CA USA, 1.4MW at Murcia, Spain and 1MW at Linddell Australia) (Völker, Heinsath, Morin, & Varas, 2009) and Ford, 2008).
- It suffers more optical losses than a parabolic trough power plant (Völker, Heinsath, Morin, & Varas, 2009).

Parabolic trough

A parabolic CSP plant has three main parts. The first is the solar field composed by the collectors, the second (which is not necessary but very useful and economically profitable) is the thermal storage and the third is the power block is composed of a generator and steam turbine assembly, pumping and cooling systems and a solar boiler. The solar boiler may be assisted by a fuel boiler during low radiation periods or for night power production.

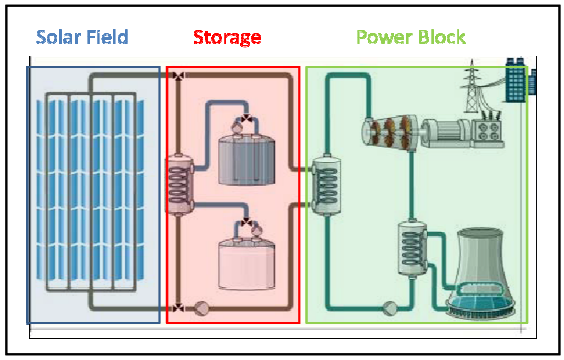

Figure 1-28: Parabolic power plant (Solarmillennium)

This technology is based on a parabolic shaped mirror that concentrates the energy in a line. Each mirror has a glass covered receiver in which the heat transfer fluid flows.

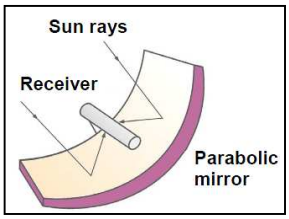

Figure 1-29: Parabolic trough (Völker, Heinsath, Morin, & Varas, 2009)

The current state-of-the-art of HTF is the use of synthetic oil in the receiver. This oil has a higher heat capacity than water, and can reach temperatures up to 400ºC. This fluid allows for thermal storage by exchanging heat in an oil-to-salt heat exchanger. The salt is used to produce the steam required for the turbine.

Another promising option is the use of the storage salt directly in the solar field, where part of it can be directed to storage and the remainder to the solar boiler. These salts used are molten due to the high temperature. However, they also have a relatively high freezing temperature. The most commonly used salt is a mixture of sodium and potassium nitrate also known as Solar Salt, which has a freezing point of around 220ºC. The newest and most promising salt is a ternary salt called Hitec XL, which has a lower

liquid temperature close to 120ºC (Gil, Medrano, Martorell, Dolado, Zalba, & Lázaro, 2009). The best option for storage is Hitec XL.

Another option is to use water for direct steam generation in the collector (Eck, Zarza, Eickhoff, Rheinländer, & Valenzuela, 2003). This option has some disadvantages, such as tube bending (Almanza, Lentz, & Gustavo, 1997), defocusing and glass breakage due to thermal deformation. Furthermore, the heat generated this way is more difficult to store because of the high pressure and temperature of the fluid as compared to other optionssuch as molten salt. One advantage of this technology is that it does not use heat exchangers, which increases its overall efficiency.

Regardless of the type of fluid used, most collectors are placed in a north-south orientation and track the solar altitude of the sun (Patnode, 2006 and Price, et al., 2002). Figure 1-30 shows the movement of the collectors .

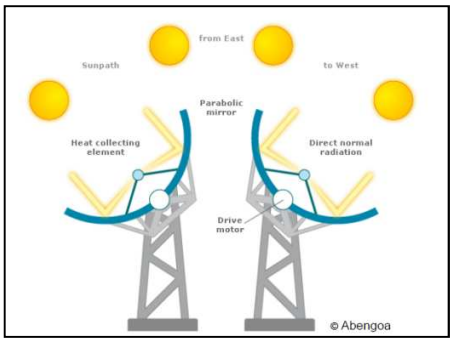

Figure 1-30: Solar movement and tracking scheme (Abengoa Solar)

The receiver is located in the focal point of the mirror and has two main functions: heating the fluid and avoiding heat losses. The first is achieved by using a selective coating to absorb most of the energy that comes from the sun. The second is accomplished with the aide of the glass cover and vacuum inside it. The glass has high transmittance and keeps air away from the inner tube in order to avoid conduction and convection losses from the tube. As a result, the only heat losses are due to radiation.

Figure 1-31 presents a sample receiver with a glass envelope and inner tube with selective coating.

Figure 1-31: Schott PTR 70 Receiver (Schott AG)

A specially developed structure must be designed to mount the mirrors. It must be capable of withstanding wind and other weather conditions. It also has to be stiff enough for the mirror not to bend and lose focus.. An example of this structure is shown in Figure 1-32.

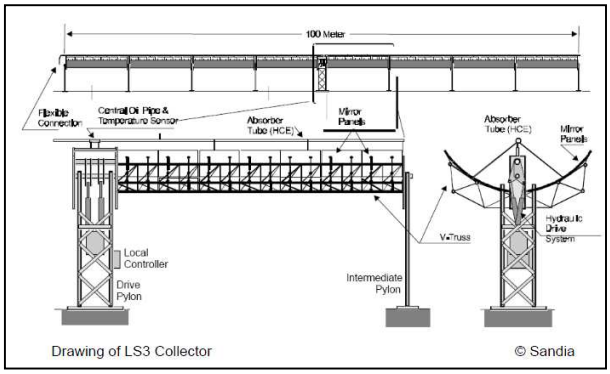

Figure 1-32: Collector structure (Pilkington Solar International, 1996)

Currently, five such structures are commercially available. They present both similarities and differences. The aperture width ranges from 4.4m to 5.77m. Module length is almost standard at around 12m and assembly length varies from 100m to 150m. The focal lengths of almost all of the models are 1.7m and optical efficiency is approximately 80%

for all of the models. The concentration factor fluctuates between 63 and 82 (Kearney D. W., 2007).

A tracking system moves the parabola, structure and receiver in order to ensure that the parabola continues to focus the light rays. One of the weak points of this system is the articulated joint of the receiver with the headers and between collectors. These pieces have to withstand high temperatures, pressure and movement without leaking.

Figure 1-33: Tracking system and Articulated joint

A common procedure in solar power plants is cleaning the mirrors and receivers in order to maximize the absorption in the receiver and reflection in the mirror. This is done with pressurized water or compressed air.

Figure 1-34: Mirror cleaning

Thermal storage is useful but not avaible in all solar power plants. Only one of the SEGS and Andasol I plant has thermal storage. This system consists of two tanks, one for cold molten salt and one for hot salt.

Figure 1-35: Thermal storage (Völker, Heinsath, Morin, & Varas, 2009)

Concentrating Solar Technologies Comparison

In conclusion, the parabolic trough is the most developed CSP technology, but it is followed closely by Fresnel and Central Receiver. The projected cost of electricity for the three systems for 2020 is the same.

Table 1-3: Technologies concentrating ration, stage, efficiency and cost (Völker, Heinsath, Morin, & Varas, 2009)

© Sandia	© Novatec	© DLR	© FVEE
C ~ 70-90 commercial η_{ann} ~ 12%-14% LEC_{2020}~ 5ct/kWh	C ~ 60 – 120 demonstration η_{ann} ~ 10%-12% LEC_{2020} ~ 5ct/kWh	C ~ 300 – 4000 commercial demo η_{ann} ~ 14%-18% LEC_{2020} ~ ?	C ~ 500 – 1000 commercial demo η_{ann} ~ 10%-15% LEC_{2020} ~ 5ct/kWh

The Stirling dish option is under development and there is no projection for this technology, but it has the advantage of easy hybridization, modularity and high efficiency of the Stirling motor.

When the land requirement of each technology is considered, the most efficient in is the Fresnel trough and the most inefficient is the central receiver.

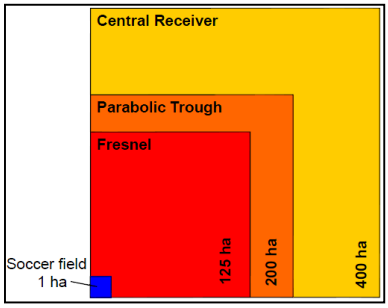

Figure 1-36: Land use for a 100MW plant (Völker, Heinsath, Morin, & Varas, 2009)

Weather and radiation data

The Atacama Desert in northern Chile is one of the best regions in the world for solar energy based on energy density data from several sources (Duffie and Beckman 2000, Goswoami et al 2000). However, no reliable data is available on the development of solar power plants in Chile.

There are five sources of radiation data available for Chile. The first is a book written by Professor Sarmiento from the Universidad Técnica Federico Santa María, which has radiation data for several locations in Chile but lacks information about the instruments used to collect the data or any specification of the weather stations that produced it.

Another source is the Chilean Bureau of Meteorology (*Dirección Meteorológica de Chile*, DMC). The information on horizontal global radiation provided by the DMC for Santiago was available for this thesis, but only for a specific location and for one year in a format that was not user-friendly.

The third source is the data collected by the developers of the software Meteonorm, which uses the data for the specific locations and interpolate for locations for which data is not available. It can produce data in different formats, such as typical meteorological year two with hourly data.

The fourth source is an online tool from the CNE, but it only shows hourly averages of global horizontal radiation for four months and the method used to obtain the data is unclear.

Finally there is a paper containing data based on satellite technology (Ortega, Escobar, & Colle, 2008), but the output is based on a satellite model validated for the weather in Brazil, not Chile.

In conclusion, there is a lack of weather and radiation data for Chile. Efforts are being made to improve this situation. For now, the available data is good enough for an initial estimate and evaluation solar plant technology, but it is not enough to be used in a solar power project. Additional information should be obtained using the proper instruments over the course of at least a few years in order to assess in the variability of the radiation and properly design the plant.

1.6 Chapter Summary

As we have seen in this chapter, Chile's energy matrix is based mostly in fossil fuels that depend on international resources. These fuels are affecting the climate of the earth. In order to stop these climate changes and reduce dependence on foreign fuels, renewable sources of energy must be discovered. Solar resources are particularly abundant in Chile, and could replace part of the fossil-generated electricity in the country, diminishing its dependence on imported oil. The most highly developed technology is the parabolic trough, which has projected prices of around US$50/MWh in 2020 (Abengoa Solar). There is thus a need to study different configurations of this type of plant.

2. THESIS OBJECTIVES

2.1 Current Knowledge in the Field

Parabolic troughs are the most promising technology in this area. This is duein part to the the experience gained with SEGS plants. This technology is well-known and has been studied thoroughly and proven to work. Though other solar concentrating configurations have been studied and are promising options for the future, the parabolic dish represents a modular technology for distributed energy production. Towers and Fresnel, which compete with the solar trough, will become more competitive as more power plants are installed (Mills, 2004 , Klaiss, Köhne, Nitsch, & Sprengel, 1995 and Trieb, Langniss, & Klaiss, 19997). One problem with solar energy is that production is intermittent and dependent on the weather, but this can be uncoupled by applying energy storage so that the plants can collect now and produce later.

There are currently two types of storage. The first and more common of the two is indirect storage. In this type of system, heat is transferred from oil to a molten salt in an oil-to-salt heat exchanger that is stored in an insulated tank. This option has been proven and reliable. (Kelly & Kearney, 2006). The second type involves passing the molten salt directly into the heat collecting element and storing part of the flow in tanks. This option is less expensive due to the absence of one heat exchanger, which reduces the cost of electricity (Kearney D. , et al., 2003 and Herrmann, Kelly, & Price, Two-tank molten salt storage for parabolic trough solar power plants, 2004). Other types of storage, such as latent heat and chemical storage are in development and represent future options but are not real options for today's plants (Pilkington Solar International GmbH, 2000). Other revolutionary options include superconducting materials, flywheels and compressed air. However, they have not yet been proven on a large scale and must be further developed (Carvallo, 2001). All plant types are expensive due to the unusual elements they require, so simulation is a low-cost option for studying behavior before moving ahead with construction (Patnode, 2006). The same is true of simulations of

the SEGS plant in TRANSYS software and EES software. The model was a complex one in that it include every part of the plant, including expansion vessels, a turbine with different extractions and inlets, deaereators and so on. The results were similar to real behavior, and it thus can be said that plant behavior can be simulated by a computer using real weather data.

Is solar energy an interesting option for limiting climate change? Is it really a source of energy? Larrain, 2008 , studied solar plants from a net energy analysis point of view in order to evaluate whether or not this technology is a net source. The author concluded that solar plants have a short energy payback time, and are not energy sinks. This research covered plants in different locations in Chile and proved that solar power plants are sources of energy in Chile.

It is not enough for technology to be a green. It also has to be profitable so that companies can invest in solar-generated electricity. Quaschning, Kistner, & Ortmanns, 2002 made an important contribution in this area by helping to evaluate the solar field. However, their study only covers a SEGS plant and a wider range of plant types exists. Their study was limited to how LEC varies with the solar field area for one type of plant at one site.

Net energy analysis demonstrated that solar plants are energy sources. Based on the fact, Chile is a solar-rich country and it is interesting to study and develop models in order to understand how the solar field size affects the cost of electricity for different locations in Chile and observe how different types of plants behave in different climates in the country.

2.2 Objectives

The aim of this thesis is to analyze thermally and economically different parabolic trough concentrator technologies in different parts of the central and northern zones of Chile in which weather and radiation data are available in order to support the decision-

making process regarding the installation of solar thermal plants in Chile. Specific targets will be selected to develop a thermal model so that researchers can quantify how much electricity can be produced annually, monthly, daily and hourly using solar resources or with fossil back-up. The second objective is to estimate the most important economic factors for each plant type and location, such as levelized sale price of electricity (LEC), present value and IRR.

2.3 Hypothesis

The hypothesis of this study is that an economic and thermodynamic model may assist specialists select the most suitable technology and field area for each location.

2.4 Methodology

The analysis considers five 100 MW solar thermal plant models with parabolic trough concentrators. The differences between the models is related to the type of thermal storage used (direct, indirect or none) and whether or not they have a fossil back-up system. These plants will be modeled at several locations in northern and central Chile. The results of these simulations are the inputs of an economic model that is to be used to obtain the present value of the projects, the minimum sale price of electricity for a project's net present value equal to zero, the installation cost and the internal rate of return the project. The thermal models for the field, storage and cycle are programmed into the software Maple 11 with inputs from EES software and input parameters and outputs in MS Excel format for later use in the economic model in MS Excel 2007 software.

3. THERMODYNAMIC MODEL

3.1 Introduction

The purpose of this chapter is to describe all of the models, so they can be reproduced. We first offer a description of each model and then describe all of the components and assumptions.

It is well known that many options are available (NREL and Völker, Heinsath, Morin, & Varas, 2009), such as direct steam production in the collector, storage systems, fossil back-up and other configurations options. The following system configurations are modeled and explained in this chapter:

Direct power production

A heat transfer fluid passes through the heat collectors and then through a heat exchanger where water is evaporated and overheated. That superheated steam is then injected into a turbine with one reheating, which moves a generator and produces electric power.

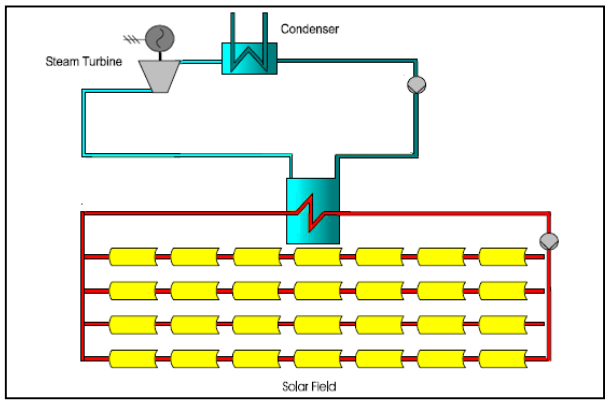

Figure 3-1: Direct power production (Kearney, et al., 2003)

Indirect storage with fossil back-up

The fluid in the collector circuit heats a secondary fluid used for thermal storage. This secondary fluid passes its energy to the water flow in order to produce steam for the reheating rankine cycle. Steam can be produced in a fossil-fired boiler when no fluid is available.

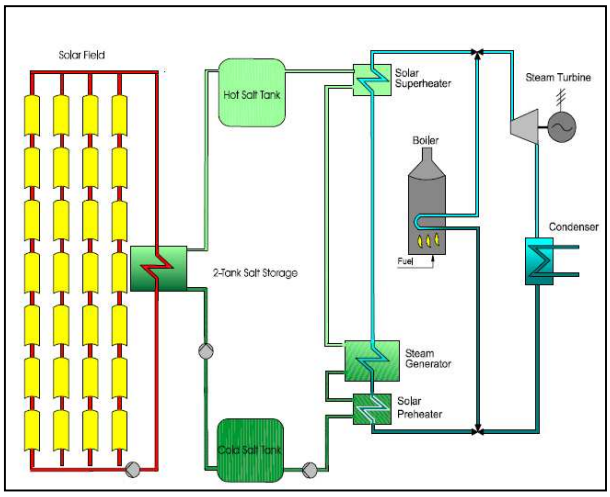

Figure 3-2: Indirect storage with back-up (Kearney, et al., 2003)

Indirect storage without back-up

The fluid in the collector circuit heats a secondary fluid that is used for thermal storage. This secondary fluid passes its energy to the water flow in order to produce steam for the rankine cycle with one reheat.

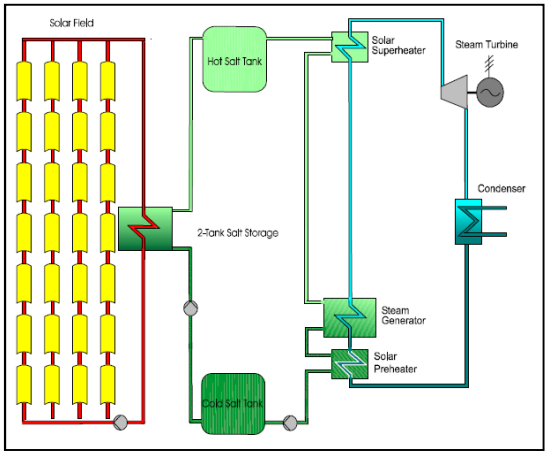

Figure 3-3 : Indirect storage without back-up (Kearney, et al., 2003)

Direct storage with fossil back-up

The fluid in the collector circuit is the same fluid used for thermal storage. This fluid passes its energy to the water flow in order to produce steam for the turbine with one reheat. Steam can be produced in a fossil-fired boiler when no fluid is available in the storage compartment.

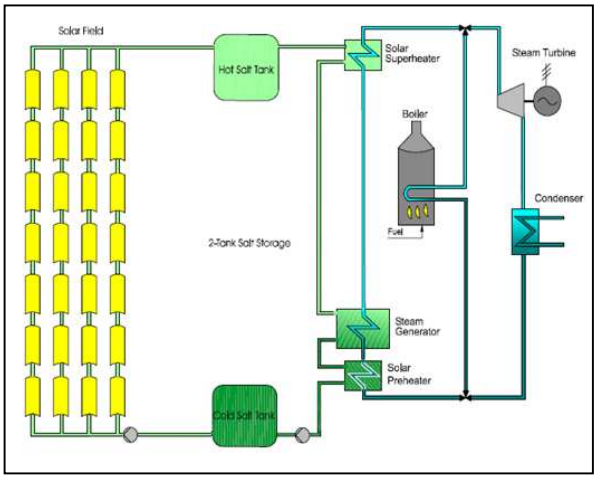

Figure 3-4: Direct storage with back-up (Kearney, et al., 2003)

Direct storage with fossil back-up

The fluid in the collector circuit is the same fluid used for thermal storage. This fluid passes its energy to the water flow in order to produce steam for the rankine cycle with one reheat.

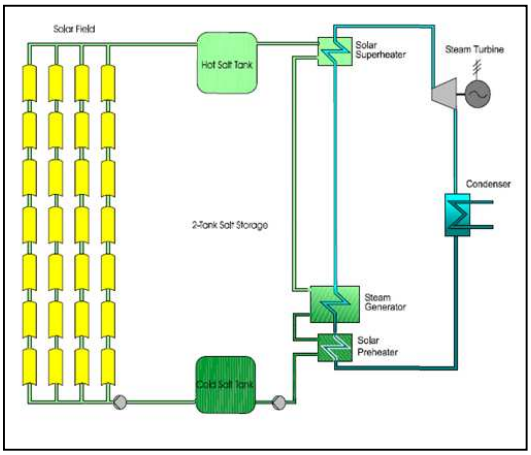

Figure 3-5: Direct storage with back-up (Kearney, et al., 2003)

This set of configurations covers most of the possible configurations for parabolic trough solar power plants.

3.2 Common information

Weather and radiation data:

The data comes from Meteonorm software in “Typical Meteorological Year 2” or “*.tmy” format.

All of the information is organized into four main columns. One is used for the day, the second for the hour corresponding to the data, the third for the direct normal irradiation measured in watts per hour per square meter and fourth is for the ambient dry bulb temperature in degrees Celsius. An example with data for hours 1 to 15 on January 1 in Antofagasta is shown in Table 3-1.

Table 3-1: Weather data table

Day	Hour	Direct normal Radiation[Wh/m^2]	Dry Bulb Temperature [°C]
1	1	0	20.1
1	2	0	19.9
1	3	0	19.6
1	4	0	19.4
1	5	0	19.2
1	6	0	19
1	7	0	19.2

Figure 3-6 presents radiation characteristics for Calama for a period of one day .

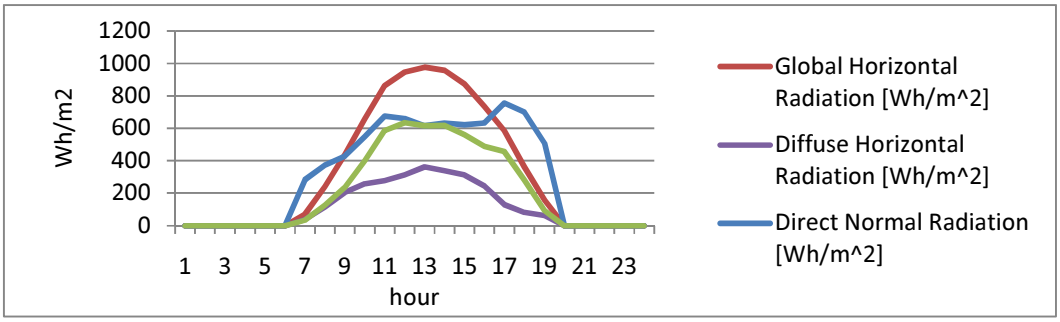

Figure 3-6: Radiation data for Calama for one day

Figure 3-7 shows radiation characteristics for a month in Calama and Figure 3-8 presents the average monthly radiation for a year in Calama.

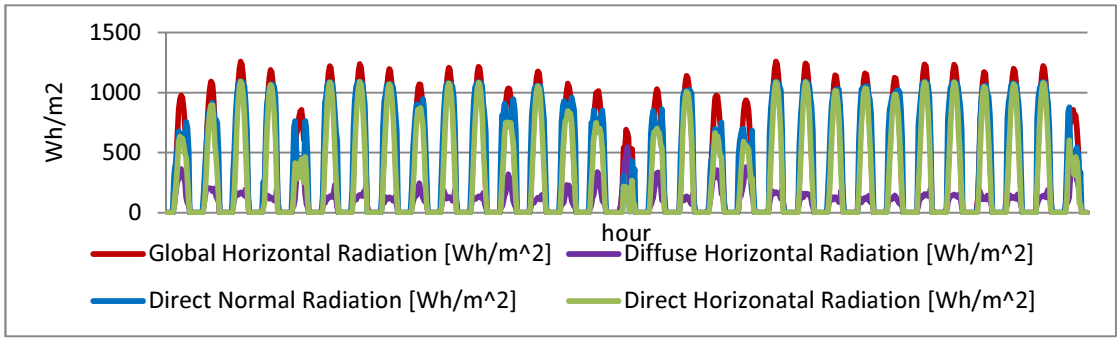

Figure 3-7: Radiation data for Calama in January

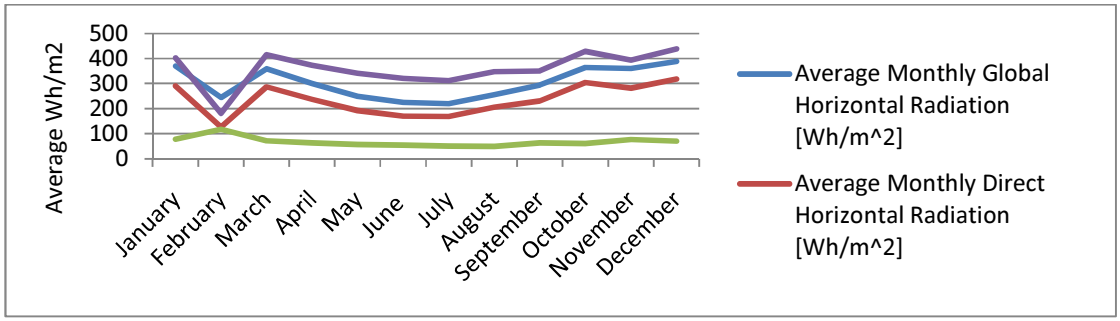

Figure 3-8: Average monthly radiation data for Calama for a year

Real data in smaller time intervals are not available. For smaller steps in simulations, interpolation in the data can be used. However, for the purposes of this thesis, hourly data is small enough given that it allows the data to be computed quickly and provides relatively accurate results.

Water Properties

The water properties for liquid water, saturated water and overheated steam come from from Engineering Equation Solver (EES) software, that contains tables for water and steam. These values should not vary a great deal from one source to the next.

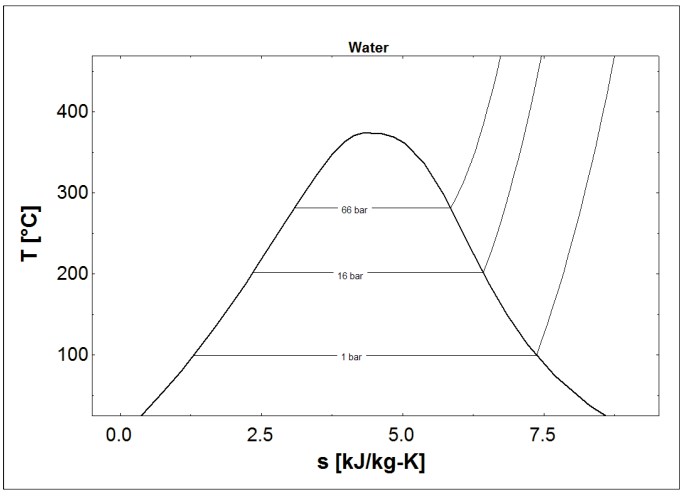

Figure 3-9: Water diagram from EES software

Hitec XL properties

Based on Kearney D. , et al., 2003 and Gil, Medrano, Martorell, Dolado, Zalba, & Lázaro, 2009 , the selected heat transfer fluid is Hitec XL because of its low freezing point compared to other salts and low vapor pressure at high temperatures compared to oils such as Therminol VP1 and Dowtherm (Kearney D. , et al., 2003). No tables or correlations for the heat capacity related to the temperature were found for this fluid. The specific heat for Hitec XL, $C_{p\ Hitec\ XL}$, was assumed to be 1.447 $\frac{kJ}{kg \cdot K}$ at all temperatures above freezing.

Therminol VP1 properties

The heat transfer fluid plays no major role in the performance of the HCE (Forristall, 2003). In view of this, Therminol VP1 was chosen from other similar products because it is the most frequently used HTF in solar fields. The data for this heat transfer fluid was obtained directly from the manufacturer's webpage. The product bulletin with liquid and vapor properties can be downloaded from the manufacturer's website (Therminol).

The following correlation for the specific heat, which was taken from the bulletin, was used:

$$C_{p\,Vp1} = 0.002414 \cdot \mathrm{T} + 5.9591 \cdot 10^{-6} \cdot \mathrm{T}^2 - 2.9879 \cdot 10^{-8} \cdot \mathrm{T}^3 + 4.4172 \cdot 10^{-11} \cdot \mathrm{T}^4 + 1.498 \frac{kJ}{kgK} \quad \textbf{(3-1)}$$

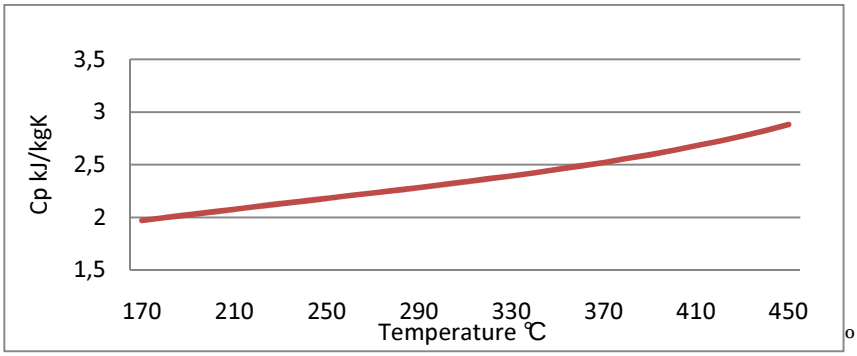

Figure 3-10: Therminol VP1 heat capacity vs. Temperature

Heat exchangers models

The heat exchangers were modeled as counter-flow exchangers with a certain efficiency given by η_{HXi}. So 1-η_{HXi} is the heat lost to the environment. The required outlet temperatures are given, so the model output is the cold fluid mass flow. The efficiency of the heat exchanger was set at η_{HXi}=95%.

$$C_{p\,Cold\,FLow} \cdot (T_{Cold\,Flow\,Out} - T_{Cold\,Flow\,In}) = \eta_{HXi} \cdot C_{p\,Hot\,Flow} \cdot (T_{Cold\,Flow\,In} - THot\,Flow\,Out\,kJkgK$$

(3-2)

Steam production

A solar boiler produces steam at 66 bar and 385°C. Water is introduced in HX as liquid water at 125°C and 66 bar. The heat added for each kg of water in this step is calculated as follows:

$$q_{Saturated\,Liquid} = (T_{Water\,Saturaton,\ 66bar} - 125°C) \cdot C_{p\,Liquid\,Water} \frac{kJ}{kg} \quad \textbf{(3-3)}$$

Where $C_{p\ Liquid\ Water}$ is $4.18\frac{kJ}{kgK}$. Next, water is taken from the liquid saturated state to that of saturated steam.The evaporation enthalpy h_{fg},is equal to $1531\frac{kj}{kg}$. So $q_{Saturated\ Steam}=h_{fg}$.

The heat necessary to overheat steam is calculated with:

$$\boldsymbol{q_{Overheat\ Steam} = h_{Steam\ 66bar\ 385℃} - h_{Saturated\ Steam\ 66bar}\frac{kJ}{kg}} \quad \textbf{(3-4)}$$

Finally, we calculate the heat necessary to reheat the steam:

$$\boldsymbol{q_{Reheat\ Steam} = h_{Steam\ 15.89bar\ 385℃} - h_{Saturated\ Steam\ 15.89bar}\frac{kJ}{Kg}} \quad \textbf{(3-5)}$$

As a result, the heat added per kg of water is:

$$\boldsymbol{q_{Steam\ Production} = q_{Saturated\ Liquid} + q_{Saturated\ Steam} + q_{Overheat\ Steam} + q_{Reheat\ Steam}} \quad \textbf{(3-6)}$$

Solar field model

Inputs:

- Aperture area measured in square meters: 1.400.000 m^2. This aperture was calculated based on the SEGS (no storage) area, which have an average of 6,150m^2 per installed MW of aperture. This was multiplied by 2 to account for storage, and multiplied by the relationship between the yearly DNI in Antofagasta (~1.8MWh/m^2) and Kramer Junction (~2.1 MWh/m^2).
- Collector Aperture in meters: 5.75 m., aperture for the LS-3 structure (Patnode, 2006).
- DNI in kJ/hrm^2: This was taken from radiation data.
- Ambient tin Celsius degrees: This was taken from radiation data.

- Heat capacity, inlet temperature and desired outlet temperature of the heat transfer fluid.
- Site latitude.
- Heat transfer fluids temperatures and heat capacities.

Output:

- Heat transfer fluid mass flow per hour

Energy absorption model (Duffie & Beckman, 1980):

$$\boldsymbol{Q_{absorbed} = DNI \cdot cos(\Theta) \cdot \eta_{Mirror} \cdot \eta_{HCE} \ \frac{kJ}{Hour \cdot m^2}} \qquad \textbf{(3-7)}$$

Where:

- $Q_{absorbed}$: energy absorbed in a square meter per hour
- DNI: direct normal irradiance
- η_{Mirror}: optical efficiency of the mirror
  η_{Mirror}=90%
- η_{HCE}: optical efficiency of the heat collecting element (HCE)
  η_{HCE}=90%
  The combined optical efficiency is 81%, which matches the efficiency level of most mirror-HCE systems (Price, et al., 2002).
- Cos(□): correction due to the angle of incidence on a north-south axis tracking surface. In order to calculate cos(□), the following equation system must be solved for every hour:
  Declination, δ (Duffie & Beckman, 1980): the angular position of the sun at solar noon with respect to the equator plane where north is positive (Cooper equation).
  $$\boldsymbol{\delta = 23.45° \cdot \sin\left(\frac{284+day}{365}\right)} \qquad \textbf{(3-8)}$$

Hour Angle, ω (Duffie & Beckman, 1980): the angular displacement of the sun east or west of the local meridian due to rotation of the earth on its axis at 15° per hour. (AM negative)

$$\boldsymbol{\omega = 15° \cdot (T - 12)} \quad \textbf{(3-9)}$$

Zenith Angle, θ_Z (Duffie & Beckman, 1980): angle between the vertical and the line to the sun.

$$\boldsymbol{\theta_Z = \cos^{-1}(\cos(\theta) \cdot \cos(Latitude_{Site}) \cdot \cos(\omega) + \sin(\theta) \cdot \sin(Latitude_{Site}))} \quad \textbf{(3-10)}$$

Angle of incidence, θ (Duffie & Beckman, 1980): the angle between the beam radiation on a surface and the normal to the surface.

$$\boldsymbol{\cos(\theta) = \sqrt{(\cos(\theta_Z)^2 + \cos(\delta)^2 \cdot \sin(\omega)^2}} \quad \textbf{(3-11)}$$

Heat losses in the HCE:

The research published by Sandia National Laboratories with DLR and NREL yielded a correlation for heat losses in the HCE, specifically Schott PTR 70 and others (Sandia National Laboratories, 2007). The following equation was used in the program:

$$\boldsymbol{Q_{Losses} = 0.39 \cdot \Delta T + 1.21 \cdot 10^{-8} \cdot \Delta T^4 \frac{W}{m}} \quad \textbf{(3-12)}$$

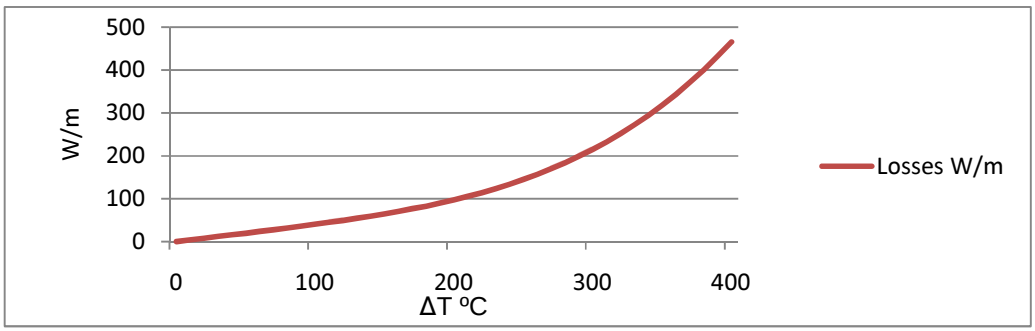

Figure 3-11: Heat losses vs. temperature difference (Therminol)

The solar field is characterized by area. An aperture of 5.75m was chosen to obtain the tube length and the losses in the solar field. The equation below is solved for every hour in order to obtain the heat transfer fluid (HTF) flow needed for the presented output temperature:

$$(\boldsymbol{Q_{absorbed}} - \boldsymbol{Q_{Losses}}) \cdot \boldsymbol{Area_{Field}} = \left(\boldsymbol{c_{p\,HTF}}(\boldsymbol{T_{out}}) \cdot \boldsymbol{T_{out}} - \boldsymbol{c_{p\,HTF}}(\boldsymbol{T_{in}}) \cdot \boldsymbol{T_{in}}\right) \cdot \dot{\boldsymbol{m}}_{\boldsymbol{HTF}} \quad \textbf{(3-13)}$$

Power block

The power block receives the steam from the heat exchanger. A fixed condition for the turbine outlet and efficiency is given to this component and the electric energy output is calculated based on this data. The turbine expands the flow from 66 bar to 15.89 bar, andthe steam flow is reheated to 385ºC for a second stage that ends at two bar saturated steam. Both expansions have an entropic efficiency of 95%.

$$\boldsymbol{E_{Out\ Power\ Block}} = \boldsymbol{\eta_{Turbine}} \cdot \boldsymbol{\eta_{Mechanic\ to\ Electric}} \cdot \dot{\boldsymbol{m}}_{\boldsymbol{Steam}} \cdot [(\boldsymbol{h_{Steam\ 66\ bar\ 385°C}} - \boldsymbol{hSaturated\ Steam15.899\ bar + hSteam\ 15.89\ bar\ 385°C - hSaturated\ Steam1.65\ bar} \quad \textbf{(3-14)}$$

The enthalpy with the entropic efficiency was calculated using equation below:

$$\boldsymbol{\eta_{Turbine}} = \frac{\boldsymbol{h_{2s} - h_1}}{\boldsymbol{h_2 - h_1}} \quad \textbf{(3-15)}$$

Where $\eta_{Turbine}$ is equal to 95% and represents the entropic efficiency, $\eta_{Mechanic\ to\ Electric}$ is equal to 93%. The enthalpies in the different stages are $h_{2s,}$ which correspond to the enthalpy at the outlet of the turbine; $h_{1,}$, which is the enthalpy at the inlet of the turbine; and h_2 , which is the isentropic enthalpy at the outlet.

Figure 3-12 shows the diagram of the rankine cycle.

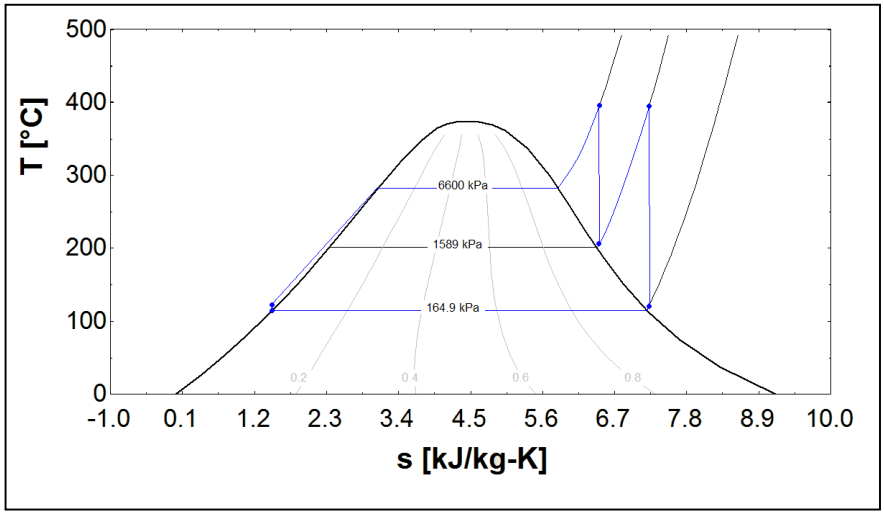

Figure 3-12: Rankine cycle T-s for water

Storage tanks

Thermal energy storage (TES) is performed in two tanks called Cold Tank (CT) and Hot Tank (HT). The fluid temperature in CT is colder than that of HT. Both tanks have one inlet and one outlet and are modeled as perfectly isolated from their surroundings so that there are no heat losses and the temperature of the fluid in the tanks is constant and uniform in time. (This was assumed after an interview with Mr. Camilo Varas, Project Manager and Solar Thermal Expert in the Renewable Energies Department at Lahmeyer).

Another source of this assumption is Figure 3-13, which shows the cooling curve for the cold tank of the Solar Two tower plant. A loss of 28ºC in 6 weeks can be neglected. A mass equilibrium equation is developed for each tank for every hour.

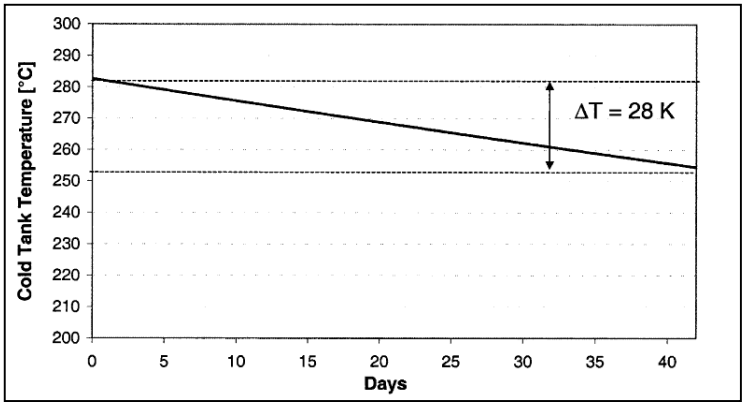

Figure 3-13: Cooling curve of cold storage tank during standby over a period of 6 weeks (Herrmann, Kelly, & Price, 2004)

The mass equations are different for the models and are explicit in each model description. The initial amount of HTF in the tanks limits the storage capacity of the plant. For the simulations, stored energy has the capacity to produce electricity for 12 hours. The total mass of Hitec XL was calculated with next equation:

$$\boldsymbol{m_{TES}} = \frac{\boldsymbol{q_{Steam\ Prodcution} \cdot \dot{m}_{steam}}}{(\boldsymbol{\eta_{HX2} \cdot \Delta_T \cdot C_{p\ Hitec\ XL}})} \qquad \textbf{(3-16)}$$

Initially, half of the mass is stored in each tank. If all of the salt is hot and stored in the HT, the plant can produce 12 hours 100MW of electricity. Given that a temperature other than indirect TES was assumed in direct storage, there are two initial masses in the storage tanks, one for each model. The initial mass per tank for direct TES is $6.26512988 \cdot 10^7$ kg. For indirect TES it is $6.40001726 \cdot 10^7$ kg.

The other constraint for the storage capacity is the solar field area and its relation to the power block. An indicator of the storage capacity is the solar multiple that is defined as the ratio between the thermal power produced by the solar field and the thermal power required by the power block at the design point (Montes, Abánades, Martínez, & Valdés, 2009).

Back-up

Back-up is not available in every model. It is a variation made to the models with TES. Having fossil back-up improves the availability and reliability of the plant and should lower the cost of electricity to said plant.

If the power plant has a back-up system, the heat produced by the hot tank can be provided in a parallel fossil fired boiler. This means that the steam is evaporated in the solar-water heat exchanger or in the fossil-fired boiler. No efficiency is measured here. The only output of this module is the heat added to the water flow. More specifically, the output is the heat amount that was not added by the HTF. It follows the next equations:

$$\boldsymbol{Q_{BU} = Q_{Steam\ Production} - Q_{Solar}} \qquad \textbf{(3-17)}$$

Where Q_{BU} is the heat added in the boiler, in kJ, $Q_{Steam\ Production}$ is the amount of heat that has to be added to take liquid water at 66 bar to overheated steam at the same pressure and 385°C and the saturated steam at 15.89 bar to steam at 385ºC and 15.89 bar in kJ and Q_{Solar} is the heat added by the HTF including efficiencies in kJ.

Condenser

The condenser is not modeled. The water inlet properties of the steam production process are assumed to be constant and a design input.

Pumps

Pumps are not modeled either. The pressure of the different flows is set as input when necessary. Parasitic consumption is accounted for in the economic evaluation, but not for the thermal part. Only the gross electricity output is studied for that section.

Simulation

The simulation was carried out in Maple 11 with one-hour steps for a period of one year. The algorithm followed for each hour in direct production is:

1. Estimates heat gain and losses in the solar field
2. Obtains heat transfer fluid mass flow in the solar field
3. Computes the steam production in the HX
4. Obtains the power output of the cycle

The algorithm for indirect TES for each hour is:

1. Estimates gain and losses in the solar field
2. Obtains heat transfer fluid mass flow in the solar field
3. Computes the mass of Hitec that is heated in the HX
4. Obtains the mass fluctuations in the hot and cold tanks
5. Calculates the steam production in the HX2
6. Obtains the power output of the cycle

For every hour for direct TES:

1. Estimates gain and losses in the solar field
2. Obtains heat transfer fluid mass flow in the solar field
3. Obtains the mass fluctuations in the hot and cold tanks
4. Calculates the steam production in the HX
5. Obtains the power output of the cycle back-up

The extra energy needed for systems with back-up is calculated in the steam production step.

3.3 Models

Direct power production

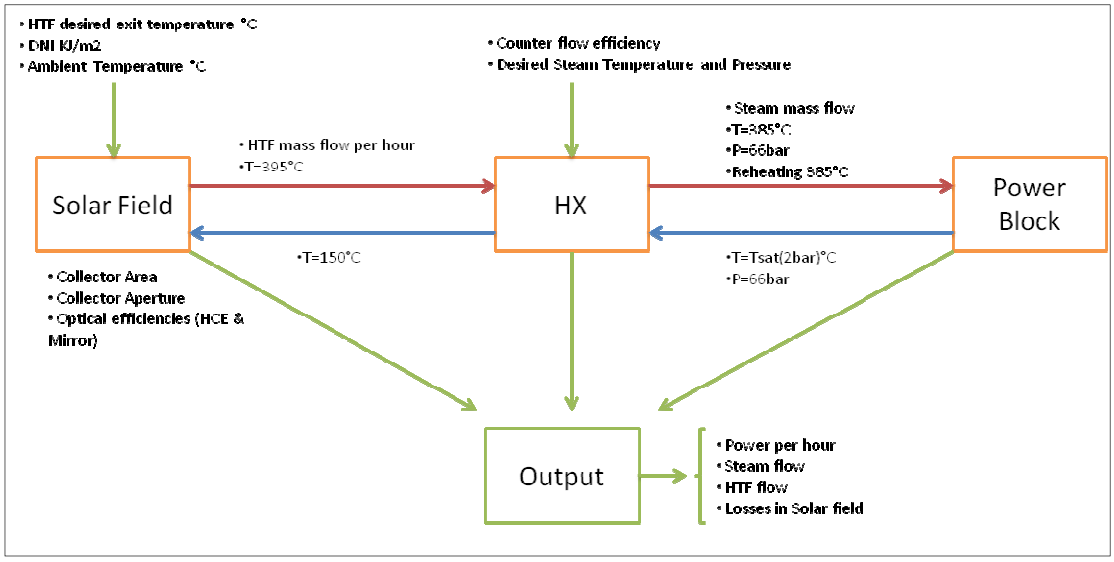

Figure 3-14: Information flow for direct power production

The heat is collected and transported by the heat transfer fluid (HTF) to a heat exchanger. The water that comes from the cooling system is heated, evaporated and super-heated in the HX. That high temperature and pressured steam is injected into a steam turbine attached to a generator where electric power is produced. The mass of HTF per hour is directly proportional to the solar radiation. Steam production will vary depending on the HTF flow. Peak electric power is close to solar noon and there is no possibility of controlling the power to a certain level or following the demand for electricity.

Therminol VP1 is assumed as HTF. It has a maximum temperature of 400°C because of its high vapor pressure at high temperatures. The efficiency of the turbine is assumed to be independent from the amount of mass flowing through it.

Indirect TES with back-up

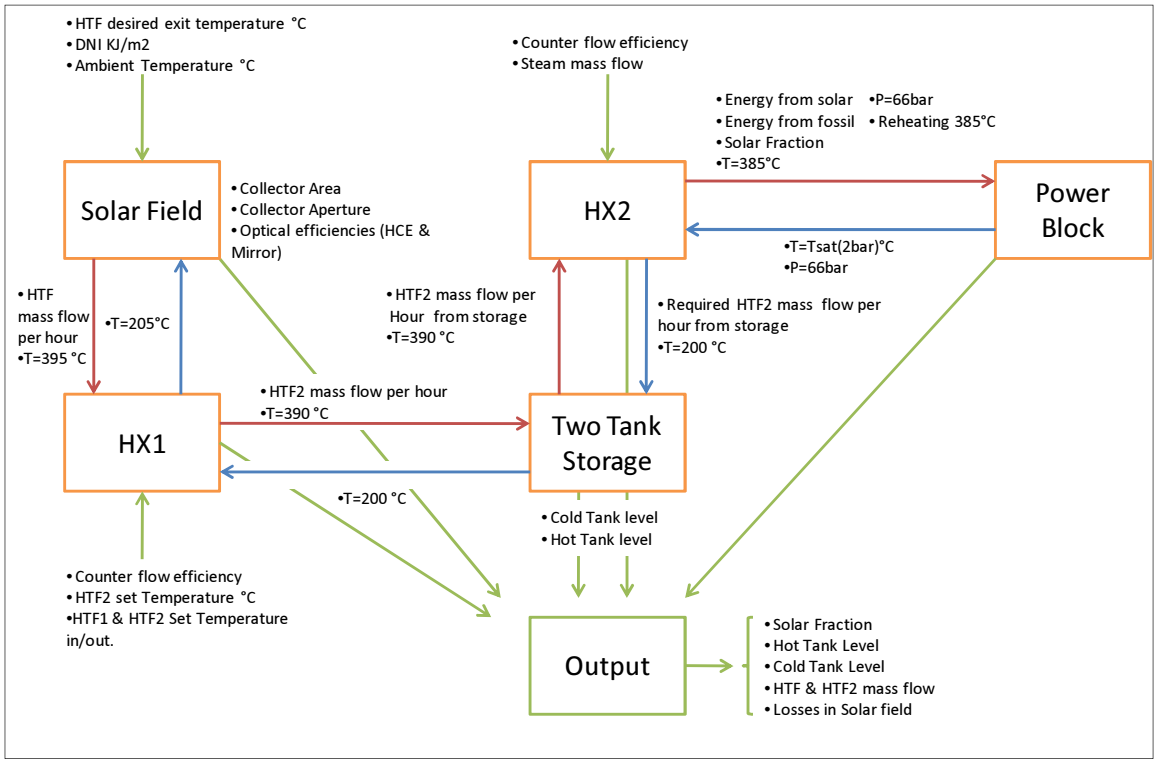

Figure 3-15: Information flow for indirect TES with back-up

According to Figure 3-15, the heat is collected and transported by the heat transfer fluid (HTF) to a heat exchanger HX1. Heat is transferred from the first fluid to the second heat transfer fluid (HTF2) in HX1. HTF2 is stored in the Cold Tank (CT). After HTF2 removes the energy from HTF in HX1, it is collected in a second storage tank. Fluid is hotter in this tank than in CT, so it is called the Hot Tank (HT). The mass of HTF per hour is proportional to the solar radiation. As the radiation changes, the amount of HTF heated in the solar field for every period of time changes, as well. HTF2 flow in HX1 will vary directly with HTF flow. The variability of the HTF2 flow is buffered in the Hot Tank. The flow from HT to HX2 will be constant. Whenever hot HTF2 available is, a constant mass of water can be evaporated in HX2 and injected to the steam turbine. When there is not enough HTF2, a secondary fossil-fired boiler can be used. This power

plant produces power at a constant rate due to the fact that it has storage and fossil back-up.

It was assumed that Therminol VP1 is used as HTF1 because it is the most frequently used solar field oil. It has a maximum temperature of 400°C because it has high vapor pressure at high temperatures. Hitec XL is used as HTF2 for storage and steam production because of its relatively low freezing temperature and low steam pressure at high temperatures. Storage tanks are at atmospheric pressure.

Specific equations apply to this model. Those listed below are mass equilibriums in the storage tanks for the hot tank:

$$\boldsymbol{m_{HT}(t+1) = m_{HT}(t) + \dot{m}_{HTF2\ from\ HX1}(t) - \dot{m}_{HTF2\ to\ HX2}(t)} \quad \textbf{(3-18)}$$

The following is used for the cold tank:

$$\boldsymbol{m_{CT}(t+1) = m_{CT}(t) - \dot{m}_{HTF2\ to\ HX1}(t) + \dot{m}_{HTF2\ from\ HX2}(t)} \quad \textbf{(3-19)}$$

The initial conditions are that there are 64,000,172.6 kilograms of heat fluid in cold and hot tanks and the power plant is working with them and fossil back-up if necessary.

Indirect TES without back-up

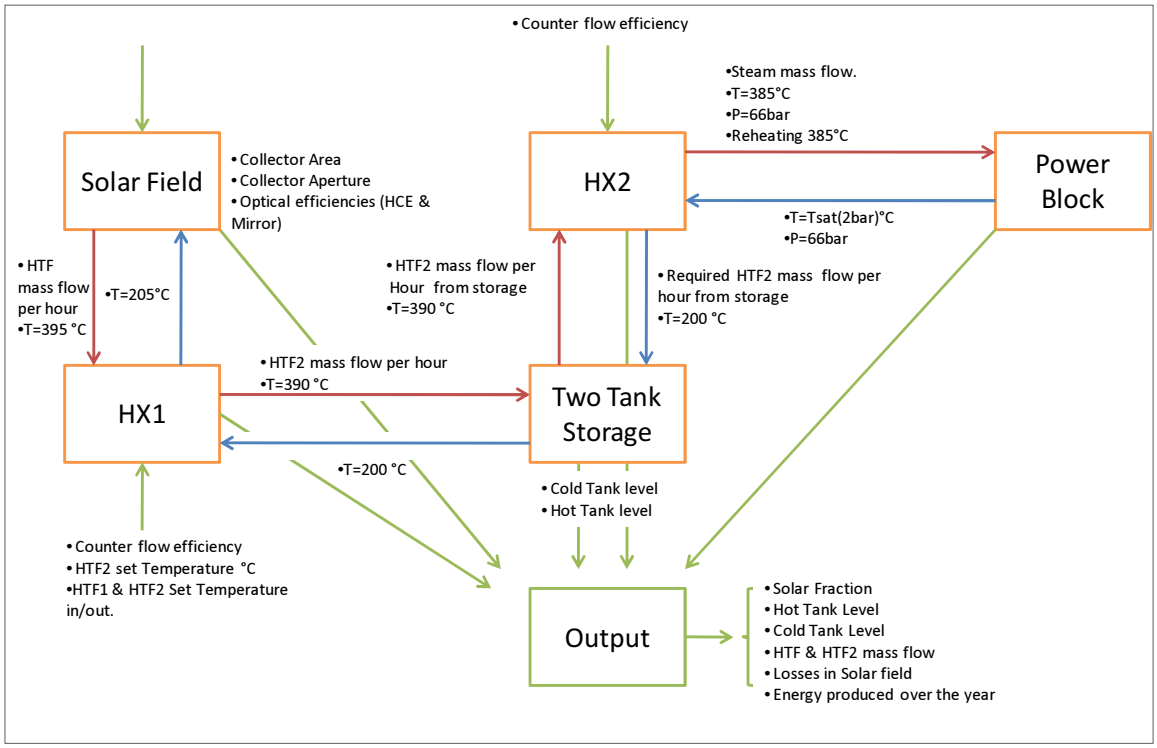

Figure 3-16: Information flow for indirect TES without back-up

This case is similar to Indirect TES with back-up. Its only difference is the absence of the fossil-fired boiler, which means that electricity production cannot take place when no hot solar salt is available.

Direct TES with back-up

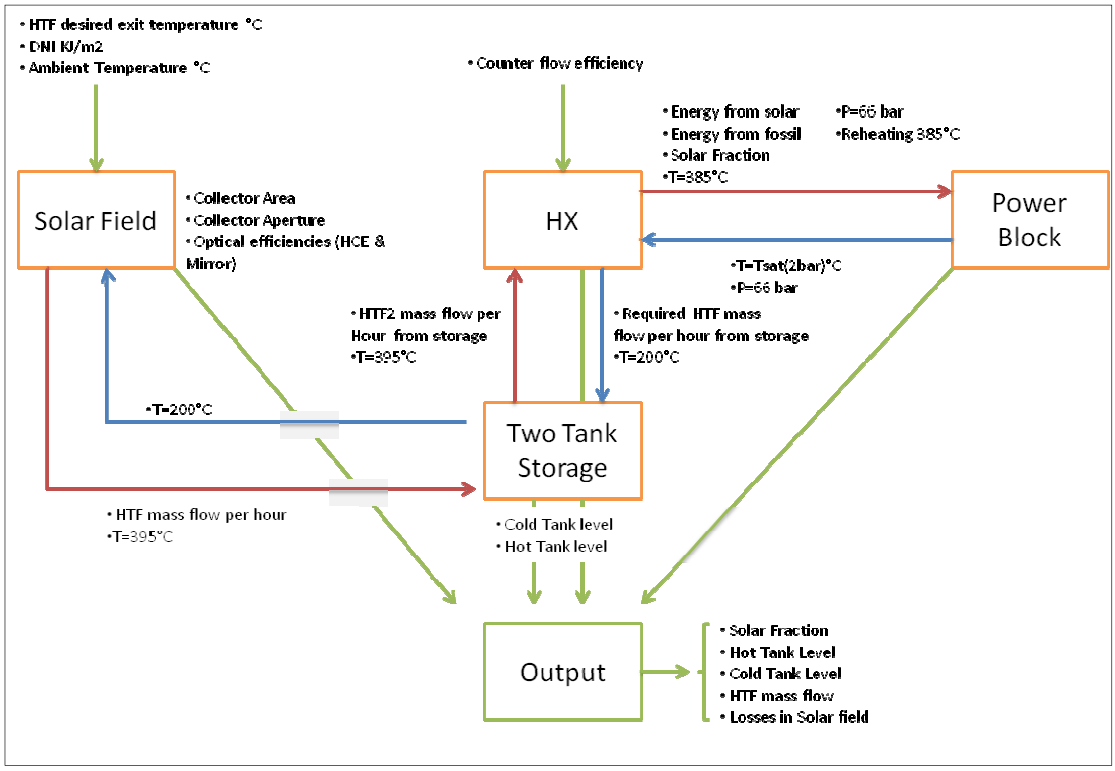

Figure 3-17: Information flow for direct TES with back-up

The heat is collected and transported by the heat transfer fluid (HTF). HTF comes from the Cold Tank (CT). After HTF passes through the collectors, it is stored in the Hot Tank (HT). The mass flow rate of HTF per hour is directly proportional to the solar radiation. The variation in the flow of HTF is buffered in the Hot Tank. The HTF flow from HT to HX is constant; when hot HTF is available, a constant mass of water can be evaporated in HX and injected into the steam turbine. If there is not enough HTF, a secondary fossil-fired boiler is used. Due to the existence of the storage and fossil back-up systems, this plant can produce electricity at a constant rate.

As in indirect TES cases, Hitec XL is chosen as storage fluid because of its relatively low freezing temperature and very low steam pressure at high temperatures. Storage

tanks are at atmospheric pressure. For this model, specific equations for the mass equilibrium in the storage tanks apply. The equations for the hot tank are:

$$m_{HT}(t+1) = m_{HT}(t) + \dot{m}_{HTF\ from\ Solar\ Field}(t) - \dot{m}_{HTF\ to\ HX}(t) \quad \textbf{(3-20)}$$

The following applies to the cold tank:

$$m_{CT}(t+1) = m_{CT}(t) - \dot{m}_{HTF\ \ to\ Solar\ Field}(t) + \dot{m}_{HTF\ to\ HX}(t) \quad \textbf{(3-21)}$$

For the initial conditions, there are 62, 651,298.8 kilograms of heat fluid in the cold and hot tanks and the power plant is working with them and fossil back-up if necessary.

Direct TES without back-up.

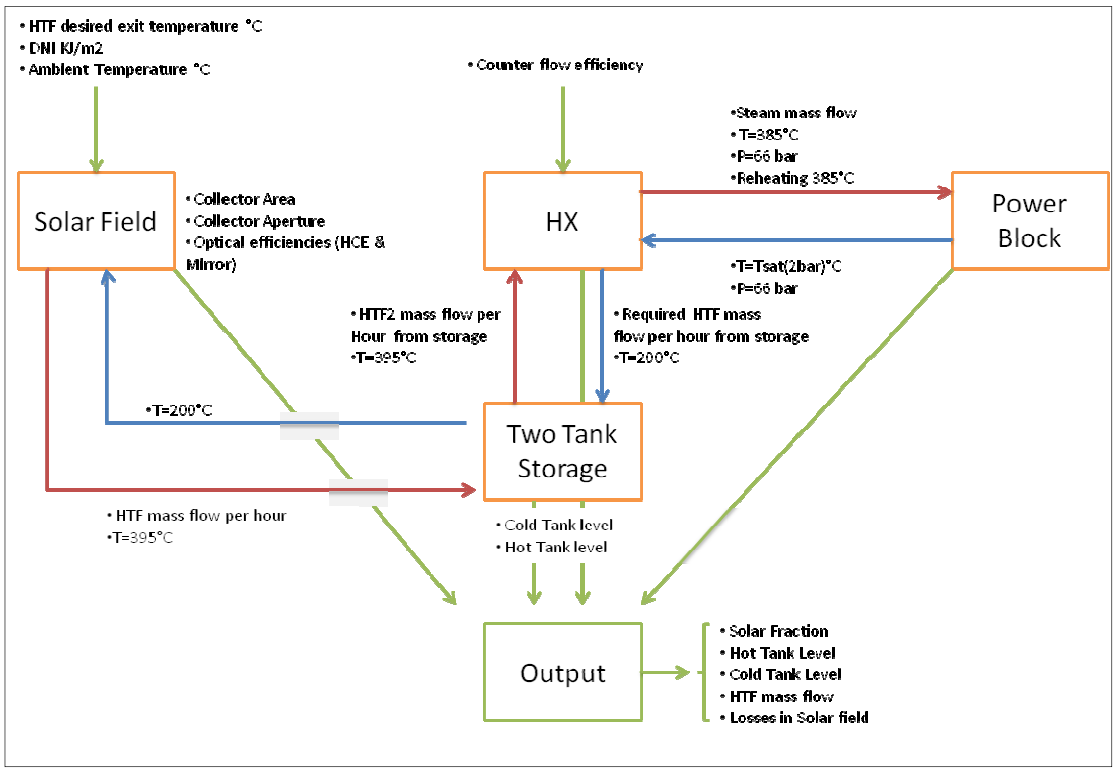

Figure 3-18: Information flow for direct TES without back-up

This case is similar to Direct TES with back-up. The only difference is the absence of the fossil-fired boiler, which means that power production is not feasible when no hot solar salt is available.

3.4 Chapter Summary

This chapter presented explanations of the different models and described how the information flows from one module to the next.

All the information required to reproduce the model and results were presented. Models go in hourly steps, which introduces some errors and imprecision, but it makes simulation relatively speedy. This makes it easier to compare the various options such as location, storage capacity and solar field size.

The purpose of the thesis is to serve as a good instrument for making decisions in regard to solar power projects. It is not intended to solve every aspect of a solar plant. The models have been developed with this in mind.

There are three main models, two with thermal storage and one that produces electricity directly.

The main features of the models are as follows:

- They have 1,400,000 square meters of collectors.
- The turbine for the models with TES is a 100MW turbine.
- The direct production model has a variable output turbine.
- Storage is done using Hitec XL.
- No back-up case is a modification of the model with back-up

Principal differences between models:

Table 3-2: Differences between models

	Solar Field Inlet/Outlet Temperature ºC	CT/HT Temperature ºC	Solar Field/Storage Fluid	Power
Direct Production	150/395	-/-	Therminol VP1/-	Variable
Indirect TES	205/395	200/390	Therminol VP1/Hitec XL	100MW
Direct TES	200/395	200/395	Hitec XL	100MW

4. SIMULATION RESULTS

4.1 Introduction

The methodology and model assumptions explained in Chapter 3 are tested in this section. Chapter 4 presents the most important results, such as solar fraction and electricity generated.

First, complete results are shown for all of the models with the radiation data from Antofagasta. Next, we compare the models in two other sites (Santiago and Calama).

The first results are organized by model, and the information is mostly presented in graphs in order to provide the reader with a better visual understanding of them.

Several representative days are shown for each model. Specifically, six consecutive days are presented for summer, autumn and winter (south hemisphere seasons) in order to show the most typical behavior during those seasons. The dates are listed below:

- January 6-11
- April 2-7
- June 1-6

The tank levels (if available) and energy delivered by solar and fossil fuel are given for each period. Given that the information for spring is similar to that provided for fall and does not add any new data, it will be omitted here.

It is important to keep in mind that the simulations are one-hour intervals for three cities. Antofagasta is located at 23º26’S 70º26’W with an average altitude of 120m above sea level.

Calama is located at 22º30’S 68º54’W with an average altitude of 2312m above sea level. Santiago is located at 22º30’S 70º47’W with an average altitude of 474m above sea level. The plants are theoretical plants that are available all year long with no

maintenance periods. This is a hard assumption. Maintenance of the solar field can be done at night and the power block can be maintained during cloudy periods (mainly winter).

4.2 Results for direct energy production in Antofagasta

Typical days by season

Six days from each season are shown for the direct energy production model. The results for the hourly fluid mass flows for water and heat transfer fluid are given. The energy output of the plant is presented in kJ per hour. Finally, the heat absorption and losses in the heat pipes are given in units of kJ/m^2 per hour. The only results for this model are shown in this section and the idea is to compare the results for the different seasons for this model.

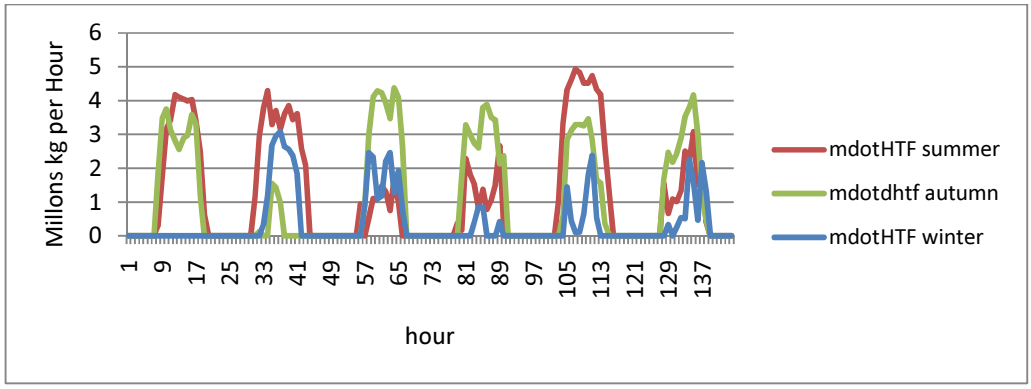

Figure 4-1: HTF flow in direct production

The flow for autumn was similar to that of summer, but much less flow is required during the winter months. If we compare Figure 4-1 with Figure 4-2, we observe a difference of the order of 10 times between the mass flow of water and VP1. This is due to the fact that water is much more capable of storing heat than Therminol VP1.

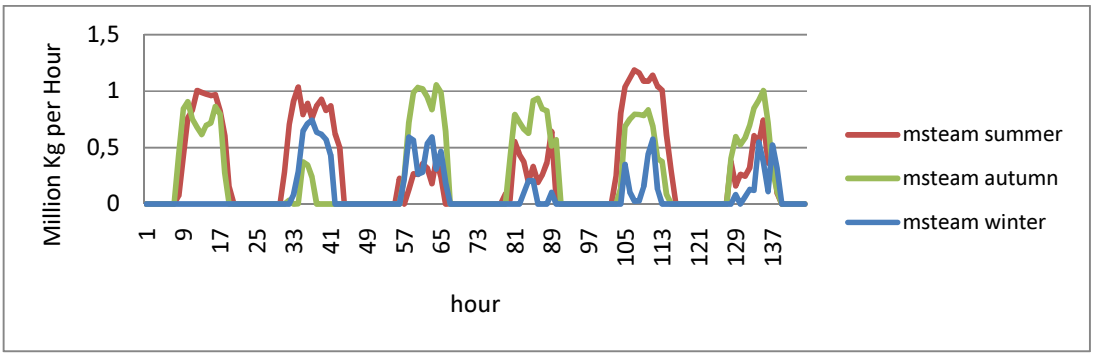

Figure 4-2: Steam flow in direct production

The delivered energy varies directly with radiation. The energy injected into the grid cannot be forecasted as in the case for TES, where it can certainly produce 100 MW for a period of time with a given level of stored fluid. High peaks appear in summer and autumn, but there is less energy available to the grid during the winter.

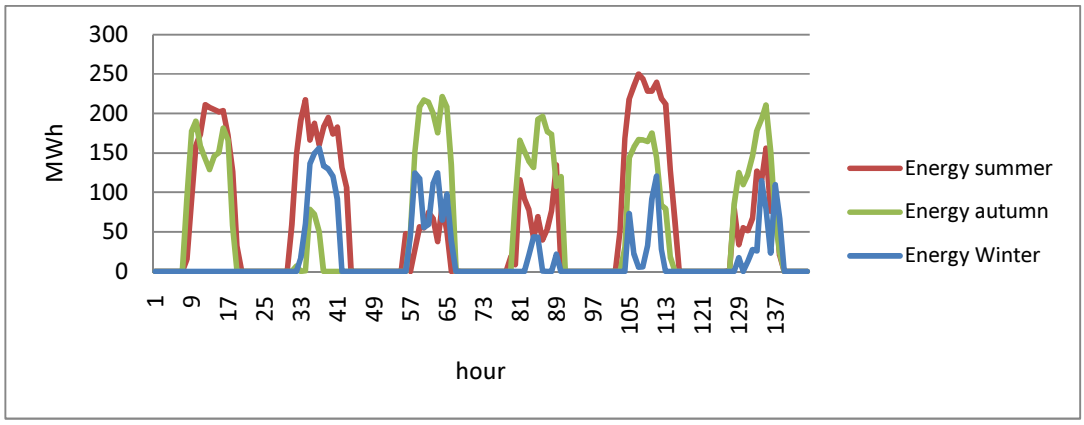

Figure 4-3: Electric energy for direct production

The energy absorbed is proportional to solar radiation. This heat is removed by the HTF, so the greater the amount of heat absorbed, the higher the mass flow through the pipes. Similar absorption rates per square meter are observed for summer and autumn.

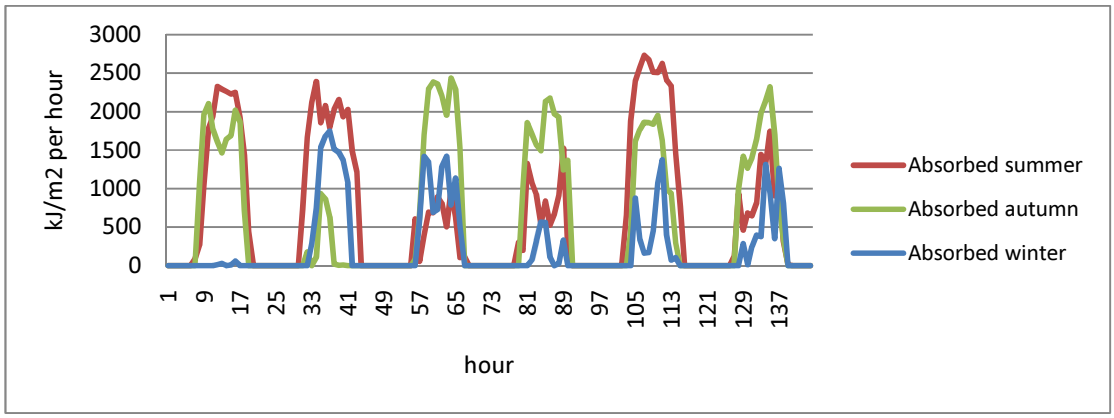

Figure 4-4: Absorbed energy in solar field for direct production

Heat losses in the collector assembly reach a limit. That limit, which is close to flat part of the curve shown in Figure 4-5, is due to the fact that the temperature difference remains almost constant during that time. Equation 3-13 shows that the losses vary only with the temperature difference between the liquid and the atmospheric temperature. As a result, when that temperature difference is constant, heat losses are also constant.

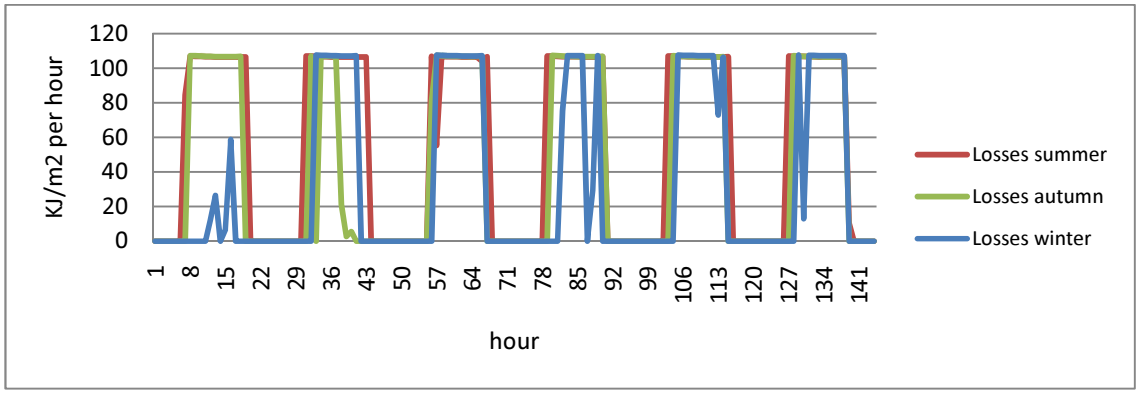

Figure 4-5: Lost energy in solar field for direct production

Losses vary along with the temperature difference between the environment and the fluid, but that difference does not vary much from season to season. The losses per square meter are almost the same for clear sky days throughout the year.

Yearly results

The solar electricity delivered in one year is 332,409 MWh, with Q_{abs} equal to 3.89 GJ/m^2 per year and Q_{loss} equivalent to 0.39 GJ/m^2 per year.

Monthly results

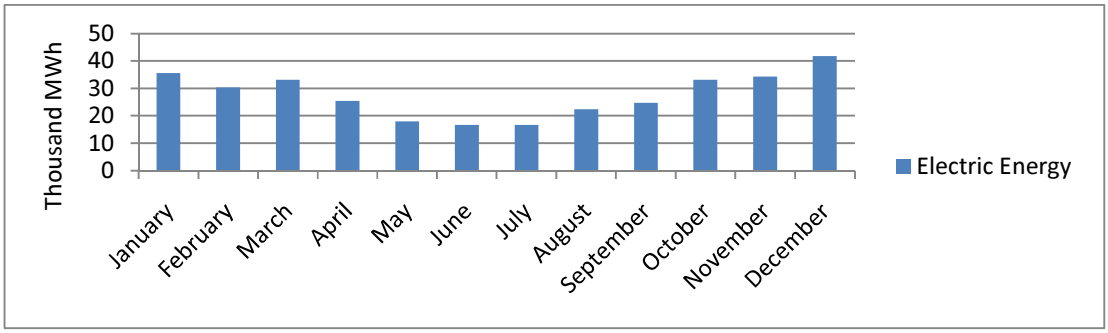

Figure 4-6: Monthly delivered electric energy

December is the highest powered month. There is flat energy production between May and July. During that period, the plant produces less than half the energy produced in December.

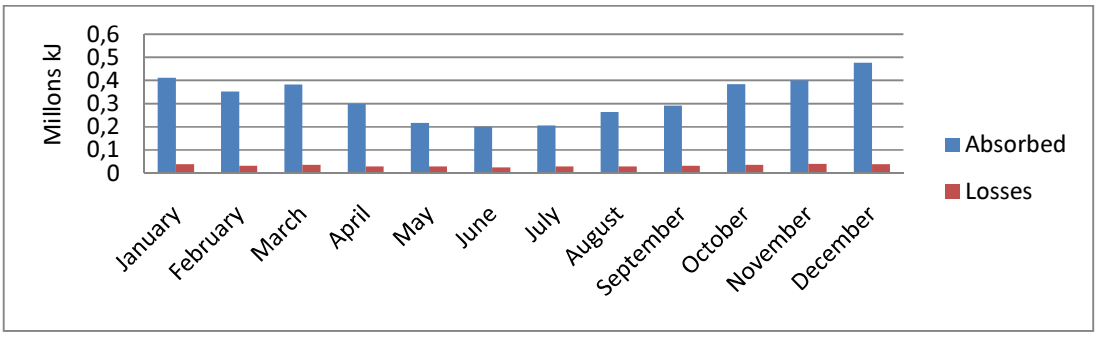

Figure 4-7: Gain and losses in solar field per month for direct production

Losses per month are similar for every month, but absorption for the best month (December) is more than two times greater than for the worst (July).

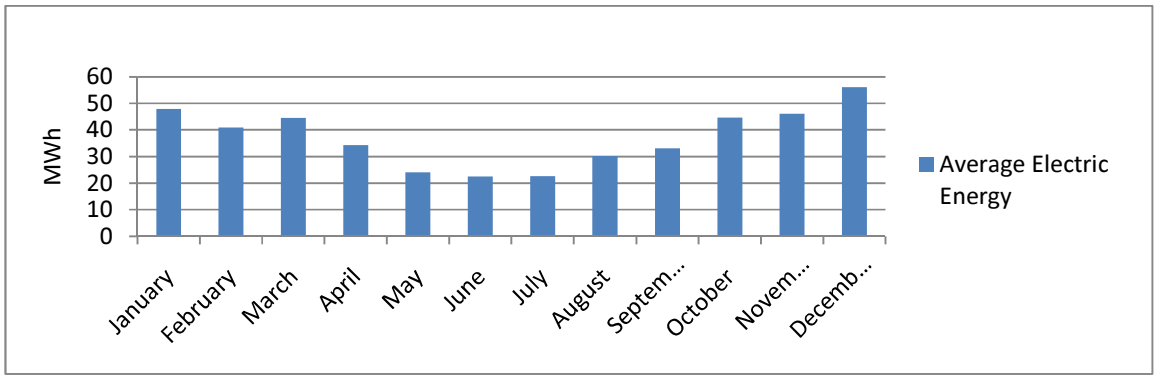

Figure 4-8: Hourly average electric energy in direct production model per month

Average electric power is calculated as the total amount of energy produced divided by the hours in the month. This is done by normalizing the energy produced each month.

The best month in energy terms is December, and the worst is July.

4.3 Results for indirect storage with fossil back-up in Antofagasta

Typical days by season

Six days for each season are shown for the indirect TES model with a back-up system. The results for the hourly fluid mass flows for heat transfer fluid are presented in Figure 4-9 and the storage media is given in Figure 4-10. The data suggest that the flows are proportional.

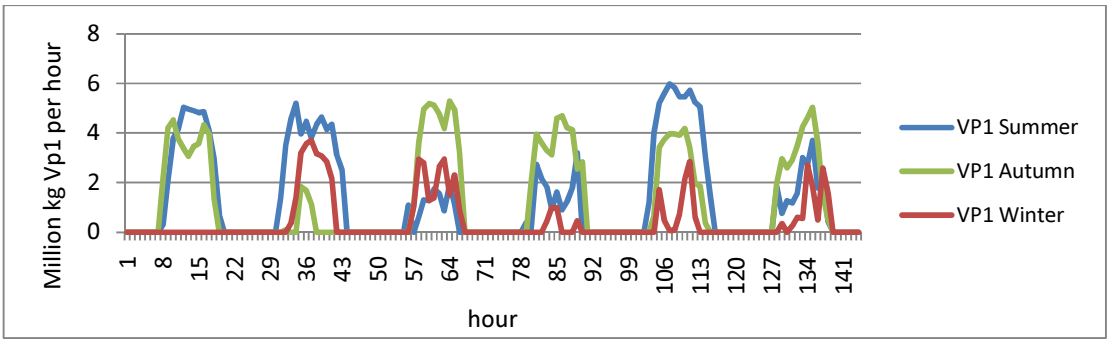

Figure 4-9: VP1 flow in solar field for indirect TES

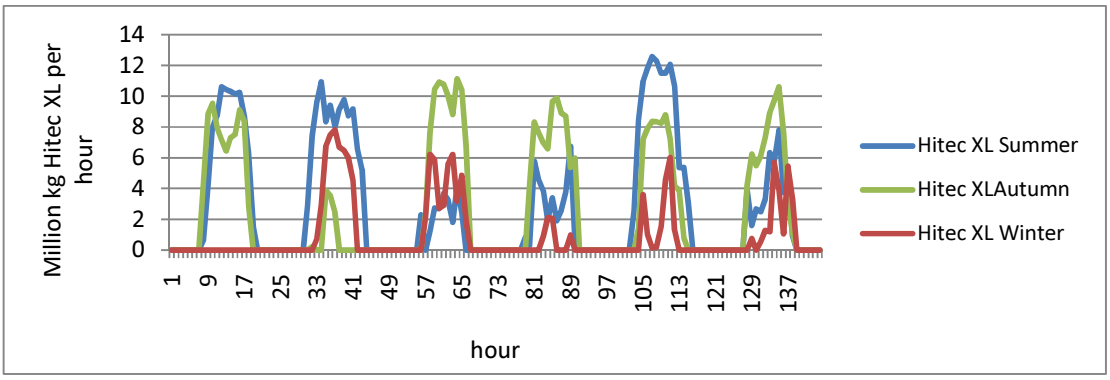

Figure 4-10: Hitec XL flow in the VP1-Hitec heat exchanger

Steam mass flow rate is constant at 476,000 kilograms per hour because of the fossil back-up, producing 100MW at all times. Hitec has a lower heat capacity than Therminol VP1, which is compensated by additional Hitec mass flow. In terms of seasonal variation, summer and autumn look similar and winter shows a smaller flow for every fluid except for steam which, as we said, is constant.

The storage fluid in both tanks is important and is measured in kg of salt for each tank. The stored fluid in CT can be observed in Figure 4-11 and data for the HT are presented in Figure 4-12. Use of the HT is higher in summer than in autumn and winter.

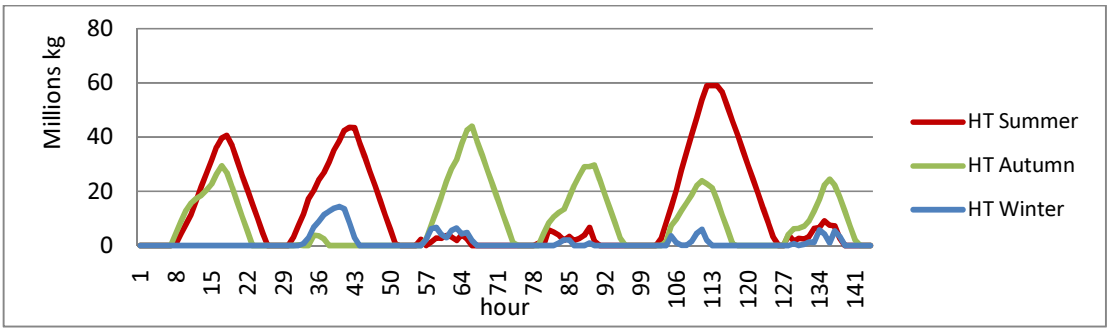

Figure 4-11: Hot tank level for indirect storage

The quantity of stored fluid in both tanks varies during the day. The HT is filled up during high radiation periods and emptied during periods in which there is little or no

radiation. Hot tank capacity is well-designed for summer days for uninterrupted salt supply. However, it could be more profitable to have a smaller capacity with breaks. An economic evaluation should be made so that a decision can be made in this regard.

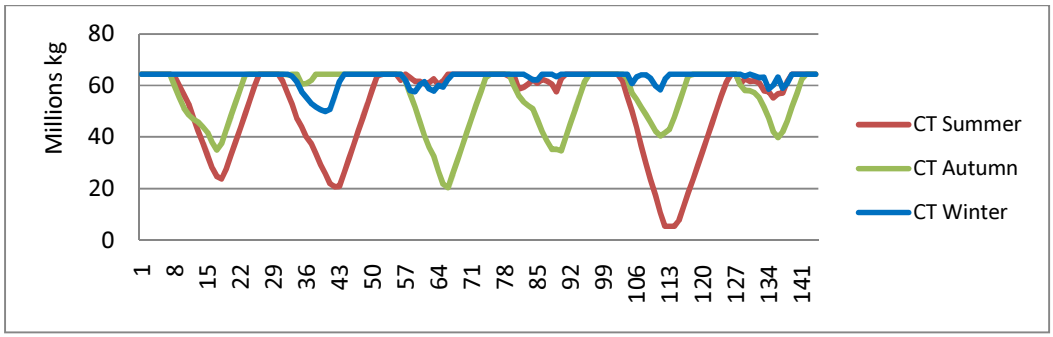

Figure 4-12: Cold tank level for indirect storage

The cold tank is almost full at all the times during the winter.

Figure 4-13 shows that solar electricity meets almost 46% of the demand during the summer months. The other 54% is produced with back-up burning fossil fuel. There are long periods of solar electric production during the summer, and during the fall, 32 % of the power is produced with solar energy. The remaining 68% is produced with back-up running on fossil fuel. Only 23% of the power is produced with solar energy during the winter. The remaining 77% has to be produced with the back-up system running on fuel.

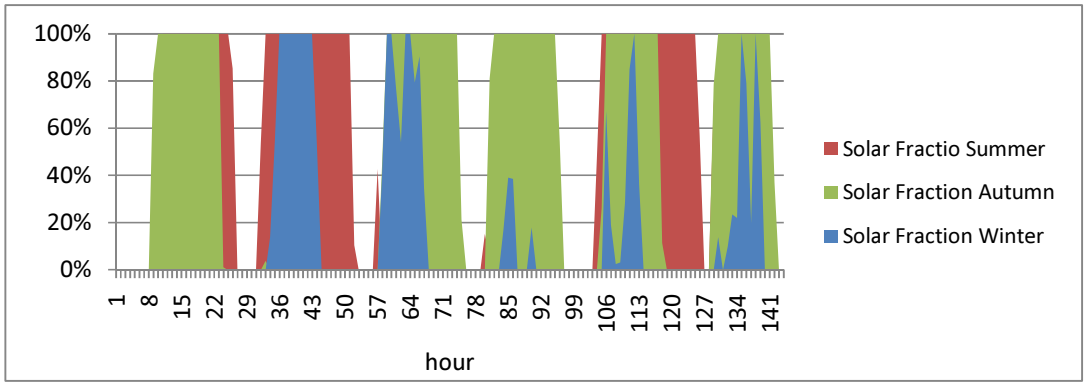

Figure 4-13: Solar fraction for indirect TES

Yearly results

The results for this section are Q_{abs} equal to 3.89 and Q_{loss} equals 0.48 GJ/m^2 per year. Losses per square meter per year are less than gains, so we have a positive result.

Thermal energy from solar power is $4.31 \cdot 10^{12}$ MJ and $7.95 \cdot 10^{12}$ MJ from fossil fuel, so most of the production is based on fossil fuels.

Electric Energy Delivered: 100MW all year. 876.000 MWh, where 35% of it is produced with solar power.

Monthly results

In Figure 4-14, the green bars show the constant energy production that is available only because there is a back-up system.

The red bar indicates that we have more power added by fuel during the winter months. The blue bar shows the same information for the summer season.

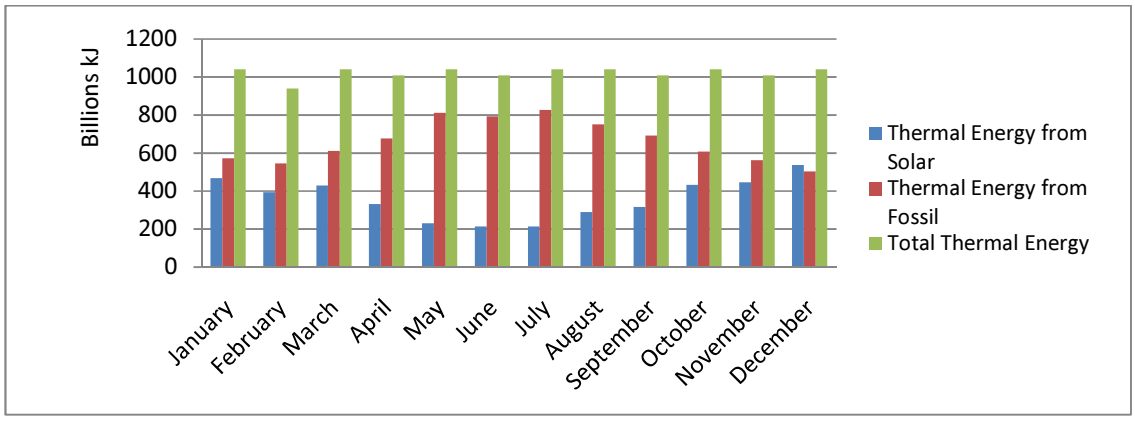

Figure 4-14: Monthly thermal energy to power block by source for indirect storage

Figure 4-15 shows the electric production per month. 100MW are produced at all times. Longer months produce slightly more energy.

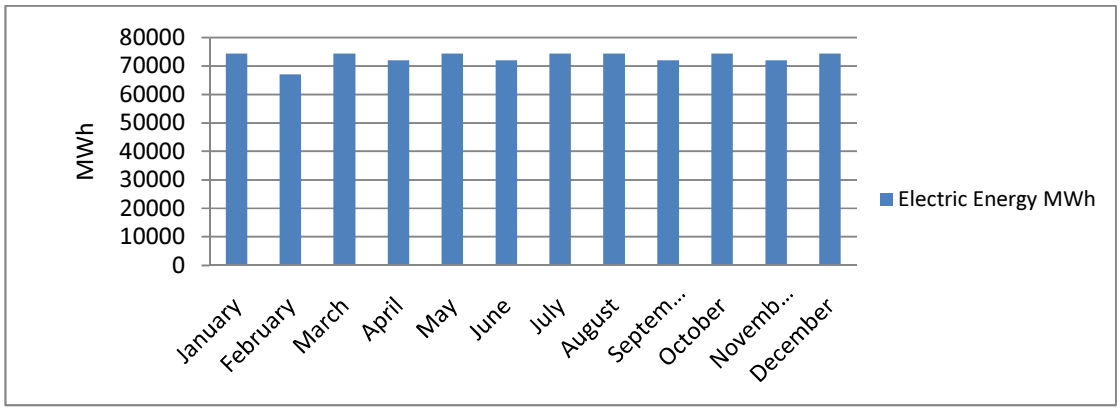

Figure 4-15: Delivered electric energy in indirect TES model

4.4 Results for indirect storage without fossil back-up in Antofagasta

Typical days by season

The relevant seasonal results for indirect storage without back-up are the same as for the case with back-up and can be seen in 4.3.

Yearly results

Electric Energy Delivered: 307,765MWh produced with solar power. This is one fourth of the normal capacity.

Monthly Results

Back-up is probably needed for winter days for this location in order to achieve higher levels of use of the plant. Figure 4-16 presents the monthly electricity. The amount of power delivered in July is less than half of that which is delivered in December.

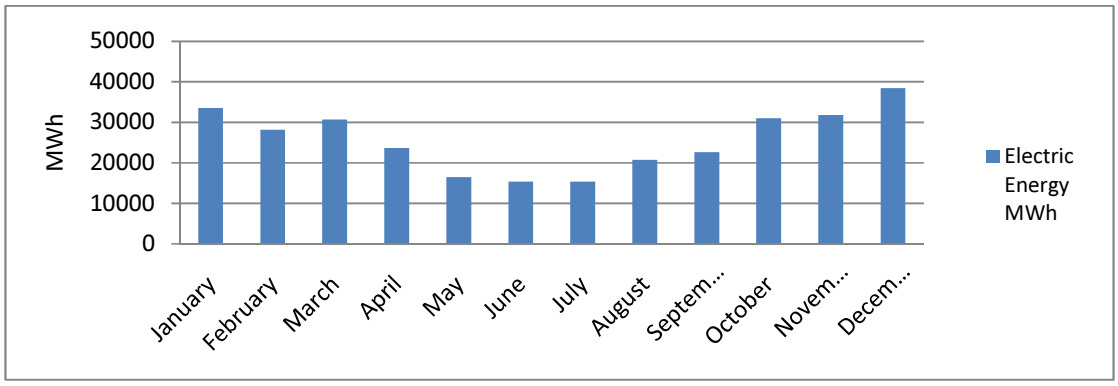

Figure 4-16: Electric energy by month for indirect TES without back-up

Figure 4-17 shows us the average power produced in an hour for every month. Winter season months produce less energy per hour than the other seasons.

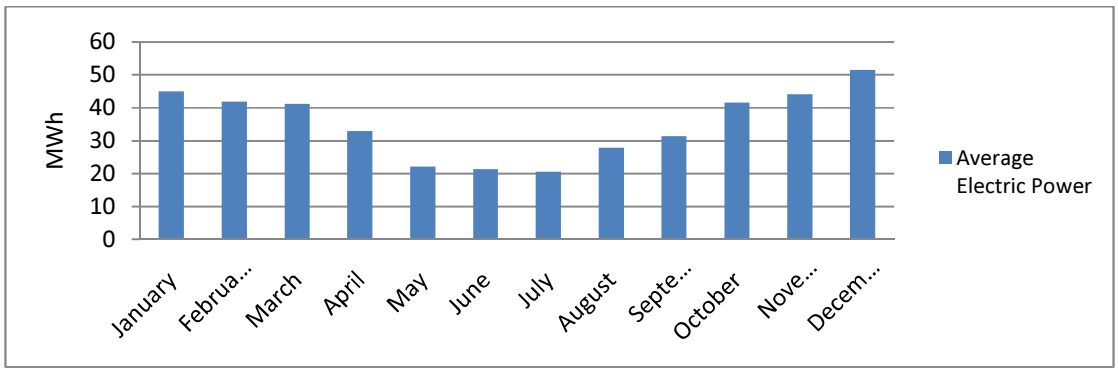

Figure 4-17: Average electric energy by month for indirect TES without back-up

4.5 Results for direct storage with fossil back-up in Antofagasta

Typical days by season

Once again, six days are shown for the direct TES model with back-up for each season. The results for the hourly fluid mass flows for the storage media are given in Figure 4-18. Flow in summer is higher than other seasons.

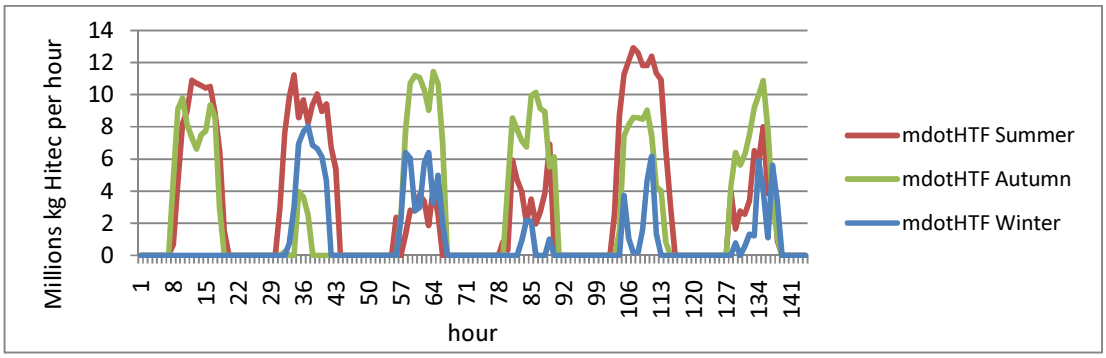

Figure 4-18: Hitec flow in solar field for direct storage

In this case Hitec XL is used in the HCE and storage system. The mass flow rates in summer and autumn are similar. In winter there is less flow of Hitec, but the steam flow remains constant in order to produce 100MW all year long.

Hot tank capacity is appropriate for summer but oversized for the other seasons. This should be optimized.

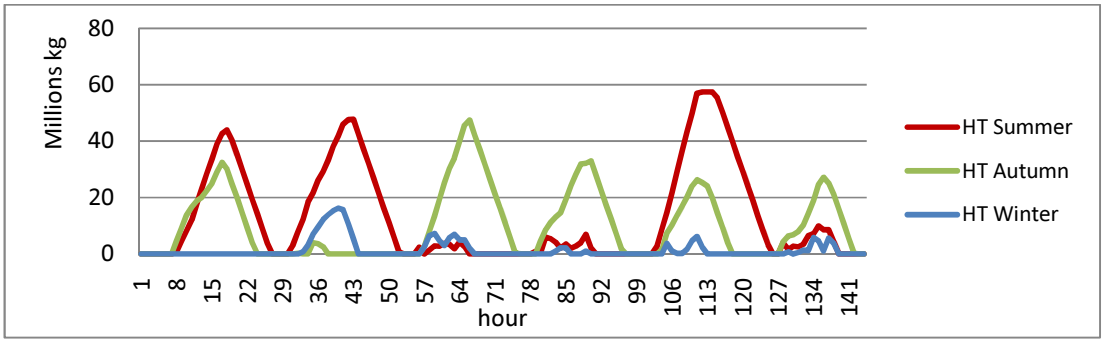

Figure 4-19: Hot tank level for direct TES

Cold tank capacity is related to hot tank capacity. Salt can be stored in either tank.

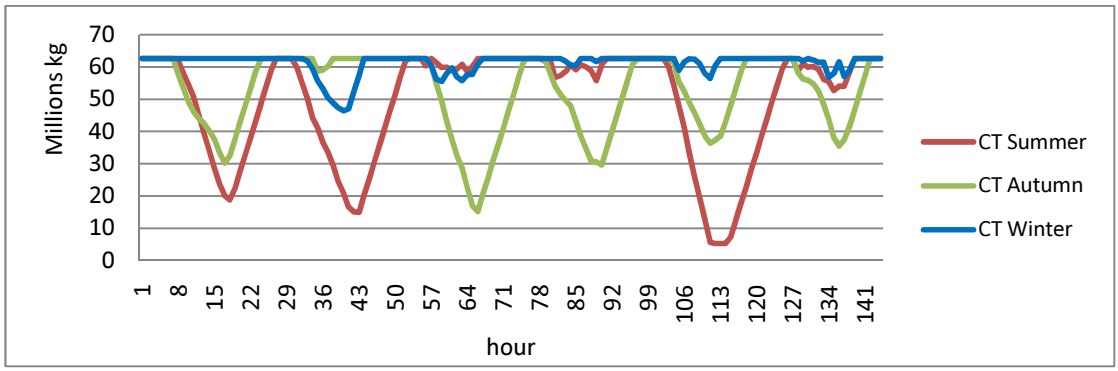

Figure 4-20: Cold tank level for direct TES

There are long periods of time with solar electricity production or solar fraction during the summer, and 48% of the power is produced with solar energy. The remaining 52% is produced with back-up burning fuel.

The results for the autumn months are similar, with 34% of the power produced with solar energy. The other 66 % is produced with back-up running on fuel.

During the winter, in contrast, we do not see long periods with solar electric production. Only 27% of the power is produced with solar energy and the remaining 73% is produced with fuel-fired back-up.

On average, 37% of the electricity produced over the course of a year is solar.

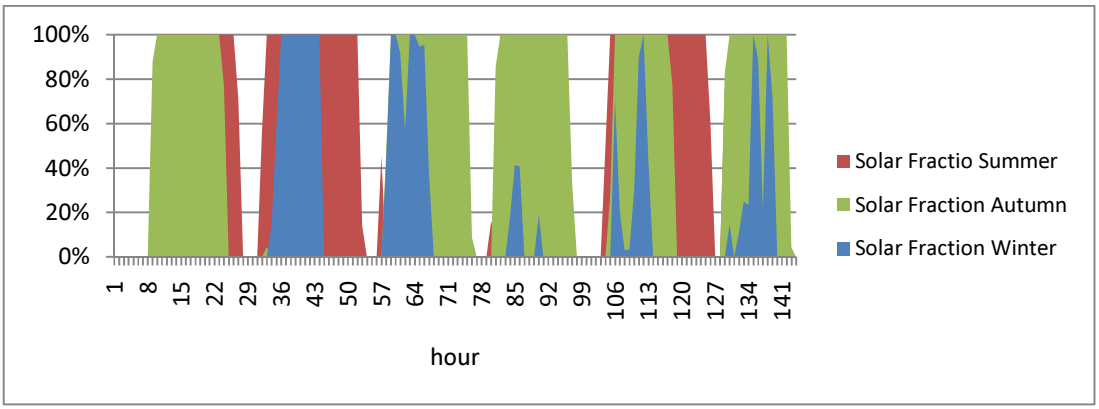

Figure 4-21: Solar fraction for direct TES

Yearly results

Thermal energy from solar production is $4.53 \cdot 10^{12}$ MJ and $7.73 \cdot 10^{12}$ MJ is from fossil.

Electric Energy Delivered: 876.000 MWh. Of this, 37% comes from solar energy.

Monthly results

Figure 4.22 shows how solar energy input decreases during winter and indicates that more fuel is needed during that time of year.

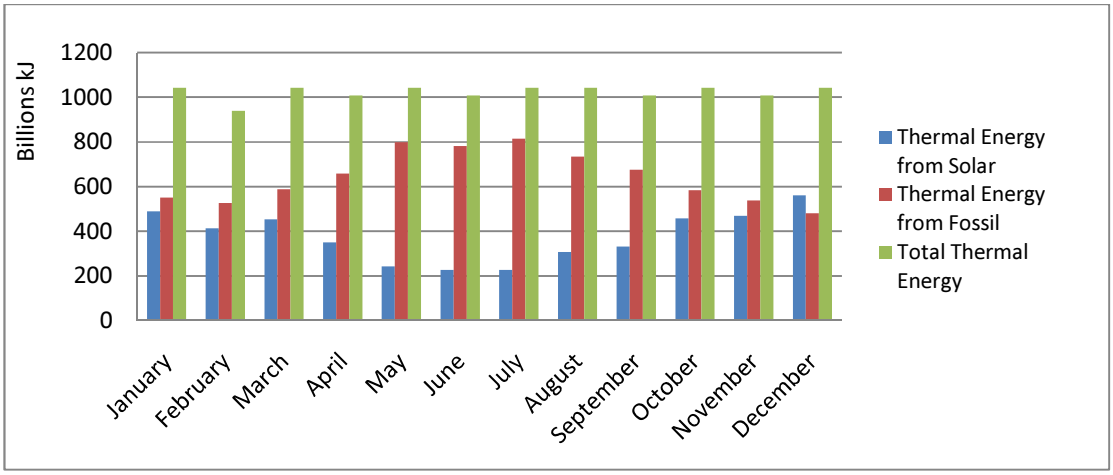

Figure 4-22: Thermal energy to power block by month per source for direct TES

Electric output is constant at 100MW for every hour every month because of the back-up.

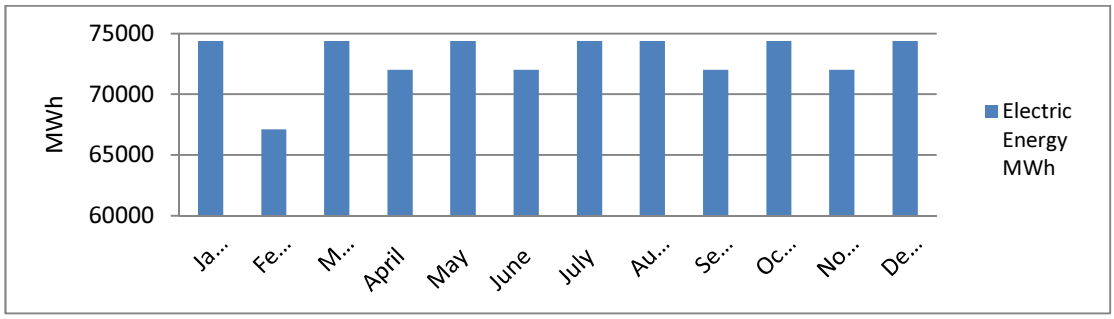

Figure 4-23: Electric energy delivered monthly for direct TES

4.6 Results for direct storage without fossil back-up in Antofagasta

Typical days by season

The relevant seasonal results for direct storage without back-up are the same as those for direct storage with back-up shown in section 4.5.

Yearly results

Electricity delivered: 323,695 MWh per year.

Monthly results

Figure 4.24 shows the electricity produced per month.

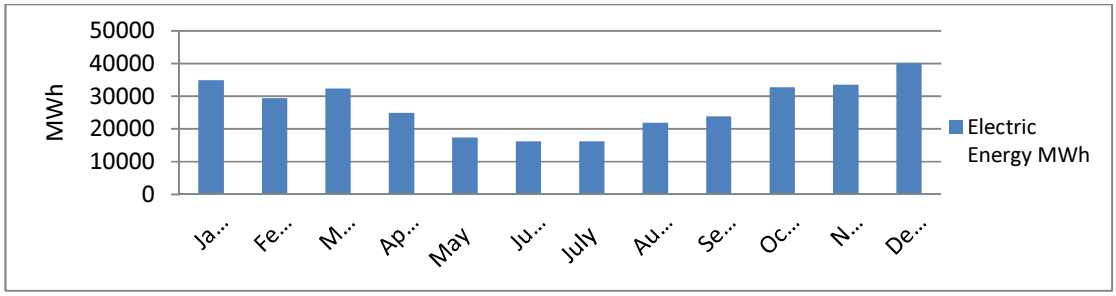

Figure 4-24 Electric energy by month for direct TES without back-up

It is even more important to have an average value of the electric energy provided to the grid per hour in order to compare months of different lengths. This is shown in Figure 4-25. Less than half as much electricity is produced during the winter months (compared to the results for summer).

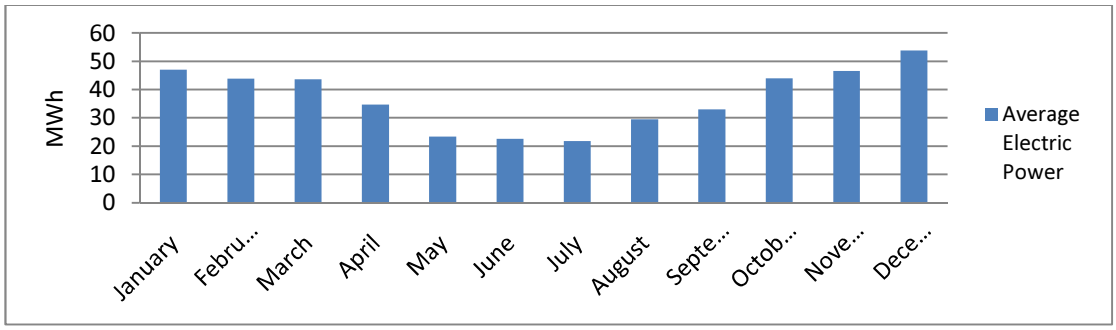

Figure 4-25: Hourly average electric power for direct TES without back-up

4.7 Models in Antofagasta comparison

Table 4-1: Summary of results

	Electric Energy MWH	Average Hourly Electric Energy MWh	Solar Fraction
Direct Production	332,409	38	100.0%
Indirect TES wBU	876,000	100	35.1%
Indirect TES woBU	307,766	35	100.0%
Direct TES wBU	876,000	100	37.0%
Direct TES woBU	323,695	37	100.0%

Indirect TES is less efficient than direct production or direct TES because it has an additional heat exchanger. Direct production is more efficient than Direct TES because it has fewer losses in the solar field due to its lower temperature at the inlet. The models with TES and without back-up are equal to the solar fraction of the same option with back-up.

Figure 4.26 shows the amount of electric energy produced using solar energy only on an hourly basis, for January 6-11. The blue line is the model without storage. It has large peaks of energy. The turbine is assumed to be as efficient producing 1MW in the morning as producing 250MW at noon, which is an assumption that introduces errors. Due to the buffer effect of the storage with Indirect TES and Direct TES, the peak radiation is transferred to the time where less or no radiation is available. Since Direct TES is more efficient than Indirect TES, the former can provide hot salt to produce steam for longer periods of time.

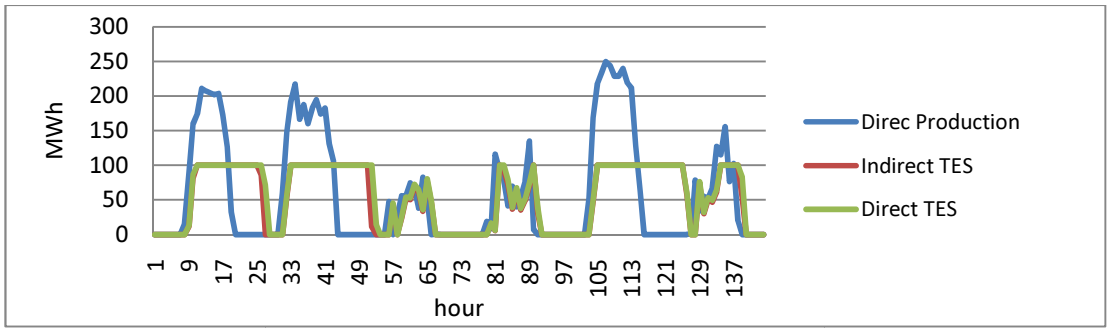

Figure 4-26: Solar electricity during the summer in Antofagasta

Figure 4-27 shows that less energy is stored and released after sunset during autumn, when there are more clouds and fewer hours of sunlight. Similarly, direct storage is more efficient than indirect TES during the summer.

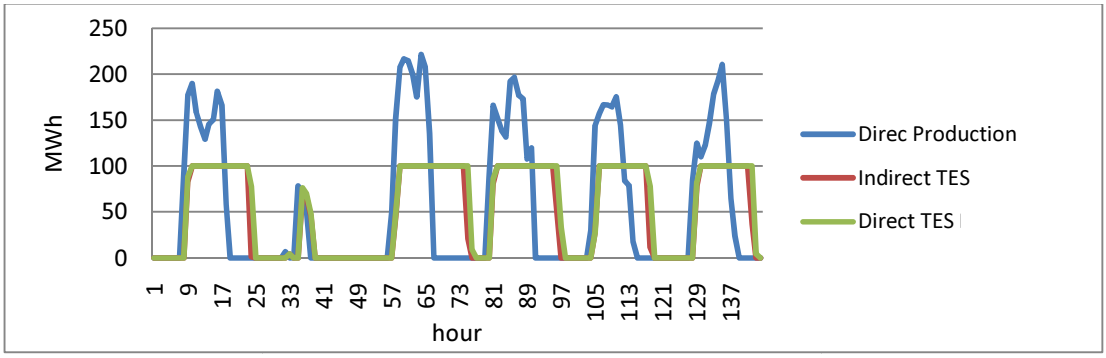

Figure 4-27: Solar electricity in autumn in Antofagasta

Figure 4-28 shows the hourly electric energy produced using solar energy only for June 1-6. There is less radiation available and during some hours no heat is stored in the models with TES. Production is the same as in the direct production model.

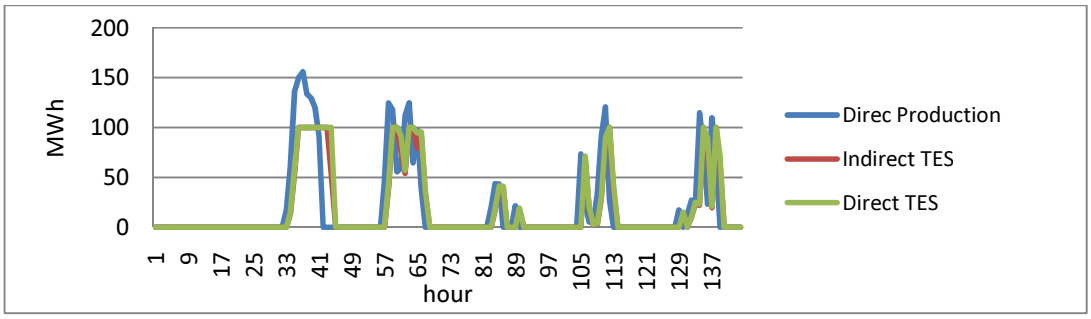

Figure 4-28: Solar electric energy per model in winter in Antofagasta

As can be seen in Figures 2-29, 2-30 and 2-31, plants with and without TES behave similar on cloudy days. This is due to the fact that all of the heat received heat is transformed into electricity.

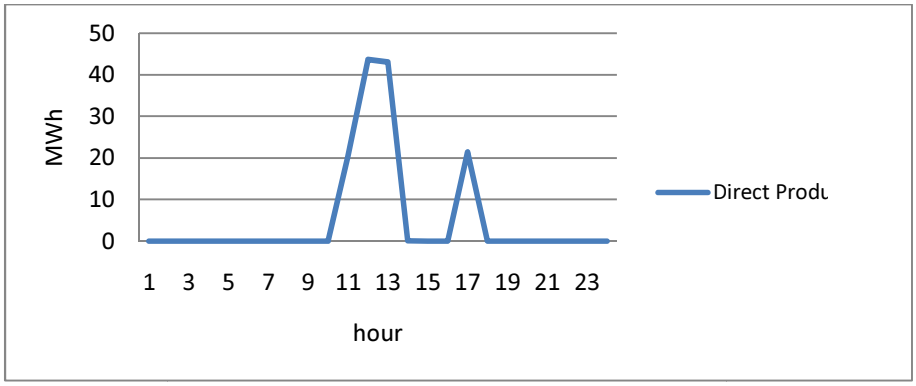

Figure 4-29: Solar electricity for direct production on a mostly cloudy day in Antofagasta

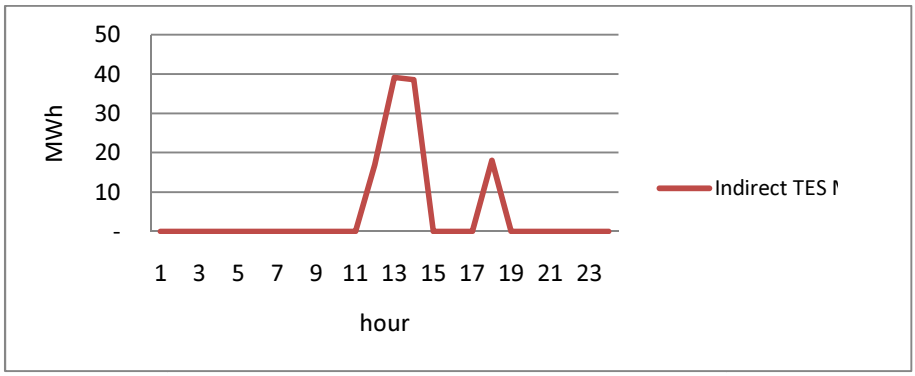

Figure 4-30: Solar electricity for indirect TES on a mostly cloudy day in Antofagasta

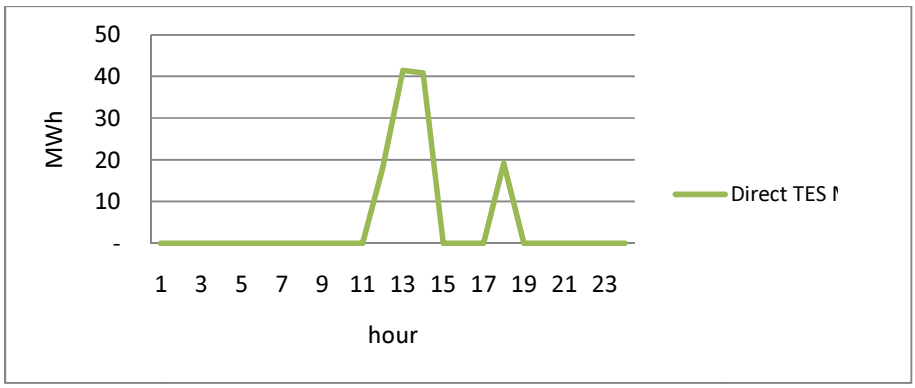

Figure 4-31: Solar electricity for direct TES on a mostly cloudy day in Antofagasta

Figures 4-32, 4-33 and 4-34 show that the plants behave similar on partly cloudy days due to that all the received heat is transformed into electricity and almost no storage can be observed.

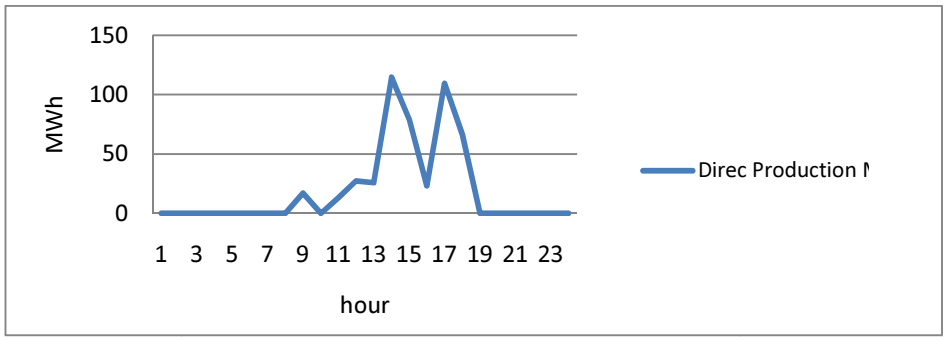

Figure 4-32: Solar electricity for direct production on a partly cloudy day in Antofagasta

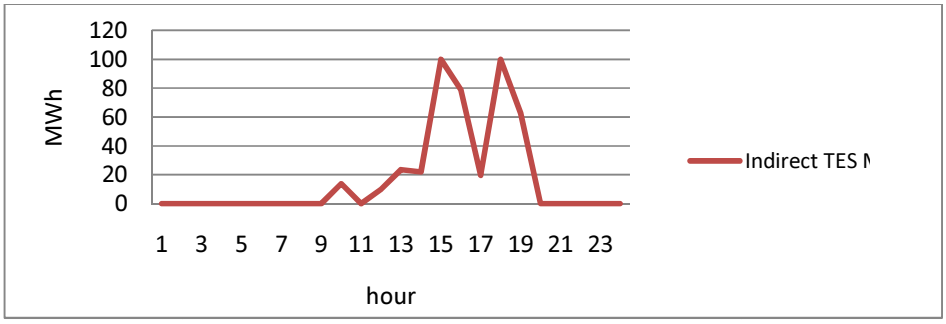

Figure 4-33: Solar electricity for indirect TES on a partly cloudy day in Antofagasta

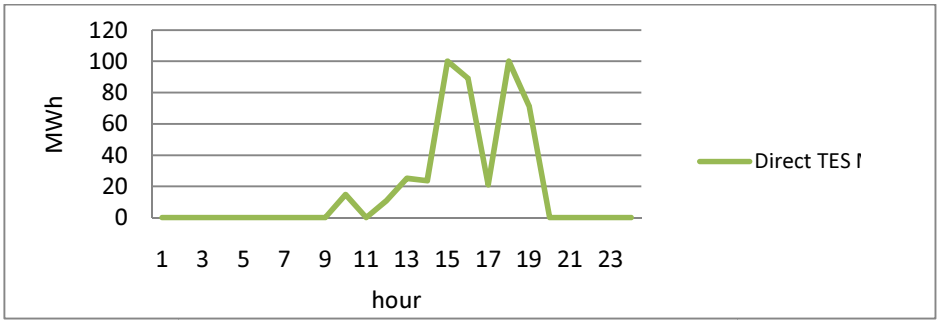

Figure 4-34: Solar electricity for direct TES on a partly cloudy day in Antofagasta

A radically different behavior can be observed in models with TES (Figures 4-35, 4-36 and 4-37). In these cases, once the maximum turbine output is achieved, the remaining heat is stored for lower radiation times. In direct production, all of the heat goes to the turbine to produce electricity, making the energy production vary.

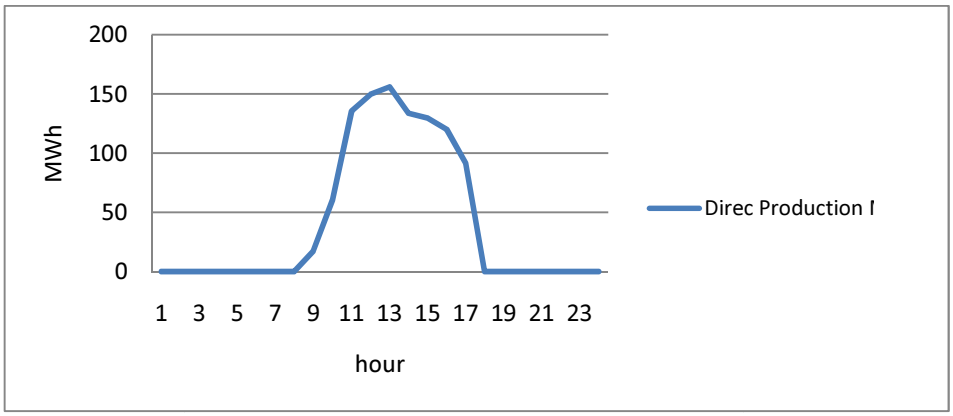

Figure 4-35: Solar electricity for direct production on a mostly sunny day in Antofagasta

Figure 4-36 shows that this model provides a shorter time of steady 100MW production (compare to Figure 4-37).

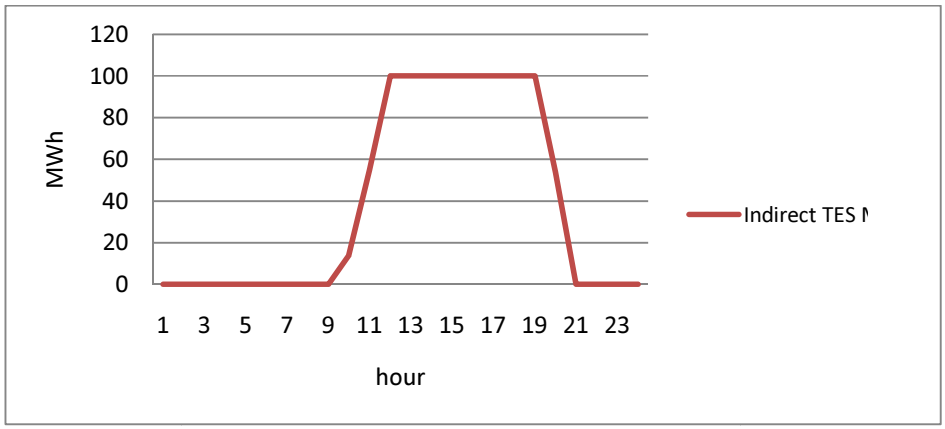

Figure 4-36: Solar electricity for indirect TES on a mostly sunny day in Antofagasta

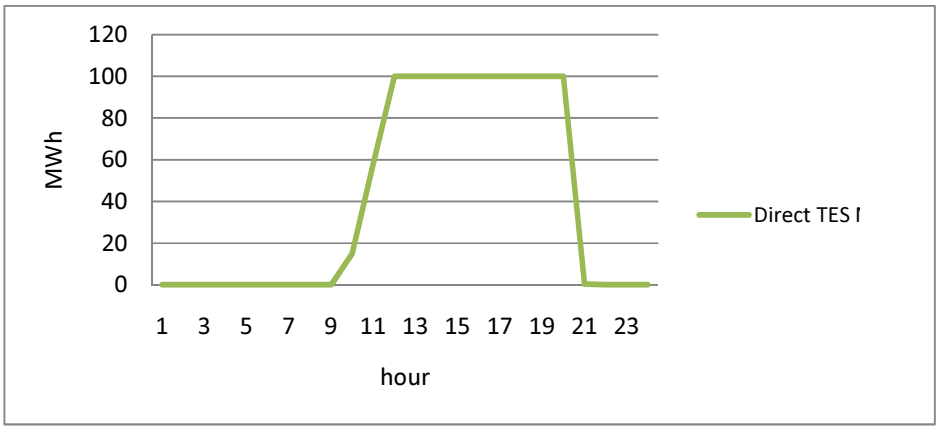

Figure 4-37: Solar electricity for direct TES on a mostly sunny day in Antofagasta

Direct storage is more efficient than indirect storage and such models can store more energy using the same area of collectors. During summer days, the initial capacity of around 60 million kilograms of Hitec XL is sufficient to meet demand. An economic model should be run to determine optimum storage capacity.

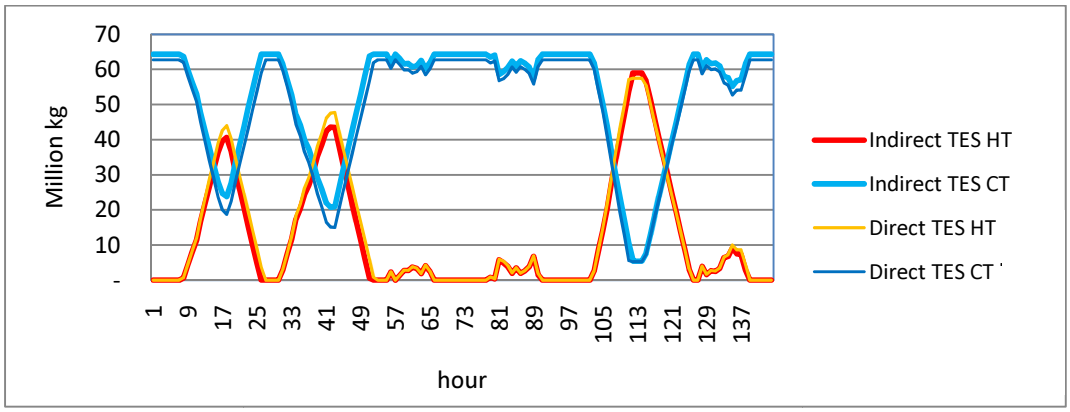

Figure 4-38: Tank levels per model during the summer in Antofagasta

On autumn days, we observe less intensive use of storage. The hot tank is used more as a device through which solar salt passes than as a storage location. The cold tank is used for storing most of the salt almost all of the time.

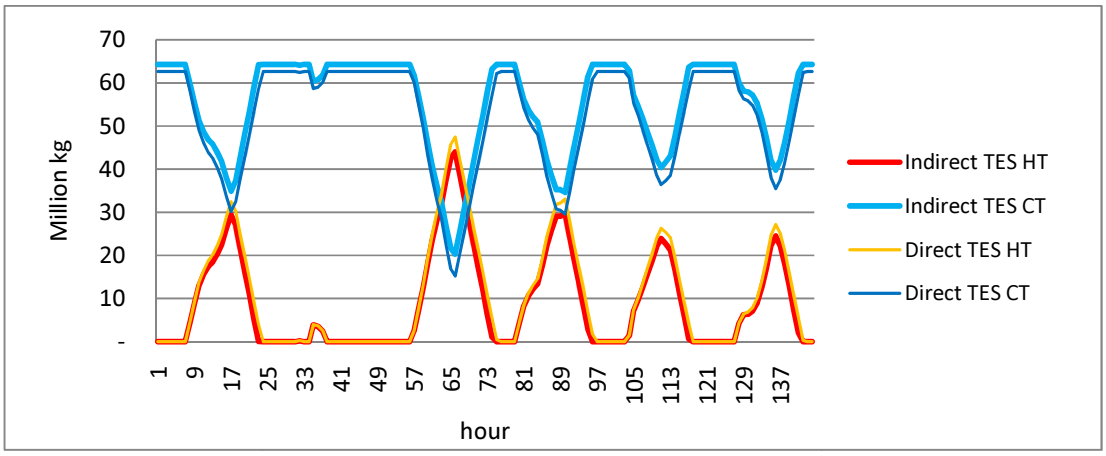

Figure 4-39: Tank levels per model during autumn in Antofagasta

Storage capacity in the collector area is barely used at all on winter days. Back-up is necessary to increase plant operation.

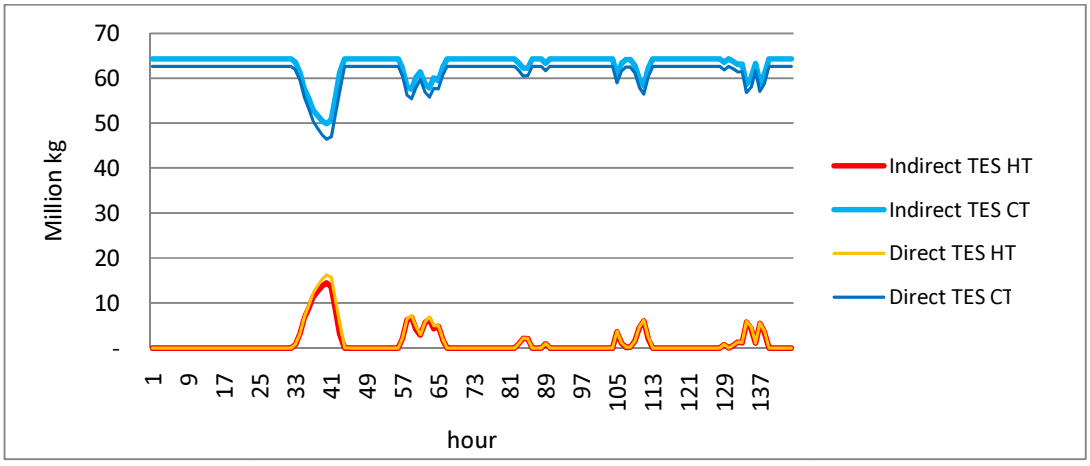

Figure 4-40: Tank levels per model in winter in Antofagasta

4.8 Monthly energy comparison for the three cities and five models

The monthly hourly average energy production is shown in Figure 4-41. This average is the sum of the energy produced per month divided by the number of hours in that month. The bar shows the range of the monthly average energy production per hour, which is

the hourly average of the worst and best months. The dot stands for the average for all months. Three conclusions can be drawn from this figure.

Calama is the best location for installing a solar trough plant for every model. The lower part of the bar for all the Calama models is above the averages of both other cities and the average annual energy for this city is approximately twice of that of other cities.

Direct energy production shows a better average and a wider range for all of the cities. TES modulates the energy production of the plants, making this kind of plants produce energy on a steadier basis.

Direct TES performs better than indirect TES because it has one less heat exchanger. This gives the plant a better average electric production, better best months and better worst months. This will certainly improve the cost of electricity.

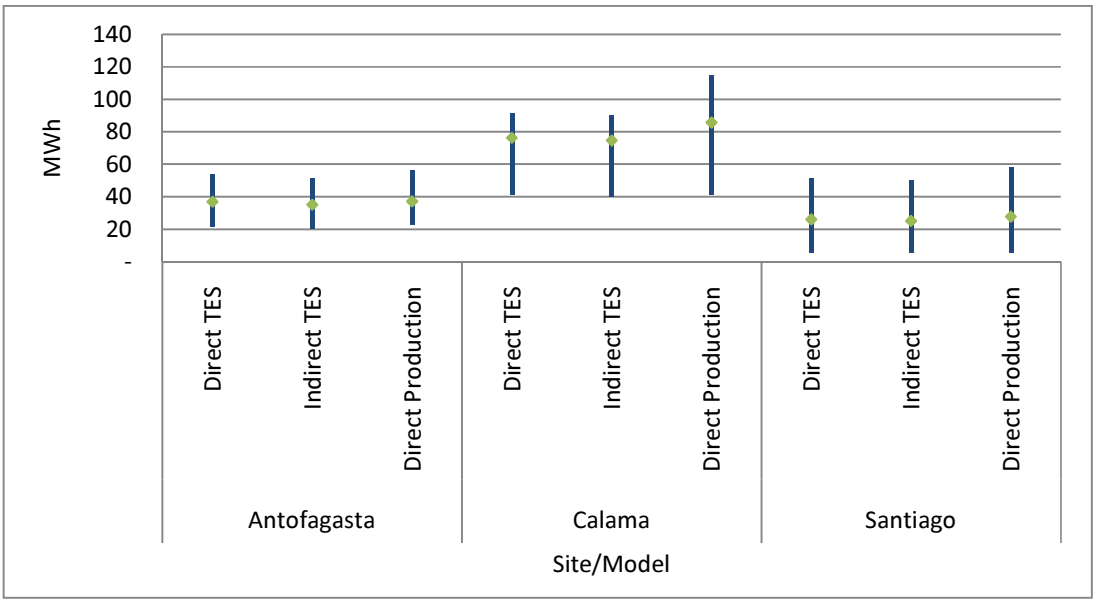

Figure 4-41: Average energy per site and model

Figure 4-42 shows the total electric production of energy for the three models in each city. Direct production is best in all of the sites followed by direct TES and finally

indirect TES. The amount of produced in this city is twice that of Santiago and Antofagasta.

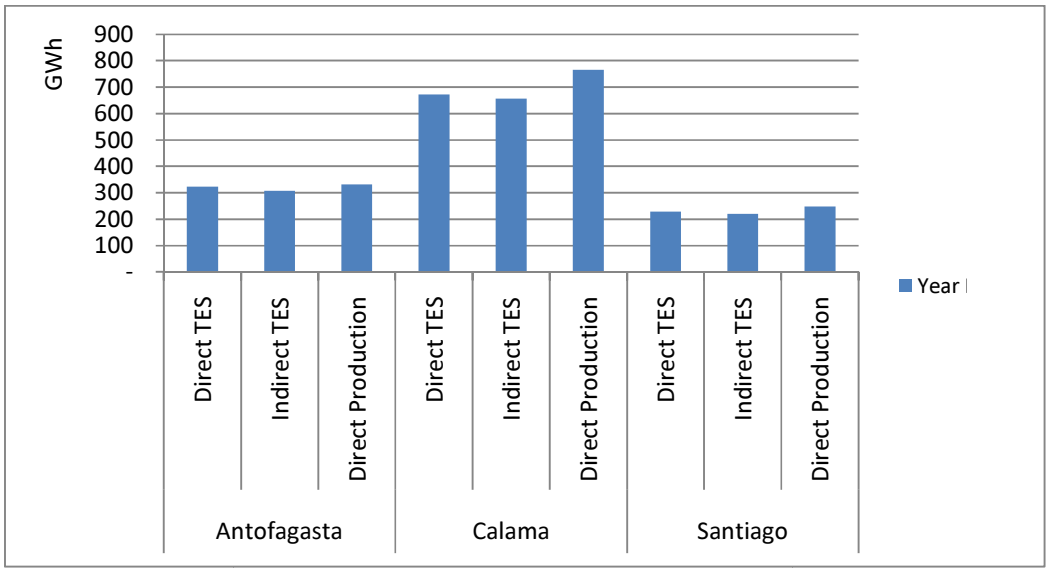

Figure 4-42: Yearly electric generation for all models and sites

Important differences in Calama

Figures 4-43, 4-44 and 4-45 show the tank occupancy for the direct TES in Calama for six days. In each figure, the left graph shows solar fraction for those six days and the right graph shows tank usage. The red line shows the quantity of salt in the hot tank and the blue line shows HTF in the cold tank.

Figure 4-43 is for summer and shows three blue zones, which means that energy production was continuous except for during a few hours. The tank levels for summer vary zero to maximal capacity every day, using the 12 hours of thermal storage.

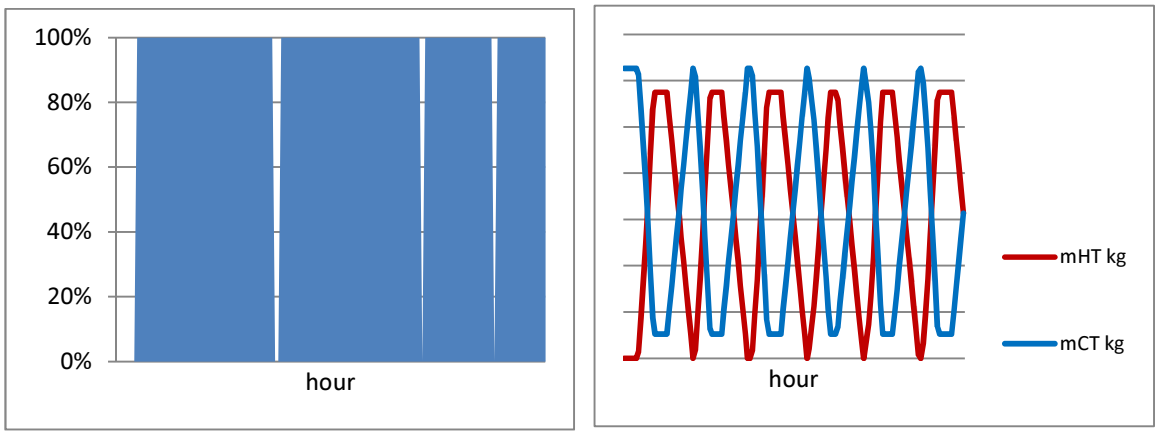

Figure 4-43: Solar fraction and tank levels for Direct TES Calama in summer

For autumn we see breaks every day and the tanks capacities are not completely used.

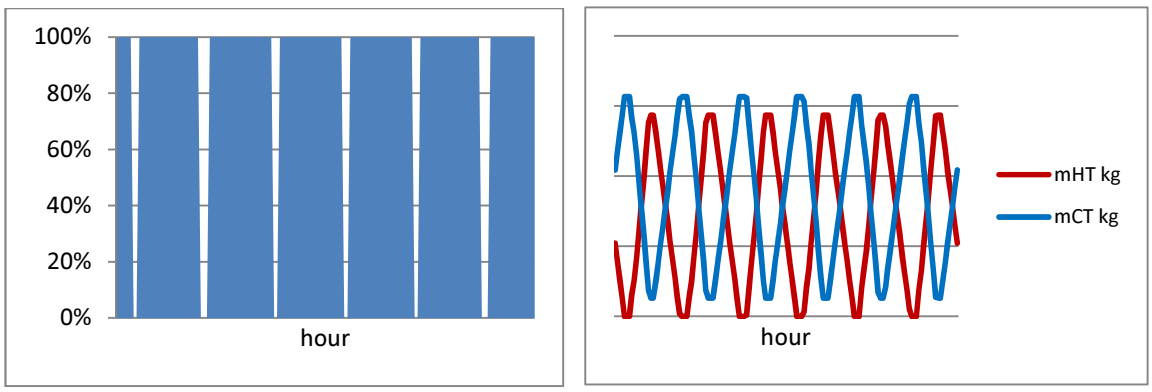

Figure 4-44: Solar fraction and tank levels for direct TES Calama in autumn

During the winter, there are large breaks in power generation and there are days when the tanks are hardly used. Comparing these results with those of Antofagasta, that plant behaves the best in days similar to autumn days in Calama. Results for indirect TES in Calama are similar to direct TES here, but not as good as those for the direct storage option.

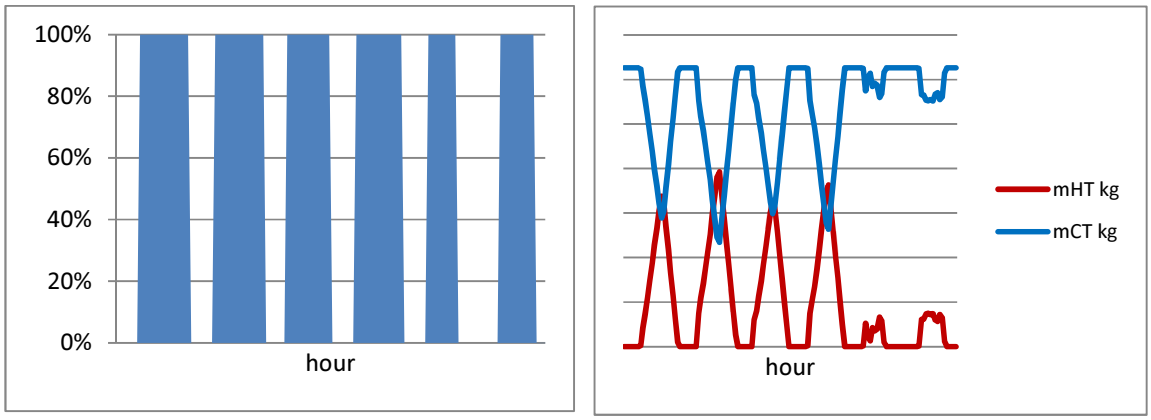

Figure 4-45: Solar fraction and tank levels for direct TES Calama in winter

Figure 4-46 shows the results for direct power production in Antofagasta and Figure 4-47 shows the direct power production model in Calama. Note that the peaks of power production are higher in Calama than in Antofagasta. More energy is produced in Calama than in Antofagasta, but neither present smooth production. There are high peaks at noon and steep decreases thereafter.

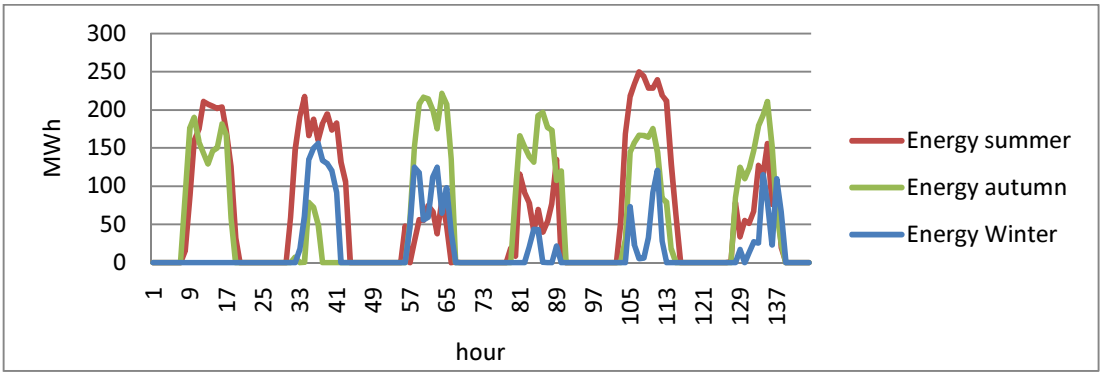

Figure 4-46: Energy production in direct production model in Antofagasta

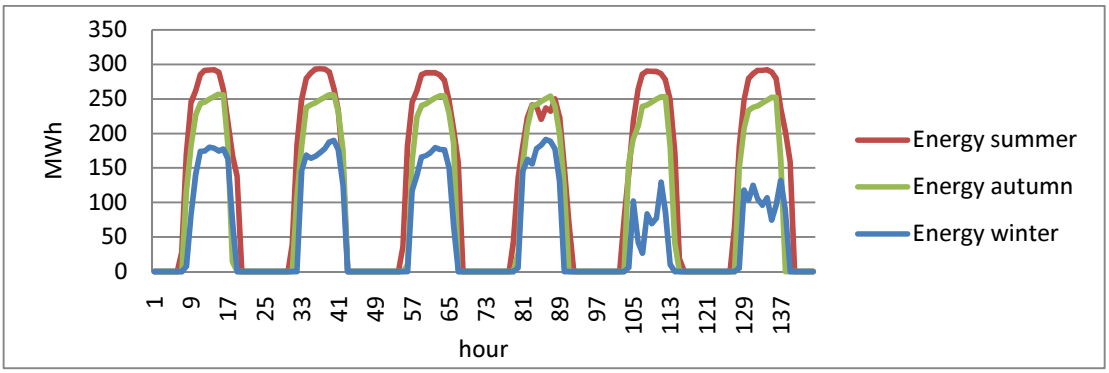

Figure 4-47: Energy in direct production model for Calama

Electricity production is mostly done using solar resources except in February, when radiation levels fall and fossil back-up is larger than solar-added heat. This decrease is probably related to a climate phenomenon known as Bolivian Winter. A yearly solar fraction of 77% is achieved in Calama with this type of plant.

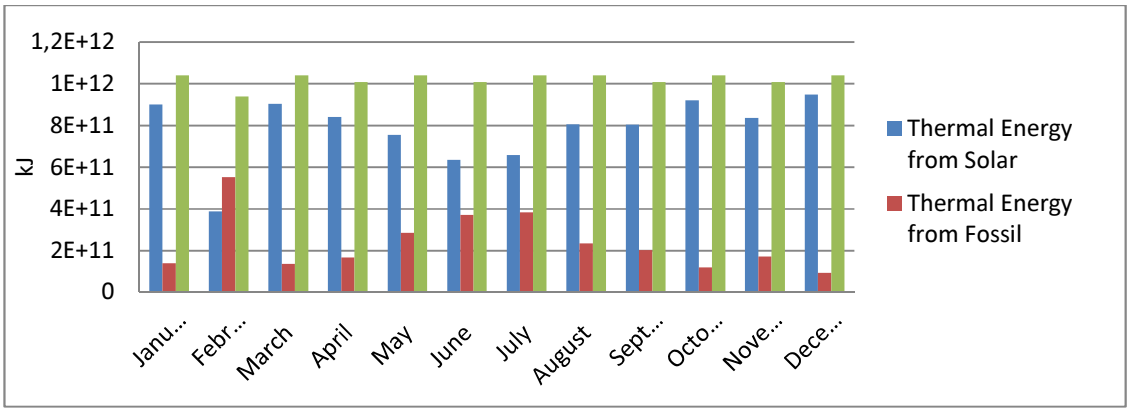

Figure 4-48: Thermal energy to power block per source in Calama for Direct TES with BU

Important differences in Santiago

For Santiago, the plant with direct and indirect TES would be a fossil plant with solar assistance rather than a solar plant with back-up. Given that the yearly solar fraction is just under 26%, it has to produce most of its energy by burning fuel.

There is practically no solar energy production during the winter. During December, the rest of the power comes from the solar source. For the other months more than half of the energy comes from the fueled back-up.

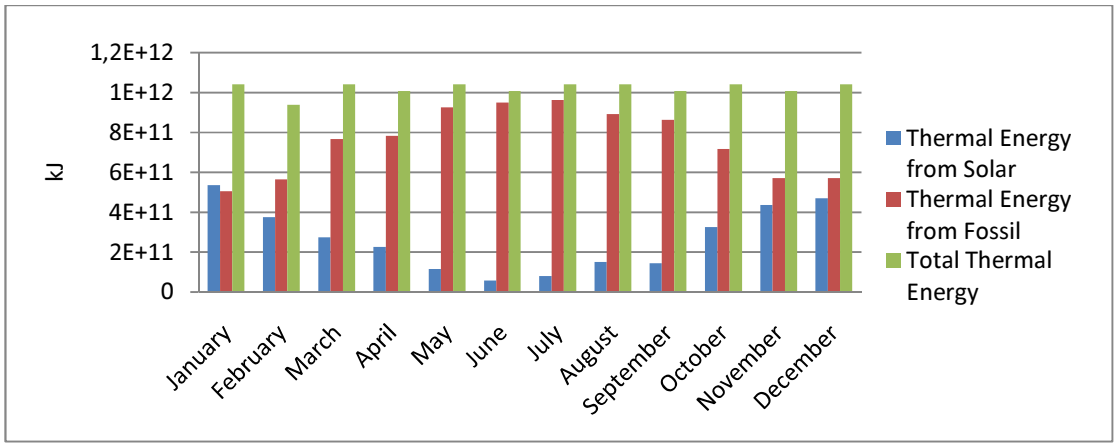

Figure 4-49: Monthly energy to power block per source for Direct TES in Santiago

4.9 Validation of the thermodynamic model

It is important to evaluate the quality of the thermodynamic model in order to achieve reliable results and produce inputs for the economic model. We thus researched and discovered a plant for which enough information available, namely the SEGS VI located in Kramer Junction, which has a net electric output of 30 MWh. A few minor modifications were made to the direct production model in order to simulate the SEGS plant as much as possible.

Assumptions

Based on the NREL webpage, it was assumed:

- Tat the fluid outlet temperature is 390ºC
- That the plant has a back-up gas boiler that can be used from noon until 6 PM to produce steam
- That the cycle efficiency was set at 37.5%

- That the solar field is 188,000m^2
- That the net output is 30MWe, the parasitic consumption is 17.3% (Sargent & Lundy LLC Consulting Group, 2003) and the gross output of the plant is 36.275 MWe.

The radiation data used was the typical meteorological year for Daggarett, where SEGS I and II are located, but it is 50 km away from Kramer Junction. No weather data for the specific location was found, but 50 km is close enough to reproduce the plant. The typical meteorological year weather data is a selection of the most representative weather data for every hour of the year for all the years for which the information is available. The historical information of the produced power and radiation comes from a presentation offered by the Kramer Junction Operating Company, (Frier, 1999) We looked for information about a plant with TES such as Andasol One, but this plant opened recently and no data is available yet.

Results

The SEGS VI plant was simulated using the meteorological data for Daggett in Southern California (NREL) with the results plotted and tabulated in Figure 4-50 and Table 4-2.

In Figure 4-50, the electric production for different years (Frier, An Overview of the Kramer Junctions SEGS Recent Performance, 1999) is plotted against the average radiation for the year. Years with radiation similar to the radiation data used for the modeled year of the SEGS VI plant were chosen.

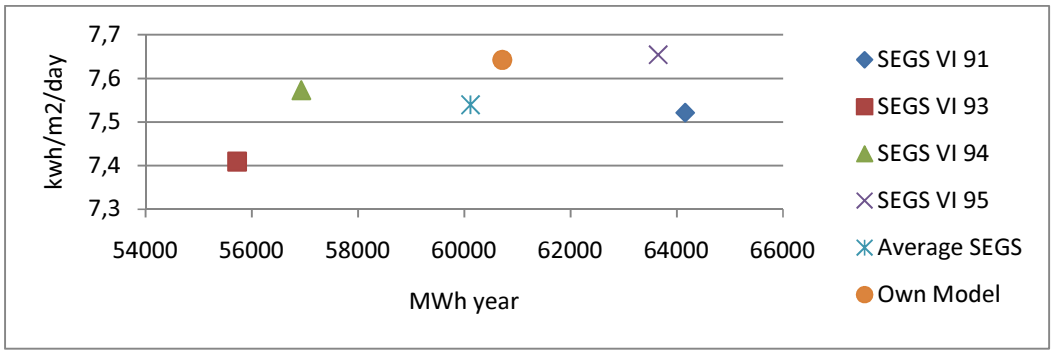

Figure 4-50: Gross electric production vs. radiation for the different plants and models

Table 4-2 presents the gross electric production of the plant for different years, the average electric production of the different years for the SEGS VI plant and the model correlated to the daily average radiation.

Table 4-2: Electric production and radiation

Plant	Yearly Electric Production MWh	Difference to own model	DNR kwh/m2/day	Difference to own model
SEGS VI 91	64155	6%	7.521	-2%
SEGS VI 93	55725	-8%	7.409	-3%
SEGS VI 94	56934	-6%	7.573	-1%
SEGS VI 95	63650	5%	7.654	0%
Average SEGS	60116	-1%	7.539	-1%
Own Model	60716		7.642	

Summary

The results of the model are similar to the historical data of the plants and it can be said that the model created is valid for the purposes of the thesis. Due to the similarity between the models and the absence of more information, it can be said that the other four models are valid, too.

4.10 Chapter Summary

As predicted, production in winter is lower than in other months, and back-up is necessary to improve low plant usage during that season. Back-up can lower the

levelized electricity cost utilizing the rankine cycle more often than it would be used in the solar mode alone.

The most efficient model for the rest of the year is direct storage. Given that very little storage is used during the winter, direct electric production should be better.

Tank capacity be determined based on the cost of the system and the energy losses due to defocusing when no fluid is available to remove heat from the HCE. On a radiant day, the hot storage could be full and the cold tank could be empty for periods of time. If that occurs, no refrigeration of the HCE could break the glass envelope and degrade its selective paint.

There is a need to study the economics of back-up. Researchers must evaluate the cost of fuel over the plant's lifetime, the cost of installation and the sale price of electricity. This should be compared to the projected value of electricity for the lifetime of the plant.

The collector area is another key milestone given that this variable would determine the storage capacity and size of the plant (how much fluid needs to be stored under the economical optimization of the storage size and the capability of the turbine).

In regard to the site, it is clear that the best site for installing a solar power plant among the cities considered in this study is a location near to Calama, which presents the highest radiation levels throughout the year.

5. ECONOMIC MODEL

5.1 Introduction

The economic value of the project is as import as the analysis of the thermodynamic results. Profitability is relevant for estimating what, if any, government subsidy will be needed. These results will vary by country. For example, if the country is rich in fossil fuels like natural gas, the electricity cost would be less expensive than it would be in a country like Chile that imports such fuels. In some cases, solar power plants will be less competitive than gas natural fueled plants.

The sale price of the electricity will depend on the diversity of the electric power producers in the network. These factors affect electricity price paid and its variability. Other factors include distance to the nearest substation and water availability and cost.

The most important aspect of solar power is the solar resource because it defines the solar field area, storage capacity and the plant's operational results. Solar resources are directly related to the project's bottom line.

The economic model was built using Microsoft Excel and uses its Solver Add-On to obtain the results.

As we know from the thermal model, only one year is computed thermodynamically, so the same energy results are used for the following years.

The cost model works as shown in Figure 5-1:

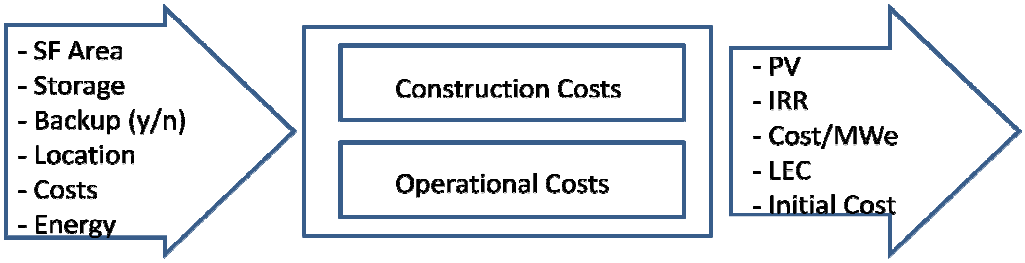

Figure 5-1: Cost model diagram

5.2 Economic concepts

This section presents descriptions of key economic concepts in order to help the reader understand the inputs and results as well as the procedure used for the economic model.

Present value

The present value of a money flow that occurs in the future is calculated as follows:

$$\boldsymbol{PV = \frac{Flow}{(1+r)^n}} \qquad \textbf{(5-1)}$$

Where *r* is the opportunity cost of capital or discount rate, and *n* the period of time ahead of the base time.

Net present value

Net present value (NPV) is the sum of all of the flow of every period *i* of a project brought to the present date with the corresponding discount rate. If the NPV is positive, the project is profitable for the investor. If it is zero, the investor should be indifferent. If it is negative, the project is not economically beneficial.

$$\boldsymbol{NPV = \sum_i \frac{Flow_i}{(1+r)^i}} \qquad \textbf{(5-2)}$$

Internal rate of return

The internal rate of return (IRR) of a project is the discount rate that makes the NPV be zero.

IRR can be positive, zero or negative. A value above the discount rate means that money flows at a higher rate earn profits. When the IRR is lower than the discount rate, the project is not suitable for that investor but could be for someone else with a less expensive cost opportunity.

Levelized energy cost

The levelized energy cost, or LEC, given by equation 5-3 is the cost of energy that makes the present value of the project zero (IEA, 1991). If the price of electricity is higher than the LEC, the project is feasible. If not, an economic incentive from government should be used in order to make it interesting to investors. (Quaschning, Kistner, & Ortmanns, 2002)

$$\boldsymbol{LEC} = \frac{\left(\boldsymbol{CC_{ii,pv}} + \boldsymbol{C_{om,pv}} + \boldsymbol{C_{fuel,pv}} + \boldsymbol{C_{tax,pv}}\right) \cdot \boldsymbol{crf}}{\boldsymbol{E_{gen}}} \qquad \textbf{(5-3)}$$

Where $CC_{ii,pv}$ is the present value of the initial investment, $CC_{om,pv}$ represents the present value of the operation and maintenance costs, $CC_{fuel,pv}$ is the present value for fuel in the back-up system, $CC_{tax,pv}$ stands for the present value of the taxes to be paid, crf is the reciprocal of the factor that brings the energy injected to the grid to present and E_{gen} is the injected energy in a given year.

IRR and NPV are two indicators of the quality of a project. NPV shows if a project is beneficial or not and can be positive, negative or zero. IRR shows how far away a project is from being good or bad. We can use these indicators to compare different projects and make decisions about their development. LEC is also a good economic indicator that can be used by the government to determine how many incentives this technology requires in order to be developed in the country.

5.3 Inputs and Assumptions

This section presents a description of the inputs to the model. Most of the inputs are equipment or installation costs. These and all other costs are listed in US$ per feature. For example, the cost of a mirror is listed in US$ per square meter of solar field. Most of the costs come from Sargent & Lundy LLC Consulting Group, 2003 because it has detailed cost drivers and is one of the only reliable sources of solar equipment cost estimates.

Energy produced

The amount of energy produced by a plant and characteristics such as location and aperture area come from the thermodynamic model developed in Chapters 3 and 4. The results of the simulations in monthly values for a period of one year are the energy inputs for the economic model. A value for solar produced energy is given to the model, and in case of fossil back-up, the amount of energy produced with the resource is given.

Parasitic

A variable parasitic level was chosen for online state. Twenty percent of the produced power is not sold or used by the power plant itself. For offline mode, parasitic is neglected and consumption is assumed equal be zero.

Mirrors

The cost of the mirrors was set at US$40 for each square meter of aperture (Sargent & Lundy LLC Consulting Group, 2003).

Structure

The cost of the structure was set at US$109 /$m^2$ (Sargent & Lundy LLC Consulting Group, 2003). Thisis the sum of cost of the concentrator structure, concentrator erection, drive, foundations and other spares per square meter in 2004.

Heat collecting element

The cost of the HCE was set at US$43/m^2 (Sargent & Lundy LLC Consulting Group, 2003).

Solar field heat transfer fluid

This cost depends on the system used. For a direct storage system, the fluid is Hitec XL, which costs US$1.19/Kg. In the case of indirect storage or direct production, the fluid used is Therminol VP1, which costs US$2.2/Kg. (Kearney D. , et al., 2003). The mass of HTF is calculated as:

$$\boldsymbol{m_{HTF} = \frac{SF_{Area}}{5.75} \cdot \left(\frac{0.054}{2}\right)^2 \cdot \pi \cdot \rho_{HTF} \cdot 1.1\ kg} \qquad \textbf{(5-4)}$$

Where SF_{Area} is the area of the collectors (m), 5.75 is the aperture of the collectors (m), 0.054: is the inner diameter of the HCE (m), and ρ_{HTF} is the density of the heat transfer fluid flowing in the solar field (kg/m^3). The result is 1992 kg/m^3 for Hitec XL and 815 kg/m^3 for Therminol VP1 and 1.1 is a factor accounting for the fluids in other pipes that are not heat collecting elements (no units).

Solar field pumping systems

The cost of SF pumping systems was set at US$31 per m^2 of solar field and accounts for interconnection piping, electronics and control and header piping (Sargent & Lundy LLC Consulting Group, 2003).

Contingency

Contingency expenses were estimated in US$11 per square meter, (Sargent & Lundy LLC Consulting Group, 2003).

Hot tank and cold tank storage

The cost of each tank was calculated based on the cost given in Kearny et al, 2003 for storage per kWh_t but for the thesis this cost must be listed in $/kg of storage fluid and is calculated as follows:

$$\boldsymbol{HT\ Cost = CT\ Cost = \frac{1}{2} \cdot C_{p\ HTF} \cdot \frac{Cost}{3600} * \Delta T\ USD} \qquad \textbf{(5-5)}$$

Where for direct storage $C_{p\ HTF}$ is1.447 kJ/kg K and Cost is 16.18 and 16.67 US/kWht for direct and indirect TES, respectively. ΔT= 190 and 185°C for direct and indirect TES, respectively.

Table 5-1: Storage cost (Kearney D. , et al., 2003)

	ΔºC	Storage cost $/kwht
	200	15.2
Direct TES	190	16.18
Indirect TES	185	16.67
	150	20.1

Thus, HT Cost=CT Cost= US$0.6178/kg for direct TES and US$0.6197/kg for indirect TES and both tanks have capacity for all of the salt.

Storage fluid

Hitec XL is always used in storage and we use the same cost as for the HTF in solar fields of US$1.19/kg is used. The mass of Hitec XL calculated was similar to that presented in Chapter 3 and provides 12 hours of heat storage for the rankine cycle. HTF needed for 12 hours of direct thermal storage is as follows: 62,652,989 kg and for 12 hours of indirect thermal storage: 64,000,173 kg.

Storage heat exchanger

In case of Indirect Storage, where Therminol VP1 transfers heat to Hitec XL, a heat exchanger with an installed cost of US$100/kWe was installed (Sargent & Lundy LLC Consulting Group, 2003).

Storage pumping system

The pumping system in the storage tanks was estimated in US$50,000 for a 12 hour TES system for both direct and indirect types.

Turbine

Turbine costs were estimated as the average of the cost for a turbine in Aspen Systems Corporation, 2000 . A range of US$400 to US$800/kW is given in this report, so 600US$/kW was chosen.

Generator

According to Sargent and Lundy, the cost of the generator for 2004 is US$367/kWe.

Cooling

The cost of the cooling system was estimated to be US$150/kWe. That is, is US$100/kWe, which is the same as that of the heat exchanger, plus 50%.

Water Pumps

The cost of water pumps in the cycle was estimated at US$10/kWe of installed capacity.

Steam generator

The cost was estimated at US$100/kWe of installed capacity (Sargent & Lundy LLC Consulting Group, 2003).

Back-up boiler

For the models with fired back-up, the boiler cost was estimated to be US$150/kWe. This is based on an estimate based on the cost of the Steam Generator plus 50%.

Transmission line

Transmission line costs were estimated by Mr. John O'Shea, General Manager of RTHO Elektrische (www.rtho.com) at US$35,000/km for 100MWe of installed capacity. RTHO Elektrische is a company that designs and sells products for power lines and substations. The US$35,000 per km can be broken down as follows:

- US$4,000 /km for labor
- US$18,000 /km for the towers
- US$9,300 /km for the conductor
- US$3,600 /km for isolators and others

Substation

As was true for the Transmission Line, substation costs were estimated by Mr. O'Shea at a cost of US$2,600/MWe of installed capacity. That amount can be broken down as follows:

- US$1,2800 /MWe for labor
- US$1,020 /MWe for switches, pedestals and lightning protection
- US$300 /MWe for connectors and others

The distance to the closest substation was set on 30 km for all of the locations.

Site

The cost of the land was at US$350 per hectare, or US$0.035 per square meter for all locations based on data from Mr. Roberto Otárola of Abengoa Chile.

The cost of the site is not an important cost driver and at US$350/ha it represents less than 1% of the total project cost. This cost was sensitized up to US$150,000/ha, in which case it represents approximately 4% of the total cost. We will make no further effort to find a more accurate price.

Engineering and planning

This cost driver was set at 15% of the direct costs. This is the default value in the Solar Advisor Model free software developed by NREL.

Mirror maintenance

Mirror maintenance represents 85% of the cost of operation and maintenance according to the Sargent & Lundy LLC Consulting Group, 2003. The cost is US$4.675/kW month.

Repairs

This item represents 15% of the O&M cost as stated in Sargent & Lundy LLC Consulting Group, 2003, or US$0.825/kW month.

Sale cost

When selling electricity, a fee must be paid to transmit the power over the grid. The table below presents the cost of transmitting some representative tracts. The fee is proportional to the plant's net maximum output power, which also is shown.

Table 5-2: Sale cost (CDEC-SIC)

Guacolda-Maitencillo 220		
Power	202.2	MW
Fee	517.0	kUS/year
Fee/Power/Moth	213.1	US/MW month
S. Luis- Quillota 220		
Power	595.7	MW
Fee	2111.0	kUS/year
Fee/Power/Moth	295.3	US/MW month
Cholgua-Charrua 220		
Power	202.6	MW
Fee	530.8	kUS/year
Fee/Power/Moth	218.3	US/MW month
A. Chillan- Parral 154		
Power	30.1	MW
Fee	1155.8	kUS/year
Fee/Power/Moth	3204.3	US/MW month
Concepcion-Charrua 154		
Power	81.9	MW
Fee	990.3	kUS/year
Fee/Power/Moth	1007.2	US/MW month
A. santa- S. Luis 220		
Power	181.9	MW
Fee	1591.6	kUS/year
Fee/Power/Moth	729.1	US/MW month
Average	944.5	US/MW month

The toll is calculated as:

$$\boldsymbol{Normalized\ Monthly\ Toll} = \frac{\boldsymbol{Fee}}{\boldsymbol{Power * 12\ Months}} \quad \frac{\boldsymbol{USD}}{\boldsymbol{MW\ Month}} \tag{5-6}$$

The fee used is the average of the normalized toll. Therefore, the toll was estimated at US$955 per installed MW per month. If the installed capacity is 100MW, the monthly transmitting cost would be US$95,500. This cost is projected to increase at a rate of 5% per year.

Fuel cost

Diesel is used as a back-up fuel for the fossil burner boiler. The cost of diesel was estimated as an average cost for diesel for the combined cycle thermal plants in the SING system in Chile (CNE, 2009) . This cost is US$112.71/MWe generated with fossil BU and is estimated to grow at a rate of 5% per year.

Natural gas is another option as a back-up fuel, but it is not reliable as diesel. We had a good supplier with low prices for natural gas, but it is no longer providing the country with the fuel. Coal is not an option because it would pollute and affect the efficiency of the mirrors and HCE. Another advantage of diesel is that it can be replaced with biodiesel.

Sale price

The sale price was estimated using past data (CNE, 2009). The used sale price is the average market price. It was 81.580CLP/kWh with an exchange rate of550CLP/US$ in April 2009. The sale price at SING is US$148.33/MWh and is estimated to grow at 5% per year.

Taxes

Two kinds of taxes apply in Chile. One is the value added tax (IVA), which is paid to the State and represents 19% of the sale price. All costs and earnings are given in net values, without including IVA. The IVA is applied to the operation costs listed for each month.

The company's earnings are taxed at a rate of 17% of the earnings after IVA and depreciation.

Depreciation

A five-year linear depreciation scheme is assumed to minimize the tax load. There is no remaining value of the assets is applied. The site and engineering do not depreciate.

Output

The output of the economic analysis is a table containing present value (PV) in US$ with a discount rate of 15% assuming that energy is sold at US$148/MWe and the plant is depreciated in 5 years.

The percentage of the internal rate of return (IRR) is given assuming that energy is sold at US$148/MWe and the plant is depreciated in 5 years.

The total construction cost (Cost) is given in US$ as if the plant were constructed "overnight" on December 31, 2009 and became available on January 1, 2010.

The cost per electric mega watt of installed capacity (Cost/MWe) is given in millions of US$/MWe.

The levelized electric cost (LEC) is presented in US$/MWh and in CLP/kWh at an exchange rate of 550 Chilean pesos per US$.

Table 5-3: Economic output example

		Units/Assumption
PV	$ (581,420,242.52)	15%, 142US/MWh 5y dep
TIR	0.7798%	142US/MWh 5y dep
Cost	$ (848,162,651.18)	C.D. 12/2009
Cost/Mwe	$ (8.48)	Mill US/Mwe
LEC	625.4017732	US/MWh
	343.9709752	CLP/kwh @ 550CLP/USD

As output, a summary of the cost divers is obtained to. The cost categories are given by Solar Field and Site, and account for the mirrors, structure, site and other considerations.

The next driver is the HTF system, which accounts for the heat exchanger and cost of the heat transfer fluid that runs through the solar field. Storage cost includes the two tank system and fluid as well as other considerations. The power block cost includes the turbine, generator, cooling system, pumping and solar steam generator. Contingency is a factor accounting for extras. Finally, the indirect costs refer to engineering and other costs.

Table 5-4: Cost drivers summary example

Costs Driver	USD		% total
Solar Field and Site	$	(212,561,632)	25%
HTF System	$	(1,450,218)	0%
Storage	$	(373,466,495)	45%
Fossil Backup	$	-	0%
Power Block	$	(122,700,000)	15%
Contingency	$	(18,262,309)	2%
Indirect	$	(108,222,284)	13%

5.4 Chapter summary

All of the information required to reproduce the models was presented. A good estimate of the cost and key economic indicators for a solar power plant can be obtained. The model is flexible enough to allow parameters to be modified as the location and plant models change.

LEC: The levelized energy cost is the cost of energy that makes the present value of the project zero. It is a good indicator of the support that this technology requires from the government.

PV: Present value shows if the project is economically feasible.

IRR: This is the discount rate that makes the present value of the project zero.

6. ECONOMIC RESULTS

6.1 Introduction

Now that the methodology and model assumptions for the economic analysis have been discussed (Chapter 5), we can turn to the results of the simulations. The most important results are the present value of the project for each concept and location and the initial investments required.

The first analysis involved considering a standard plant at different locations.The main characteristics of this plant are:

- Solar field area: 1,400,000 m^2
- Storage Capacity: 12 hours
- Turbine electric output: 100MW for direct and indirect TES plants, variable for direct production
- Parasitic consumption: 20% when online, 0% when offline
- Lifetime: 30 years
- For plants with back-up, a boiler is added.

The second analysis involves amplifying the solar field area of all of the plants. This is done by multiplying by one plus the factor between the annual energy produced by the best plant without back-up and the annual energy produced by the corresponding plant.

$$\boldsymbol{SF_{Area,Site}} = \left(\mathbf{1} + \frac{\boldsymbol{Energy_{year\ best\ plant}}}{\boldsymbol{Energy_{year,Site}}}\right) \cdot \boldsymbol{SF_{Original\ Area,\ \ Site}} \qquad \textbf{(6-1)}$$

This demonstrates the impact of extra investment in the solar field area in the power production and levelized cost of electricity.

6.2 Results for plants without back-up

The best LEC and thus the best present value and higher IRR are those obtained for Calama, so the amplified areas are based on that result. The amplifying factors (multiplier) are presented in the table below:

Table 6-1: Solar Field Amplifiers and Areas

	No BU								
	Calama			Antofagasta			Santiago		
	Direct Storage	Indirect Storage	Direct Prod	Dir	InDir	Prod dir	Dir	InDir	Prod dir
	Original Area	Original Area	Original Area	Original Area	Original Area	Original Area	Original Area	Original Area	Original Area
Original Area (m2)	1400000	1400000	1400000	1400000	1400000	1400000	1400000	1400000	1400000
Anual energy (MWh)	671666	656869	765686	323695	307766	332409	227679	219898	248217
Multiplier	1.140	1.166	1.000	2.365	2.488	2.303	3.363	3.482	3.085
Modified Area (m2)	1595974	1631925	1400000	3311639	3483042	3224824	4708201	4874811	4318650

Results for Antofagasta

Table 6-2: Economic results for Antofagasta, no back-up

	Antofagasta						
	Direct TES		Indirect TES		Direct Production		
	Original Area	Modified Area	Original Area	Modified Area	Original Area	Modified Area	Units/Assumption
PV	$ (325,755,867)	$ (265,175,101)	$ (347,269,429)	$ (382,529,787)	$ (304,213,337)	$ (723,460,598)	15%, 148US/MWh 5y dep
IRR	5.56%	9.05%	4.96%	7.57%	2.75%	2.40%	148US/MWh 5y dep
Cost	-725680991	-926438619	-737728564	-1085132190	-588070870	-1373007884	C.D. 12/2009
Cost/MWe	-7.3	-9.3	-7.4	-10.9	-2.4	-2.3	Mill US/MWe
LEC	342	245	365	288	324	330	US/MWh
	188	135	201	159	178	182	CLP/kWh @ 550CLP/USD
Produced Energy	323695	527563	307766	526505	332409	765686	MWh year

All of the projects have a negative PV and thus an IRR that is lower than the 15% discount rate with a sale price of US$148/MWe.

We can see a large improvement in the projects' LEC when the collector area is increased. However, an improvement is not always evident in the energy output and its present value. IRR also is improved.

Results for Calama

Table 6-3: Economic results for Calama, no back-up

	Calama						
	Direct TES		Indirect TES		Direct Production		
	Original Area	Modified Area	Original Area	Modified Area	Original Area	-	Units/Assumption
PV	$ (59,827,277)	$ (222,431,993)	$ (80,249,332)	$ (158,084,721)	$ (57,368,368)		15%, 148US/MWh 5y dep
IRR	13.51%	10.80%	13.02%	11.73%	13.37%		148US/MWh 5y dep
Cost	-725680991	-1044498500	-737728564	-960961786	-658907413		C.D. 12/2009
Cost/MWe	-7.3	-10.4	-7.4	-9.6	-2.2		Mill US/MWe
LEC	166	210	172	192	163		US/MWh
	91	115	95	106	90		CLP/kWh @ 550CLP/USD
Produced Energy	671666	703042	656869	696437	765686		MWh year

Direct storage in Calama is the best site for the plant, with LEC of US$233/MWh. The net present value of the project is negative with a discount rate of 15%, but in this case the IRR is 9.28%.

Results for Santiago

Table 6-4: Economic results for Santiago, no back-up

	Santiago						
	Direct TES		Indirect TES		Direct Production		
	Original Area	Modified Area	Original Area	Modified Area	Original Area	Modified Area	Units/Assumption
PV	$ (398,614,665)	$ (593,214,550)	$ (413,858,510)	$ (621,030,231)	$ (436,553,337)	$ (1,372,152,332)	15%, 148US/MWh 5y dep
IRR	2.24%	4.03%	1.80%	3.77%	-	-	148US/MWh 5y dep
Cost	-725680991	-1277413123	-737728564	-1317247377	-644767013	-2012887579	C.D. 12/2009
Cost/MWe	-7.3	-12.8	-7.4	-13.2	-2.2	-2.2	Mill US/MWe
LEC	483	437	508	453	484	491	US/MWh
	266	241	279	249	266	270	CLP/kWh @ 550CLP/USD
Produced Energy	227679	393854	219898	390824	248217	765686	MWh year

Solar energy produced in Santiago is relatively more expensive than in northern locations. Furthermore, the plant operational factor for solely solar energy is very small compared to the other sites. The factor energy produced with the amplified area over not amplified (~1.7) is smaller than the solar field area amplifier (~3).

The energy produced varies in accordance with the collector area and can improve the financials for different sites. However, increasing the mirror area does not always make the plant perform at its optimum level, so location is fundamental for economic feasibility.

6.3 Results for plants with back-up

The amplifier factor is the same for plants with and without fossil burners. However, more energy is produced with the solar resource and less is produced using fossil fuel if all other variables remain constant.

Results for Antofagasta

Table 6-5: Economic results for Antofagasta

	Antofagasta				
	DIR TES		INDIR TES		
	O AREA	M AREA	O AREA	M AREA	Units/Assumption
PV	$ (386,578,018)	$ (388,725,565)	$ (299,417,195)	$ (415,570,928)	15%, 148US/MWh 5y dep
IRR	1.27%	6.66%	0.11%	6.35%	148US/MWh 5y dep
Cost	-742930991	-1044498500	-754978564	-1085132190	C.D. 12/2009
Cost/MWe	-7.4	-10.4	-7.5	-10.9	Mill US/MWe
LEC	234	234	239	240	US/MWh
	129	129	131	132	CLP/kWh @ 550CLP/USD
Produced Energy	876000	876000	876000	876000	MWh year

Amplified area reduces the LEC; IRR is also improved, but not the present value of the plant, because of the higher initial cost.

Results for Calama

Table 6-6: Economic results for Calama

	Calama				
	DIR TES		INDIR TES		
	O AREA	M AREA	O AREA	M AREA	Units/Assumption
PV	$ (53,254,392)	$ (222,431,993)	$ (303,135,503)	$ (173,176,269)	15%, 148US/MWh 5y dep
IRR	13.55%	10.80%	12.14%	11.31%	148US/MWh 5y dep
Cost	-693021027	-1044498500	-754978564	-960961786	C.D. 12/2009
Cost/MWe	-6.9	-10.4	-7.5	-9.6	Mill US/MWe
LEC	160	210	173	187	US/MWh
	88	115	95	103	CLP/kWh @ 550CLP/USD
Produced Energy	876000	876000	876000	876000	MWh year

Present value and LEC is not improved with the amplified area. The IRR is better than that of the original direct storage case. This suggests that there must be a more optimal

solar field area for the Calama direct storage case. This case is more efficient than the indirect case because it has less heat exchanger units and thus a lower cost.

Results for Santiago

Table 6-7: Economic results for Santiago

	Santiago				
	DIR TES		INDIR TES		
	O AREA	M AREA	O AREA	M AREA	Units/Assumption
PV	$ (478,521,439)	$ (641,466,346)	$ (637,677,038)	$ (669,439,691)	15%, 148US/MWh 5y dep
IRR	12.04%	1.60%	-8.23%	1.31%	148US/MWh 5y dep
Cost	-754978564	-1277413123	-865412651	-1317247377	C.D. 12/2009
Cost/MWe	-7.5	-12.8	-8.7	-13.2	Mill US/MWe
LEC	254	290	290	296	US/MWh
	140	160	159	163	CLP/kWh @ 550CLP/USD
Produced Energy	876000	876000	876000	876000	MWh year

LEC is not improved with enhanced surface. This option is worse than than others.

Initial cost

The initial cost by different drivers is shown in the table below for the three models without back-up.

Table 6-8: Cost drivers for no back-up models

	Direct TES	Indirect TES	Direct Production
Solar Field and Site	$(186,212,630)	$(186,212,630)	$ (186,212,630)
HTF System	$ (1,429,924)	$ (11,429,924)	$ (1,312,931)
Storage	$(303,983,981)	$(304,460,131)	$ -
Fossil Backup	$ -	$ -	$ -
Power Block	$(122,700,000)	$(122,700,000)	$ (306,750,000)
Contingency	$ (16,710,000)	$ (16,710,000)	$ (17,100,000)
Indirect	$ (94,644,455)	$ (96,215,878)	$ (76,695,309)
Total	**$(725,680,991)**	**$(737,728,564)**	**$ (588,070,870)**

The initial cost for each driver is shown in Table 6-9 for the three models with back-up.

Table 6-9: Cost drivers for back-up models

	Direct TES	Indirect TES
Solar Field and Site	$(186,212,630)	$(186,212,630)
HTF System	$ (1,429,924)	$ (11,429,924)
Storage	$(303,983,981)	$(304,460,131)
Fossil Backup	$ (15,000,000)	$ (15,000,000)
Power Block	$(122,700,000)	$(122,700,000)
Contingency	$ (16,710,000)	$ (16,710,000)
Indirect	$ (96,894,455)	$ (98,465,878)
Total	**$(742,930,991)**	**$(754,978,564)**

The plants are roughly the same for all locations, so the costs are the same for all locations.

6.4 Chapter summary

The LEC is a good indicator of the competitiveness of an electric project. It needs to be compared to the electricity sale price that is paid today in the country. The SING has a predominant use of fuel for generating electricity, so prices are stable in the range of US$80-150/MWe, with the lower price corresponding to coal. In SIC, close to 50% are hydroelectric plants and the rest are mostly natural gas or diesel fueled cycles. However, coal participation has increased as natural gas has become less prevalent and given the higher costs of producing power with diesel. As such, the cost of SIC is more variable, ranging from values close to zero to US$150 per MWe depending on the plans that are online.

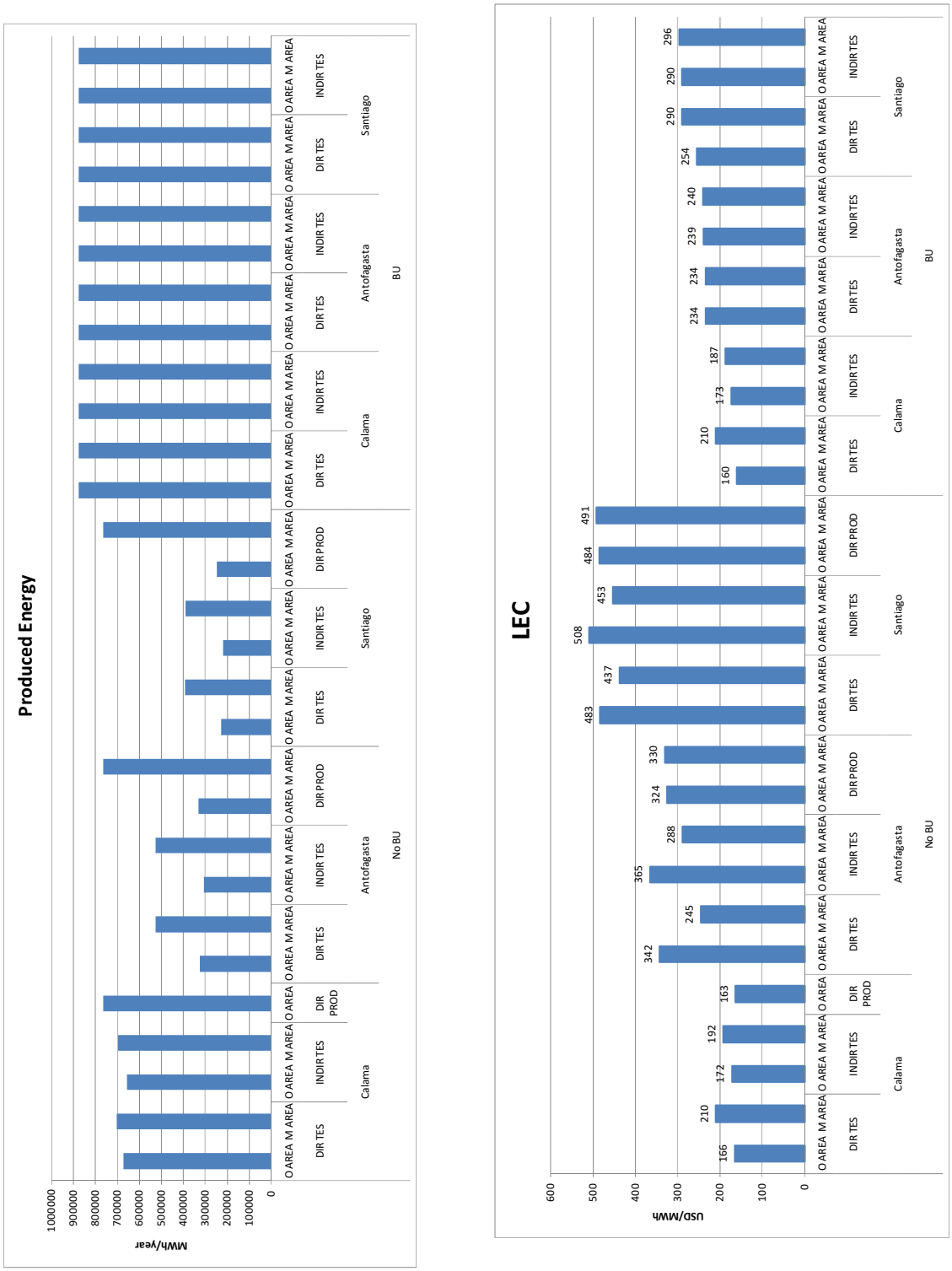

Figure 6-1: LEC for different locations and models

Figure 6-2 shows the installation costs for the different concepts. Twelve-hour storage systems are expensive and account for one fourth of the initial investment for models with this option. As a result, efforts should be focused on lower LEC.

Due to the variable output of the turbine used in the direct production model, a larger power block should be installed, but used at full capacity only once in a while as this increases the cost of the plant.

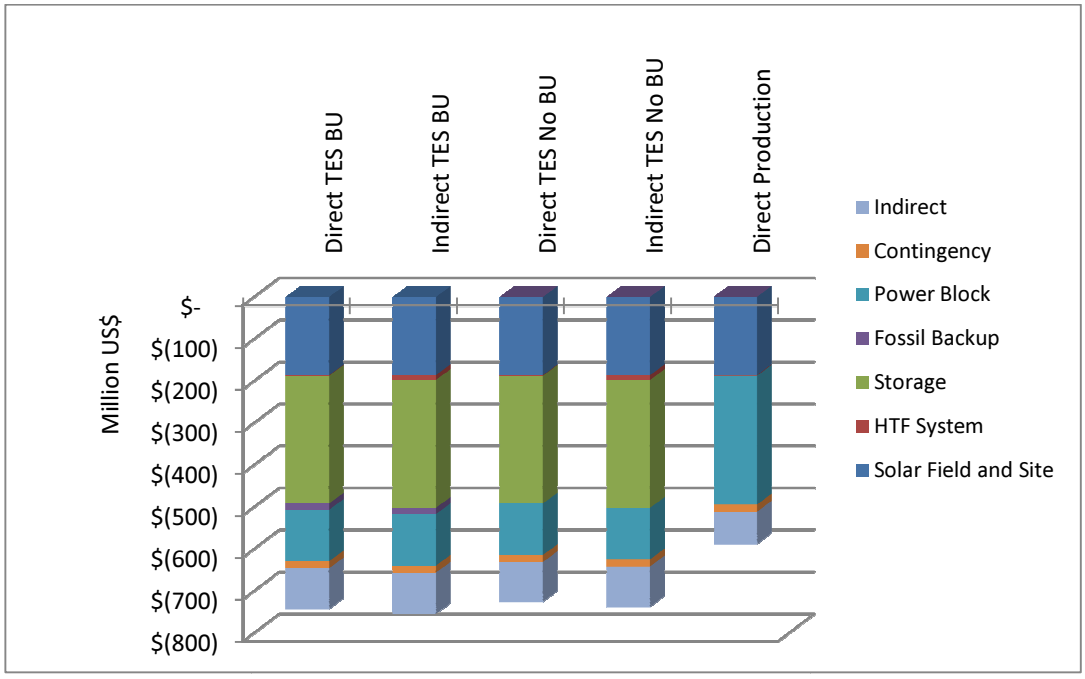

Figure 6-2: Cost drivers for different technologies

Figure 6-3 presents the yearly electric energy produced by all of the plants in the different sites. All models are non-BU models. Modifying the areas to try to produce the same energy as the most productive model increases energy production but it does not necessarily reduce the LEC, as can be seen in Figure 6-4, which compares options with and without BU.

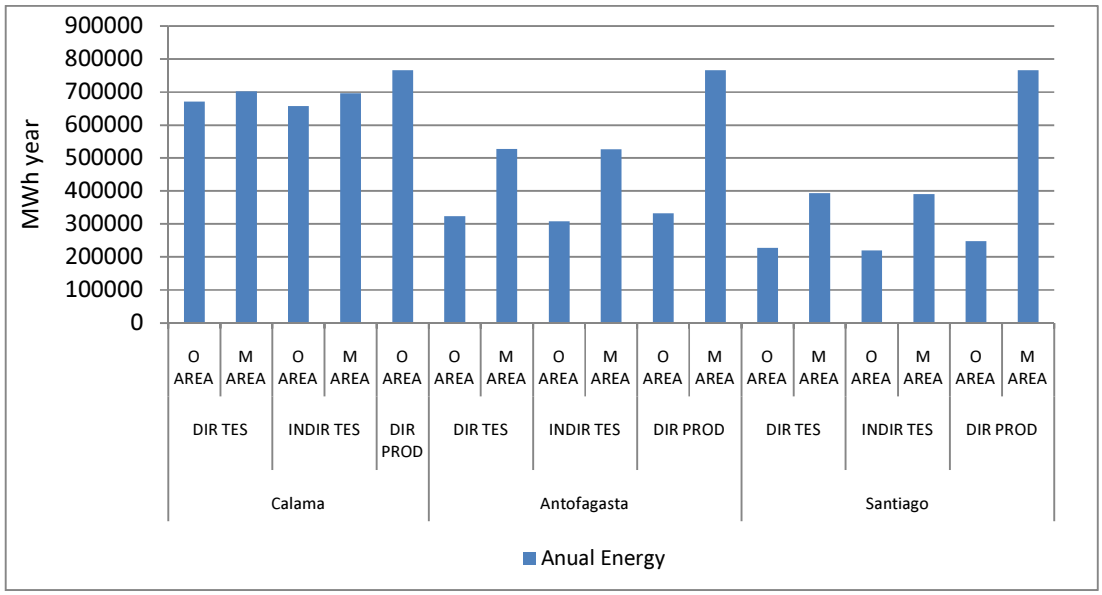

Figure 6-3: Annual energy by model

Figure 6-4 shows the LEC for Santiago and Antofagasta increases, when amplifying the solar field. However, this value decreases in Calama. This means that there has to be an optimum area for each model and the radiation characteristics of the site.

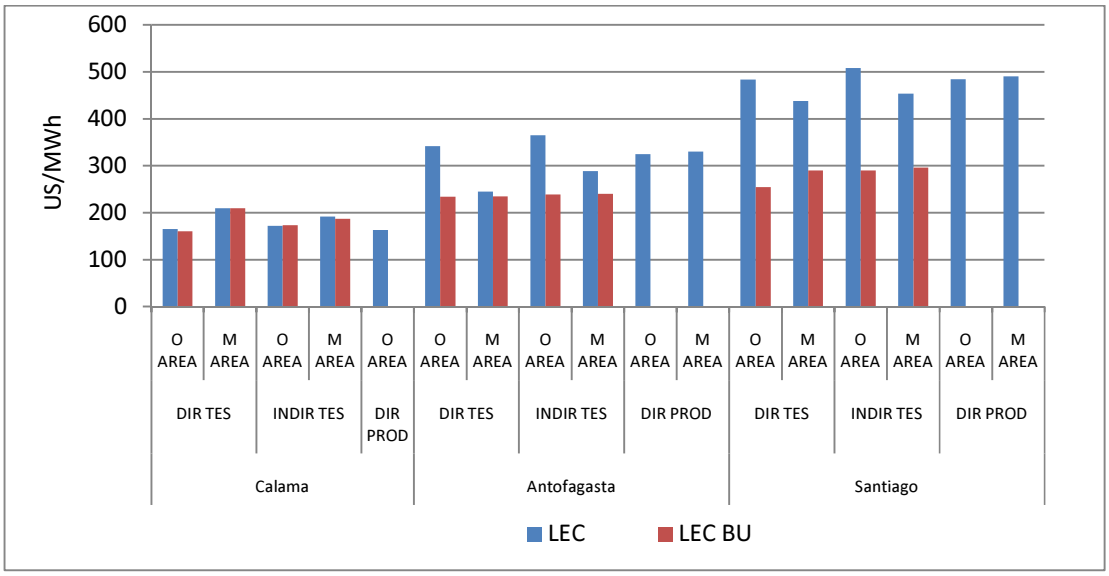

Figure 6-4: LEC by model and site

7. TOOL DEVELOPED

7.1 Introduction

Quaschning, Kistner, & Ortmanns, 2002 , worked with Greenius software for their study of a 50MWe SEGS-type plant. Specifically, they studied the behavior of LEC in regard to solar field area for one type of plant at three different radiation levels. In order to carry out this work, they had to consider several aspects. First, they needed higher radiation levels according to Chilean weather conditions. Secondly, they had to take into account various technologies including the option of hybridization with a fuel boiler.

This chapter presents an evaluation tool developed to assist experts as they make decisions regarding different radiation levels, technologies and areas for different locations in Chile using the assumptions presented in the previous chapters. Thermodynamic and economic simulations of the five types of plants were run for different collector areas and sites with different radiation levels. They are as follows:

- 1,000,000
- 1,400,000
- 1,800,000
- 2,200,000
- 2,600,000
- 3,000,000
- 3,400,000
- And others as necessary

For the following locations:

- Calama, with approximately 3,200 kWh/m^2 year
- Antofagasta, with slightly more than 1,800 kWh/m^2 year
- Santiago, with almost 1,400 kWh/m^2 year
- Copiapo, with more than 2,500 kWh/m^2 year for an intermediate radiation between Calama and Antofagasta. The radiation data for Copiapo was obtained using Meteonorm software.

The output of these simulations is the LEC and annual electric generation; the data is presented in graphs for easy use and comprehension.

7.2 Results

Figures 7-1 to 7-4 present the radiation levels for different values. LEC are plotted as solid lines in different colors for the various models. The energy output of the different plants is printed in the same color as the model's LEC but in a dashed line. The four options of plants with TES are 100MW plants, but turbine size for direct production plants varies with the size of the solar field in order to match the power block requirements of the best hour of the year for each solar field area.

Figure 7-1 shows the results for the plants if they were in Calama. The best model is the direct production model, which presents almost constant LEC for different collector areas. Direct production is the best option for scenarios in which TES is used without back-up, with a field area of 1,600,000m^2. The break in the energy curves at 1,400 and 2,200 thousand square meters is due to the change in the scale of the solar field area, which moves from intervals of 200,000 square meters to intervals of 400,000 square meters

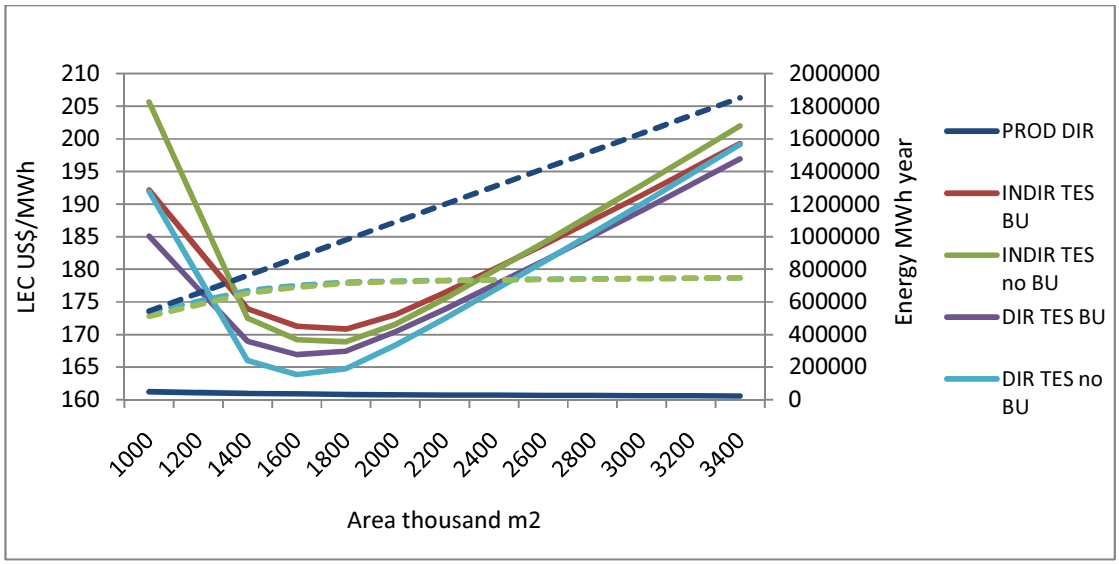

Figure 7-1: LEC and energy for Calama or locations with 3200kWh/m2 year

Figure 7-2 shows the results for Copiapo. The best model is the direct production model with back-up, with a field area of 2,000,000m^2. A close second is the option without back-up, which costs only US$3 more.

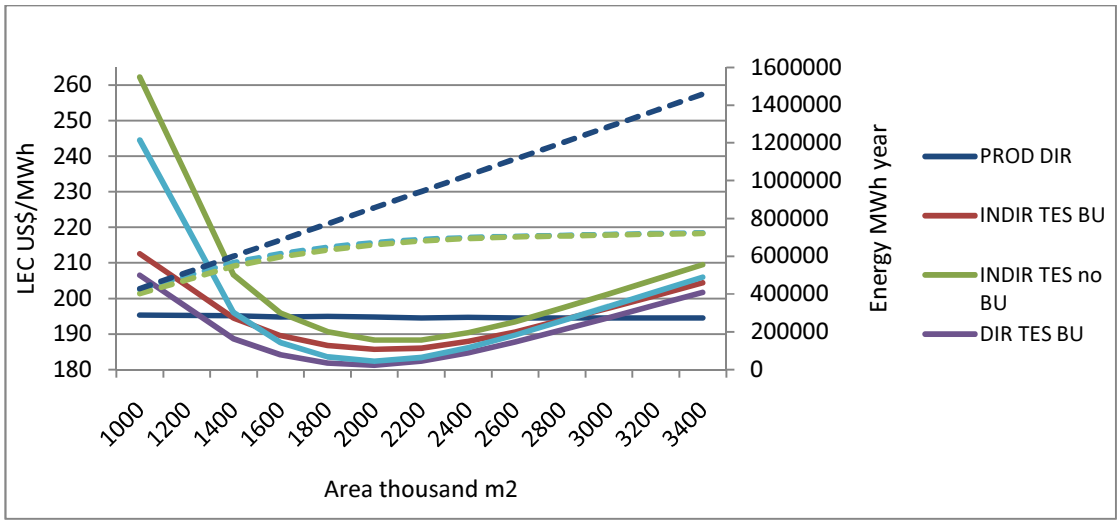

Figure 7-2:LEC and energy for Copiapo or locations with 2500kWh/m2 year

Figure 7-3 shows the results for Antofagasta. The best model is the direct production model with back-up, with a field area of 2,200,000m^2, followed closely by the option with indirect TES and back-up. When the two best LEC's are compared, the indirect TES option costs just US$5 more than the direct TES option. Direct production has a flat LEC and, based on this variable, is the worst option .

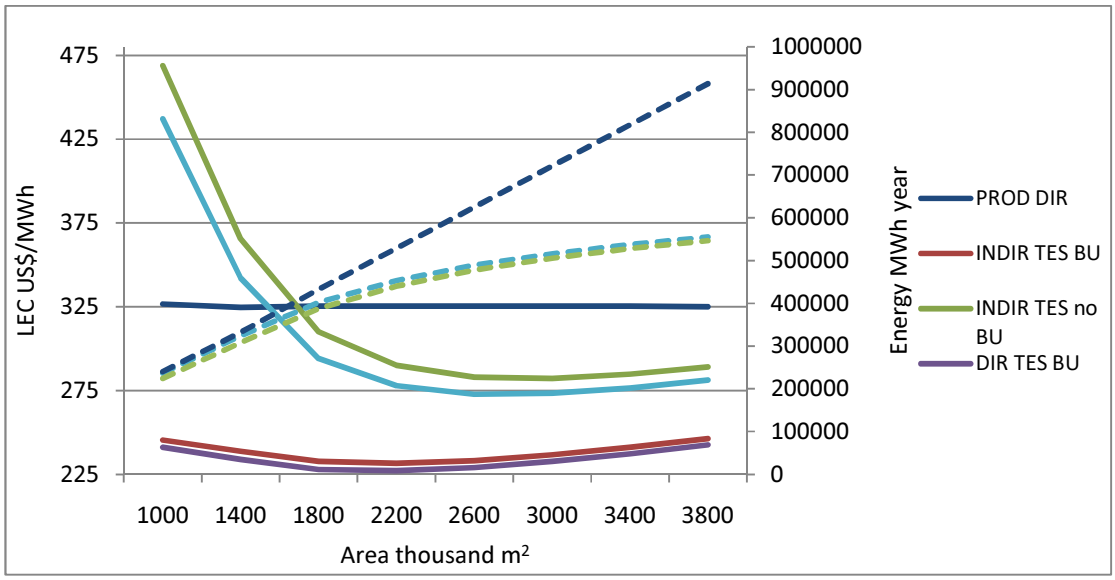

Figure 7-3: LEC and energy for Antofagasta or locations with 1800kWh/m2 year

Figure 7-4 shows the results for Santiago. The best model is the direct TES model with back-up, with a field area of 1,400,000m^2, followed closely by the option with indirect TES and back-up given that its optimal LEC costs just US$5 more than direct TES.

This option shows that, relative to the other locations, a decrease in the solar field area improves economic performance due to the reduced use of solar equipment and higher and less expensive use of the fossil burner.

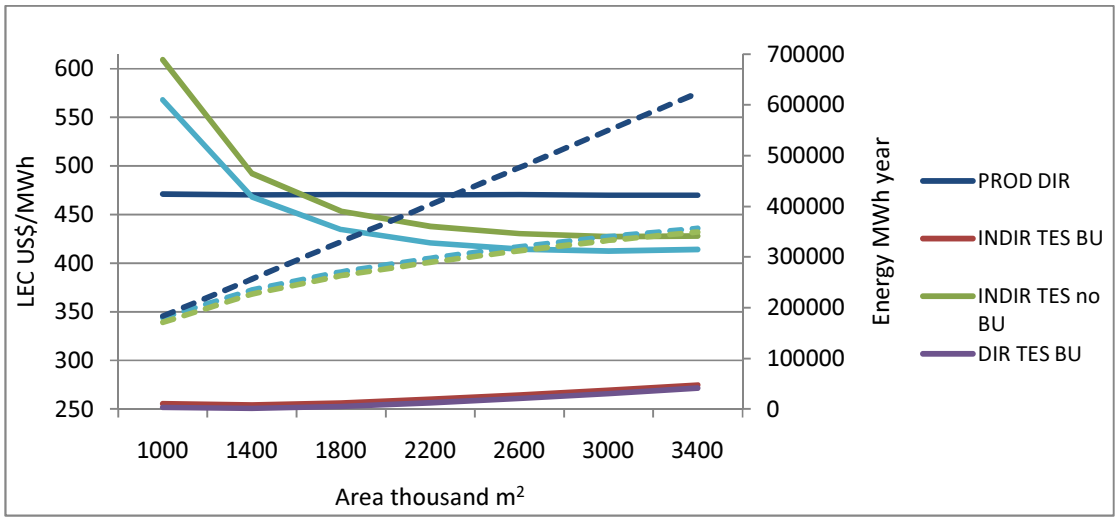

Figure 7-4: LEC and energy for Santiago or locations with 1500kWh/m2 year

Figures 7-5 through 7-9 show the LEC for each technology for different radiation levels in order to illustrate the relationship between the radiation in the site and the plant's LEC. The LEC is the solid line and its color varies by site. The dashed line is the electric energy produced and is presented in the same color as the corresponding LEC line. Figure 7-5 shows the results for direct TES without back-up. The lower LEC is achieved with the higher radiation for the same type of plant, and each radiation level has an optimum area.

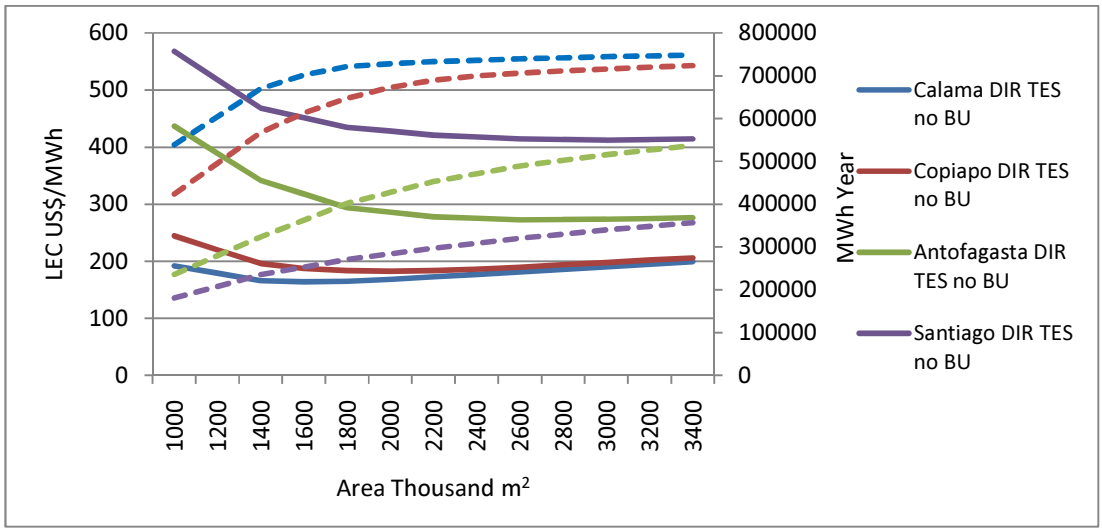

Figure 7-5: LEC for different sites for direct TES technology

Figure 7-6 shows the results for the direct TES with back-up model. Radiation is inversely proportional to LEC, but in the cases with back-up, the range of the LEC among different technologies is less than the option without back-up. The energy produced is 876,000 MWh because the plants have back-up system and run 24 hours a day and 365 days a year.

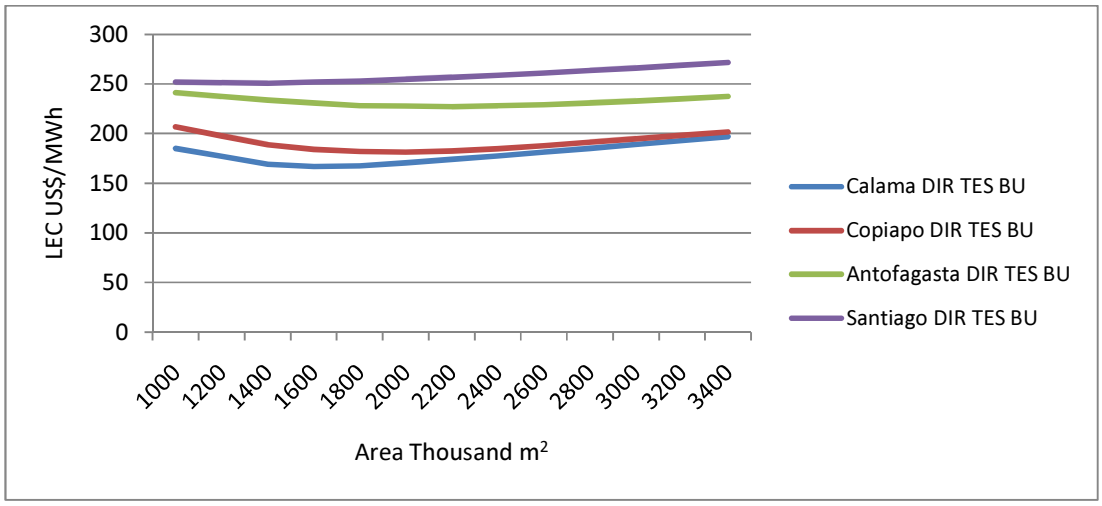

Figure 7-6: LEC for different sites for direct TES with back-up technology

Figure 7-7 shows the results for indirect TES without back-up. As was true in the direct TES case, better radiation means better LEC.

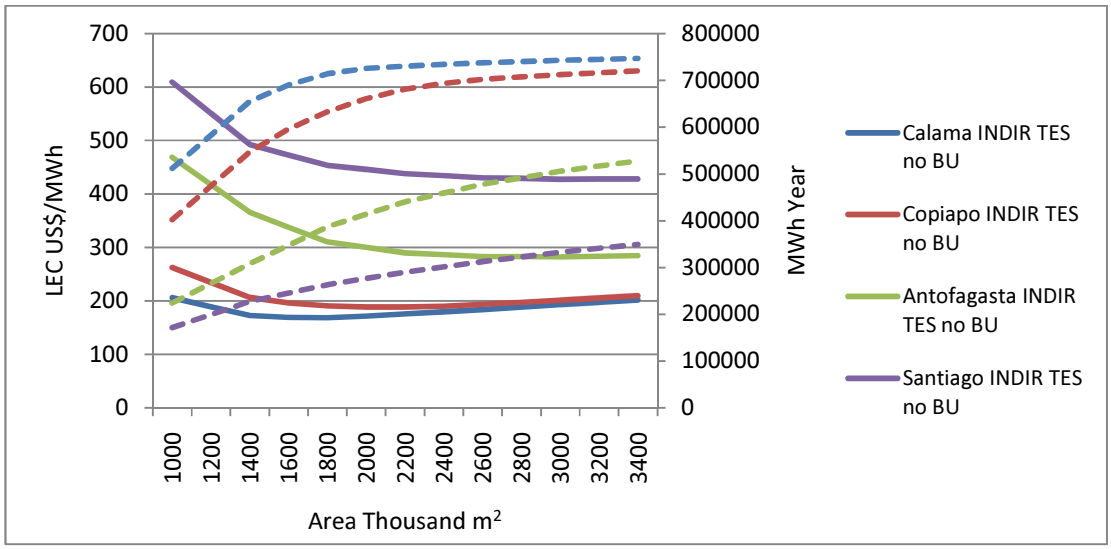

Figure 7-7: LEC for different sites for indirect TES technology

Figure 7-8 shows the results for the indirect TES with back-up option. As was true for direct TES, the range of the LEC is less than in the non back-up plant.

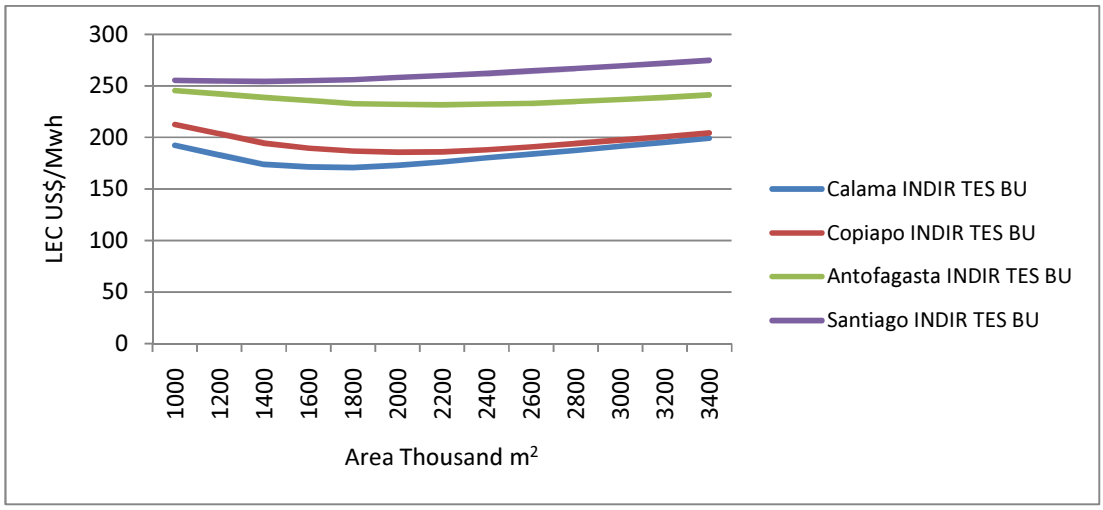

Figure 7-8: LEC for different sites for indirect TES with back-up technology

Figure 7-9 shows the direct production case The radiation level is inversely proportional to the LEC.

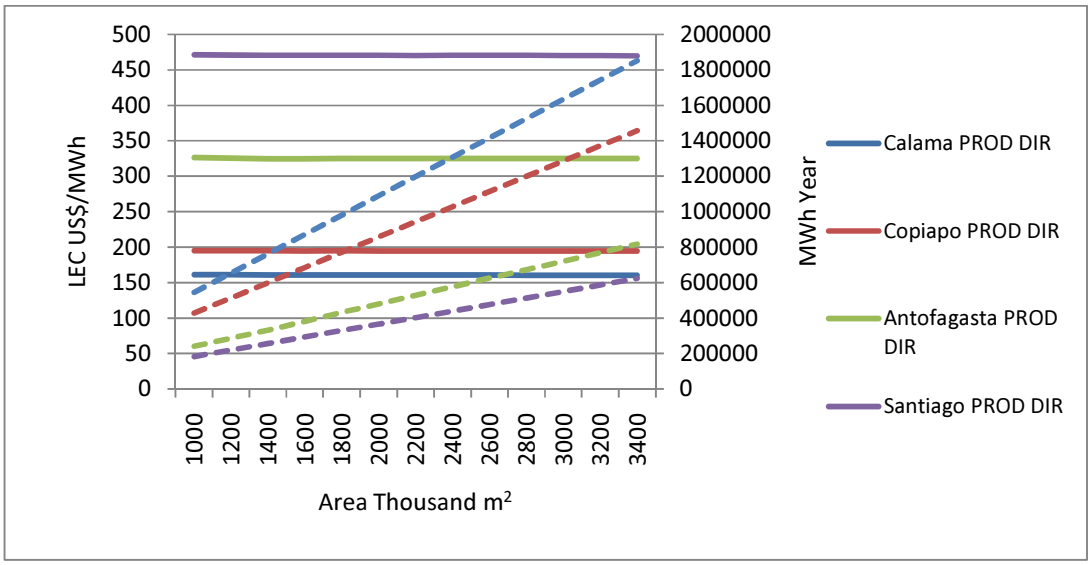

Figure 7-9: LEC for different sites for Direct Production technology

Figure 7-10 shows the best LEC for each model and radiation level.

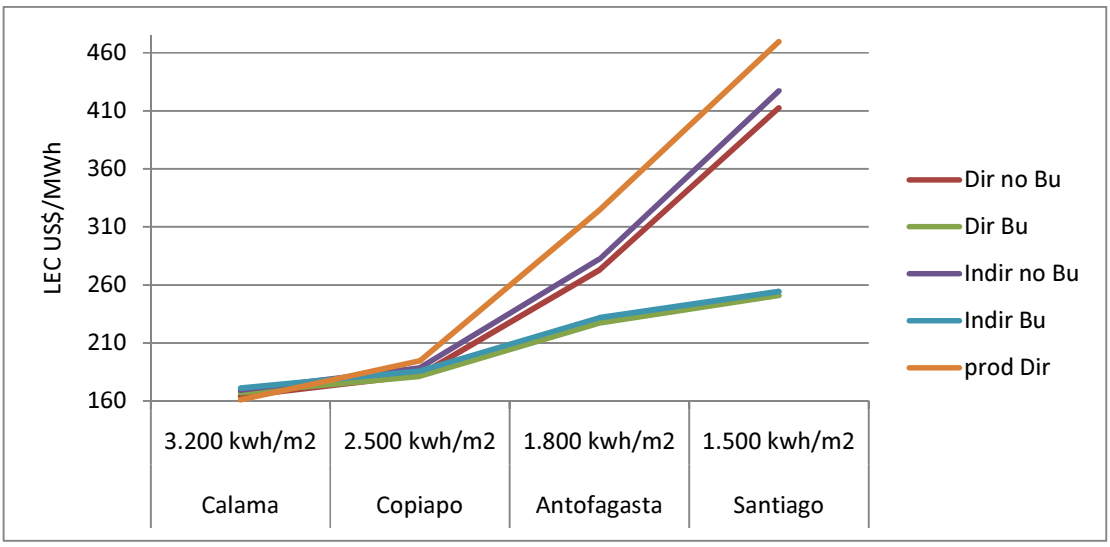

Figure 7-10: Best LEC by model

7.3 Weather variability

Due to the fact that limited data is available on the weather and radiation conditions for the different locations in Chile, the DNI for Copiapo was sensitized to a range of ±10%. This was done in order to examine the behavior of the LEC when the radiation in Copiapo was 10% worse or better than originally thought.

The ambient temperature was not changed, though this should have been done in order to better reflect real conditions. (It would be warmer if there was more radiation and cooler if there was less). However, given that it is difficult to estimate the exact temperature difference, we decided to omit this aspect.

Three different areas were chosen for the simulations of the five different models. The results are plotted below. The dashed lines correspond to the gross electric energy produced and the solid line represents the LEC for each case.

As it can be seen in Figure 7-11 and 7-12, the difference in the LEC decreases as the collector aperture area shrinks. This indicates that a slightly oversized area has a bounded LEC than an undersized solar field.

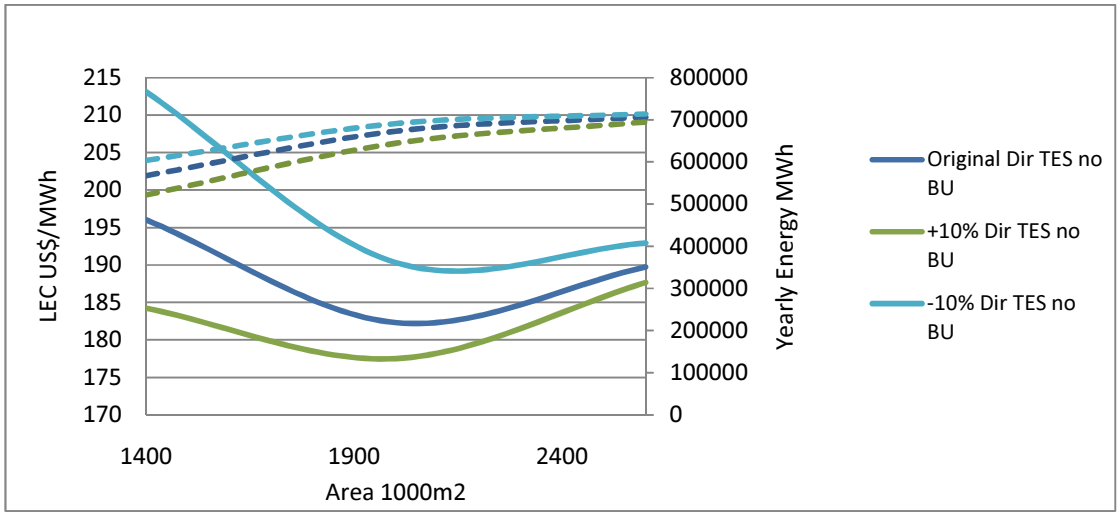

Figure 7-11: LEC and energy for +-10% radiation in Copiapo for direct TES no BU

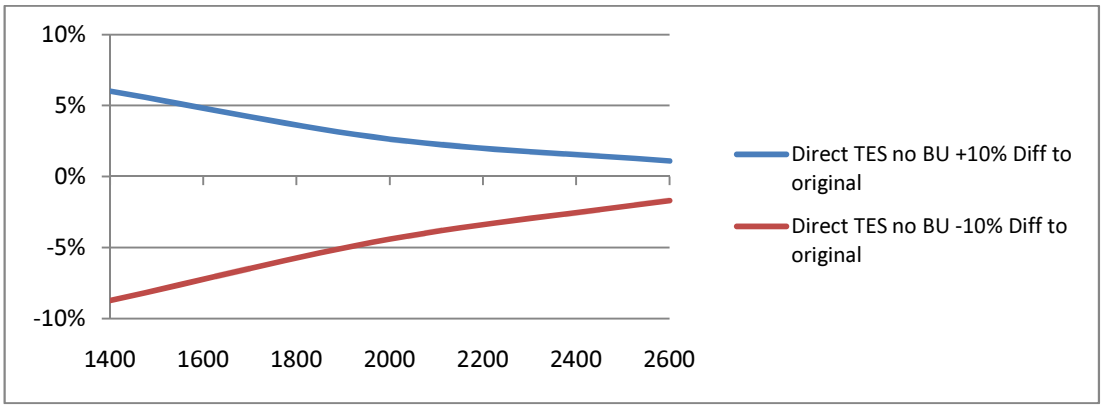

Figure 7-12: LEC difference for +-10% radiation in Copiapo for direct TES no BU

Figure 7-13 shows the results for direct TES with back-up. As was observed in the direct TES with no BU option, the dispersion diminishes as the solar field area expands.

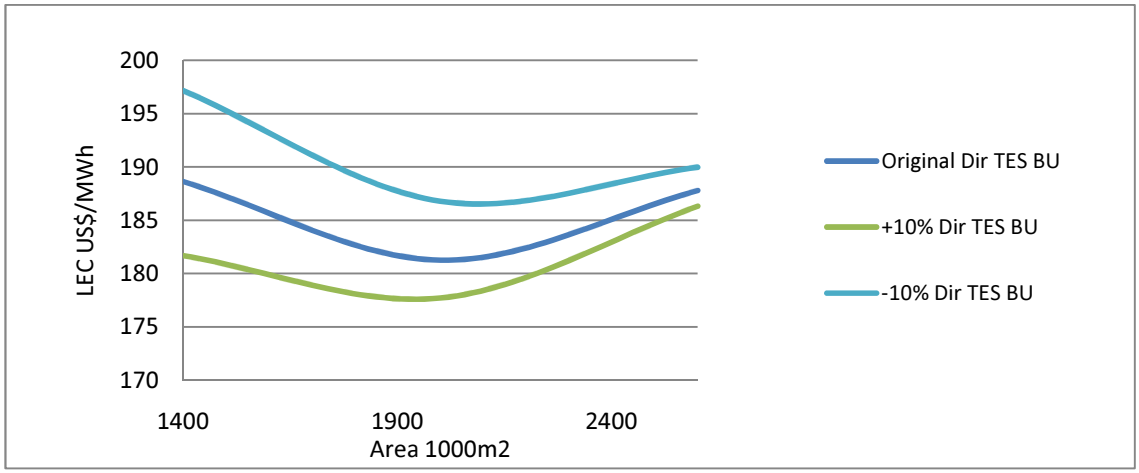

Figure 7-13: LEC and energy for +-10% radiation in Copiapo for direct TES with BU

Figure 7-14 shows the results for the indirect TES without back-up scenario. As was the case of direct TES without BU, LEC variability increases as the area increases.

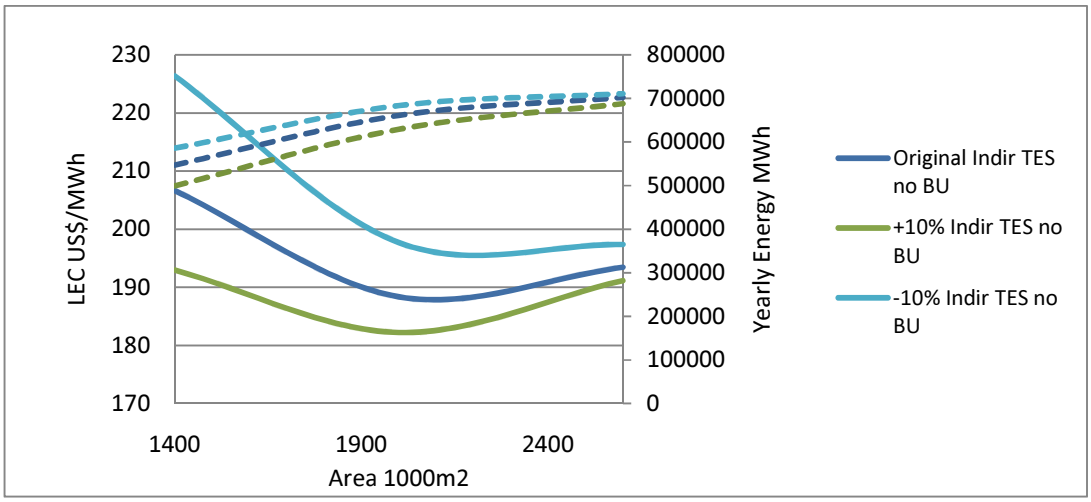

Figure 7-14: LEC and energy for +-10% radiation in Copiapo for indirect TES no BU

Figure 7-15 shows the results for the indirect TES with back-up scenario. As was the case for direct TES without BU, LEC variability decreases as the amount of area increases.

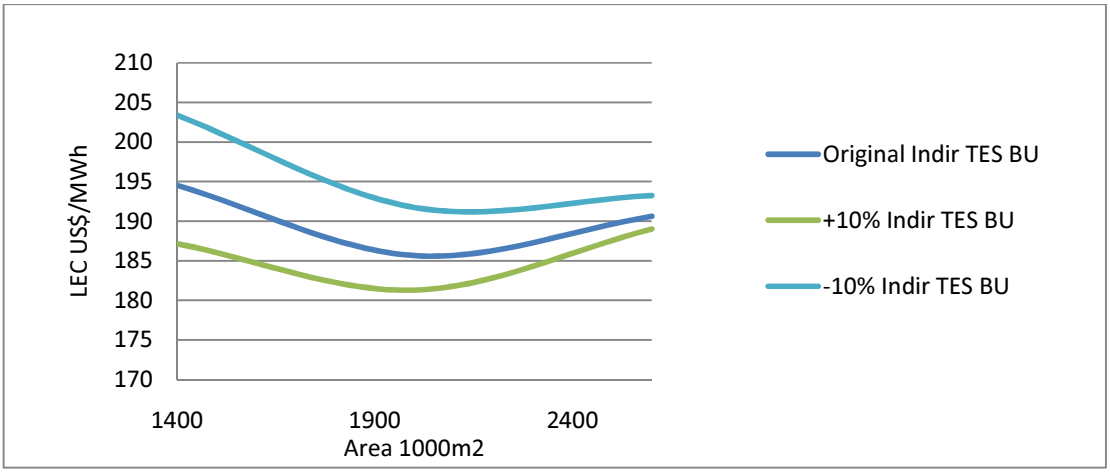

Figure 7-15: LEC and energy for +-10% radiation in Copiapo for indirect TES with BU

Figure 7-16 shows the direct production case. The differences seem to be roughly equal for all areas. Figure 7-17 shows the differences in LEC with +10% radiation compared to the original value.

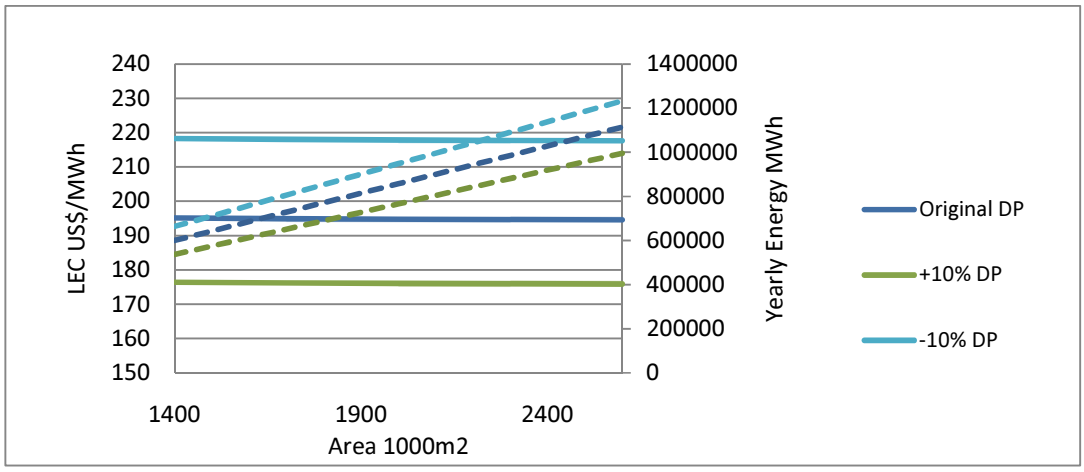

Figure 7-16: LEC and energy for +-10% radiation in Copiapo for direct production

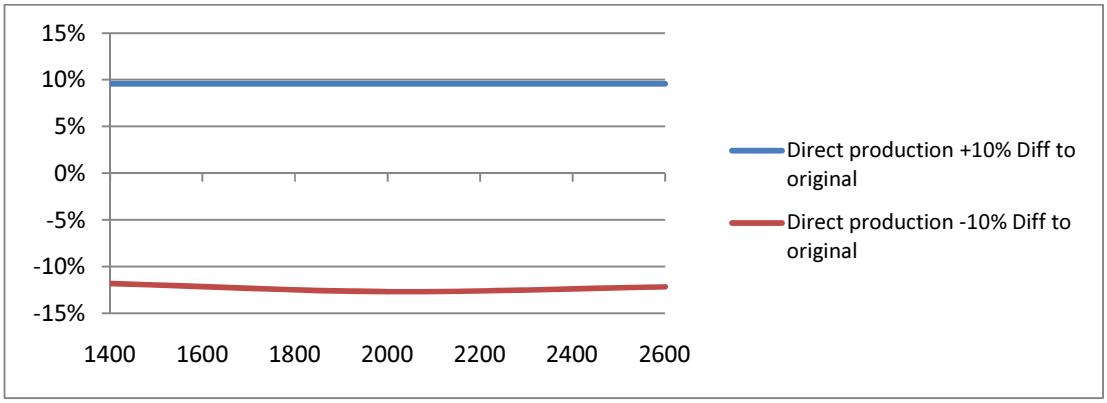

Figure 7-17: LEC difference for +-10% radiation in Copiapo for direct production

7.4 Discount rate sensitization

A case study was developed in order to understand the discount rate effect on the LEC. This example is valid for a direct TES solar plant in Copiapo without back-up with an optimal solar field aperture of 200 hectares. The discount rate was varied from zero to 30% en intervals of two percent. The result is shown below in Figure 7-18.

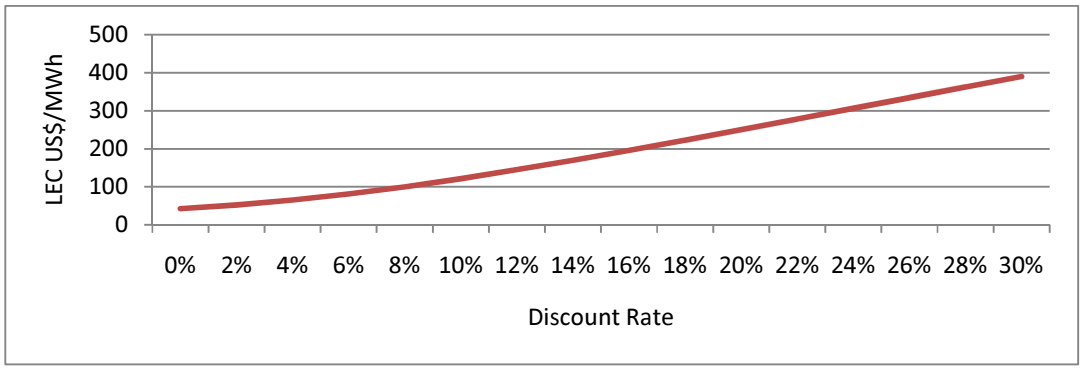

Figure 7-18: LEC vs. Discount Rate

The original LEC with a discount rate of 15% was US$182.32/MWh. If we consider the proportional variation of the LEC related to the proportional variation in the discount rate, the result can be more useful and can be extrapolated to other examples in better way.

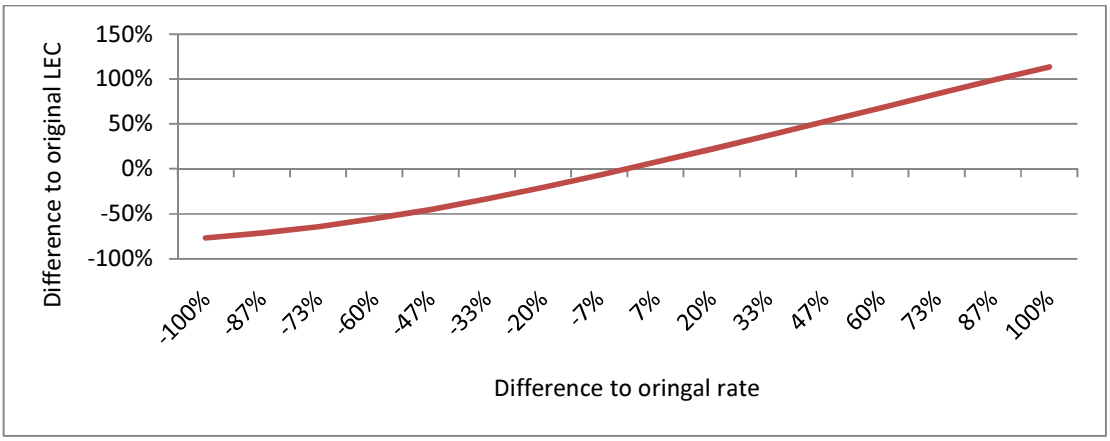

Figure 7-19: LEC vs Discount Rate

Changes in the rate from -20% to +100% are directly proportional to the change in LEC, with a factor greater than one (average in the range~1.12); this tendency is not valid for changes in the rate for differences beyond -20% or a discount rate of less than 12%.

A variation in the discount rate larger than -20%, affects the LEC in the same proportion as the discount rate with a factor of 1.12. Thus, if the rate is changed from 15% to 20% (33% increase) the LEC changes in LEC·33%·1.12 with a final value of US$250/MWh.

7.5 Chapter Summary

The best option is Calama direct TES without back-up and 160 hectares of solar field aperture. With this plant, assuming a discount rate of 15%, the cost that makes the investor indifferent or LEC is US$167/MWh.

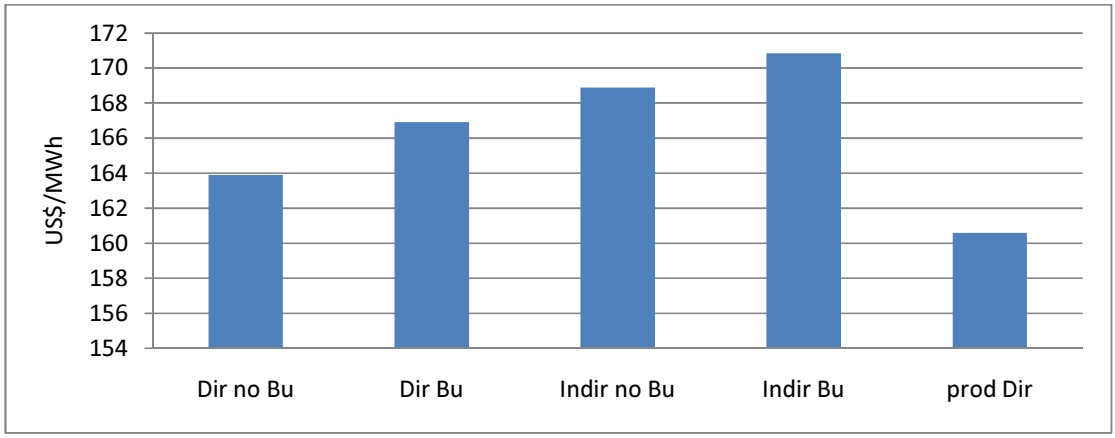

Figure 7-20: Best LEC for Calama by type of technology

LEC is inversely proportional to radiation. The range of the LEC for each type of technology and radiation level varying the SF area, is wider in the non-back-up options and narrower in the plants with back-up. This is due to the fact that the sale price tends to be closer to the sale price with fuel back-up in the last case.

Finally, for options with TES, it is better to have an oversized collector area in order to have a more tightly bounded LEC independent of the decision to include back-up. However, in the case of direct production, the only option for having a narrower LEC band is to have highly accurate data for several years. This would optimize the collector area for the radiation level of the site.

8. CONCLUSIONS

Chile is not a fossil energy producer. The country satisfies its internal consumption with imported fuels. This makes the country dependent on other countries to satisfy the demand for energy. One-third of the energy is generated using hydraulic technology and two-thirds of the electricity consumed in Chile comes from fossil fueled plants. These numbers and the IPCC claims on global warming caused by anthropogenic emissions make solar energy a resource worth considering.

Parabolic troughs are the most developed solar electric energy production device. With the addition of thermal storage and back-up boilers, this technology is a reliable source of energy with low dependence on international energy prices that is also environmentally friendly.

A few conclusions were reached based on the thermodynamic simulations. All of the models studied here are highly dependent on weather variability. Winter is a bad season and autumn and spring are not as good as summer. However, the performance in lower radiation seasons is better in Calama and Copiapo than it is in Santiago and Antofagasta due to the weather characteristics on the different sites. In a solar power plant, a relatively stable climate has a highly positive impact on the results. During the summer, only few hours are not useful. The availability of the solar resource decreases in autumn and again in winter. The seasonal variability is a key point to consider when making a decision regarding the size of the thermal storage. One must consider the cost of building a storage system with more capacity and its economic benefits. The results also are very sensitive to the collector area and the availability of fossil back-up and thermal storage.

The economic performance of the power plants is at least as important as the thermal behavior of the plants . The solar field accounts for one-fourth of the costs, while one-third of the cost of the models with TES is the storage system. In the direct production model, the power block is the most expensive aspect due to the peaks of power produced by a solar field that is connected directly to a turbine.

A system without TES is less expensive than an option with it, but the investment in and use of the power block is more regular and it remains on the same level of power for a long period of time. However, the level of direct production is completely variable.

The optimum system can be chosen based on the levelized electric cost. This decision is dependent on the radiation and the technology that can be applied. This means that there is an optimum technology and solar field size for a certain radiation level. It is clear that the higher radiation levels the best the LEC is. However, the difference in the LEC tends to be less for higher radiation levels.

The optimal SF size for different radiation levels varies. In less radiation scenarios a larger SF is needed, for optimum LEC, than in sites with higher radiation. Furthermore, the solar field area for an optimal LEC does not maximize the plant's energy output.

Based on weather data sensitization, the spread of LEC is decreased when the solar field is oversized as compared to a plant that was planned for a specific solar resource. When the weather is not reliable, it is better to over-estimate the aperture area of the collectors.

In summary, based on the LEC indicator:

- There is an optimal model for every solar radiation level
- That optimal model has an optimal SF size
- The more radiation, the smaller the SF
- The optimal SF area is not the one that maximizes the energy output of the plant
- Back-up can lower LEC, especially in lower radiation sites, but it can increase the cost of electricity in higher radiation zones.
- The variability of the weather data may introduce variations in the LEC. In order to diminish the variation, a solar field size that is larger than the optimal size should be used.

REFERENCES

Abengoa Solar. (n.d.). *http://www.abengoasolar.com.* Retrieved November 23, 2009, from http://www.abengoasolar.com/sites/solar/es/tecnologias/termosolar/tecnologia_ccp/index.html

Almanza, R., Lentz, A. J., & Gustavo. (1997). Receiver behavior in direct steam generation with prabolic troughs. *Solar Energy , 61* (4), 275-278.

Aspen Systems Corporation. (2000). *Combined Heat & Power: A Federal Manager's Resource Guide Final Report.*

ATSE. (2009). *The hidden costs of electricity: Externalities of power generation in Australia.*

Bernardes, M. D., Voß, A., & Weinrebe, G. (2003). Thermal and technical analyses of solar chimneys. *Solar Energy , 75*, 511–524.

Boyle, G. (2004). *Renewable Energy.* United Kingdom: Oxford University Press.

Carvallo, A. (2001). Energy Storage Technologies for utility scale intermittent renewable energy systems. *Journal of solar energy engineering , 123*, 387-389.

CDEC-SIC. (s.f.). Obtenido de https://www.cdec-sic.cl/

CNE. (n.d.). *Explorador de Energía Eolica y Solar*. Retrieved November 25, 2009, from http://condor.dgf.uchile.cl/EnergiaRenovable/Norte/

CNE. (2009, April). *http://www.cne.cl*. Retrieved November 23, 2009, from http://www.cne.cl/cnewww/opencms/07_Tarificacion/01_Electricidad/Otros/Precios_nudo/otros_precios_de_nudo/archivos_bajar/abril2009/ITD_SING_ABR09.rar

CNE. (2008). *Política Energética: Nuevos Lineamientos.* Santiago.

Duffie, J. A., & Beckman, A. W. (1980). *Thermal engineering of thermal processes.* New York, USA: Wiley & Sons, INC.

Eck, M., Zarza, E., Eickhoff, M., Rheinländer, J., & Valenzuela, L. (2003). Applied research concerning the direct steam generation in parabolic troughs2003. *Solar energy* , 341-351.

Energy, U. D. (2006). *Solar Energy Technologies Program 2007-2011.*

Ford, G. (2008). CSP: bright future for linear fresnel technology? *Renewable Energy Focus* (9), 48-49, 51.

Forristall, R. (2003). *Heat Transfer Analysis and Modeling of a Parabolic Trough Solar Receiver Implemented in Engineering Equation Solver.* NREL.

Frier, S. (1999). An Overview of the Kramer Junctions SEGS Recent Performance. *Parabolic Trough Workshop.* Ontario, CA.

Frier, S. (1999). *http://www.nrel.gov*. Retrieved November 23, 2009, from http://www.nrel.gov/csp/troughnet/pdfs/1999_kjc.pdf

Galetovic, A. (2007, December 2). Energías no convencionales: ¿Cuánto nos costarán? *La tercera* .

Gil, A., Medrano, M., Martorell, I., Dolado, P., Zalba, B., & Lázaro, A. (2009). State of the art on high temperature thermal energy storage for power generation. *Renewable and Sustainable Energy Reviews* .

Herrmann, U., Kelly, B., & Price, H. (2004). Two-tank molten salt storage for parabolic trough solar power plants. *Energy* , *29*, 883-893.

IEA. (2006). *CO2 emissions from fuel combustion.*

IEA. (1991). Guidelines for the economic analysis of renewable energy technology applications.

IPCC. (2007). *Climate Change: Synthesis Report.*

ISES World Congress 2009. (2009). Resolution. Johannesburg.

Kearney, D. W. (Performer). (2007). *Parabolic Trough Collector Overview*.

Kearney, D., Herrmann, U., Nava, P., Kelly, B., Mahoney, R., Pacheco, J., et al. (2003, May). Assessment of a Molten Salt Heat Transfer Fluid in a Parabolic Trough Solar Field. *Journal of Solar Engineering* , 170-176.

Kelly, B., & Kearney, D. (2006). *Thermal storage commercial plant for 2-tank indirect molen salt system.*

Klaiss, H., Köhne, R., Nitsch, J., & Sprengel, U. (1995). Solar thermal power plants for solar countries - Technology, ecnonomics and market potential. *aplied Energy* , *52*, 165-183.

Larrain, T. (2008). *Net energy analysis of hybrid concentrated solar thermal powerplants in chile: a design of a selection methodology for optimal plant location based on sustainability attributes.* PUC, Santiago.

Libertad y Desarrollo. (2008). Energías Renovables No Convencionales y Eficiencia Energetica.

Mills, D. (2004). Advances in solar thermal electricity technology. *Solar Energy* , *76*, 19-31.

Montes, M., Abánades, A., Martínez, J., & Valdés, M. (2009). Solar multiple optimization for a solar-only thermal power plant, using oil as heat transfer fluid in the parabolic trough collectors. *Solar Energy* (89), 2165–2176.

Nieuwlaar, E., & Alsema, E. (1997). *Environmental Aspects of PV Power Systems.*

NREL. (s.f.). *www.nrel.gov.* Recuperado el 2009 de November de 2009, de http://rredc.nrel.gov/solar/old_data/nsrdb/tmy2/unix/23161.tm2.Z

Ortega, A., Escobar, R., & Colle, S. (2008). Solar energy resourse assesment for Chile.

Patnode, A. (2006). *Simulation and Performance Evaluation of Parabolic Trough Solar Power Plants.* University of Wisconsin-Madison.

Pilkington Solar International GmbH. (2000). *Survey of thermal Storage for parabolic trough power plants.*

Pilkington Solar International. (1996). Status Report on Solar Thermal Power Plants.

Plataforma Solar de Almeria. (n.d.). *www.psa.es.* Retrieved November 23, 2009, from http://www.psa.es/webesp/instalaciones/discos.html

Price, H., Lüpfert, E., Kearney, D., Zarza, E., Cohen, G., Gee, R., et al. (2002). Advances in parabolic trough solar power technology. *Journal of solar energy , 124* (2).

PRLOG. (2009, March). *http://www.prlog.org*. Retrieved November 23, 2009, from http://www.prlog.org/10198293-global-solar-photovoltaic-market-analysis-and-forecasts-to-2020.html

Quaschning, V., Kistner, R., & Ortmanns, W. (2002, May). Influence of Direct Normal Irradiance Variation on the Optimal Parabolic Trough Field Size: A problem Solved with Technical and Economical Simulations. *Journal of Solar Energy Engineering* , 160-164.

Sandia National Laboratories. (2004, November 9). Retrieved November 24, 2009, from http://www.sandia.gov: http://www.sandia.gov/news/resources/releases/2004/renew-energy-batt/Stirling.html

Sandia National Laboratories, N. D. (2007, March). *Parabolic Trough Receiver Thermal Performance.* Golden, Colorado, USA.

Sargent & Lundy LLC Consulting Group. (2003). *Assessment of Parabolic Trough and Power Tower Solar Technology Cost and Performance Forecasts.*

Schott AG. (n.d.). *http://www.schottsolar.com.* Retrieved November 23, 2009, from http://www.schottsolar.com/global/products/concentrated-solar-power/schott-ptr-70-receiver/

Solarmillennium. (n.d.). *http://www.solarmillennium.de.* Retrieved 11 23, 2009, from http://www.solarmillennium.de/Technology/Parabolic_Trough_Power_Plants/Operation/Parabolic_Trough_Power_Plants_Generate_Electricity_from_Solar_Heat_,lang2,104.html

SWERA. (n.d.). *http://swera.unep.net/index.php?id=7*. Retrieved November 25, 2009, from http://swera.unep.net/typo3conf/ext/metadata_tool/archive/download/samglo_234.pdf

The Western Governors' Association's Clean and Diversified Energy. (2006). *Solar Task Force Report.*

Therminol. (n.d.). *http://www.therminol.com.* Retrieved from http://www.therminol.com/pages/bulletins/default.asp?where=E_VP1

Trieb, F., Langniss, O., & Klaiss, H. (19997). Solar electricity generation - A comparative view of technologies, costs and enviromental impact. *Solar Energy , 59*, 89-99.

Völker, T., Heinsath, A., Morin, G., & Varas, C. (2009, April 21-22). *Centrales termosolares - una perspectiva para Chile.* Casa Piedra, Santiago, RM, Chile.